



**HAL**  
open science

# The Numerical Zoom method for the elliptic perturbed problems and non-linear problems

Adnan Alahmad

► **To cite this version:**

Adnan Alahmad. The Numerical Zoom method for the elliptic perturbed problems and non-linear problems. Numerical Analysis [math.NA]. Université Bourgogne Franche-Comté, 2020. English. NNT : 2020UBFCD047 . tel-03510225

**HAL Id: tel-03510225**

**<https://theses.hal.science/tel-03510225>**

Submitted on 4 Jan 2022

**HAL** is a multi-disciplinary open access archive for the deposit and dissemination of scientific research documents, whether they are published or not. The documents may come from teaching and research institutions in France or abroad, or from public or private research centers.

L'archive ouverte pluridisciplinaire **HAL**, est destinée au dépôt et à la diffusion de documents scientifiques de niveau recherche, publiés ou non, émanant des établissements d'enseignement et de recherche français ou étrangers, des laboratoires publics ou privés.

---

**THESE DE DOCTORAT DE L'ETABLISSEMENT  
UNIVERSITE BOURGOGNE FRANCHE-COMTE  
PREPAREE AU LABORATOIRE DE MATHEMATIQUES DE  
BESANCON**

**Ecole doctorale n° 553 Carnot-Pasteur  
Doctorat de spécialité  
Mathématiques appliquées et applications des  
mathématiques**

par

**M. Adnan ALAHMAD**

---

**La méthode du Zoom Numérique  
pour des problèmes elliptiques  
perturbés  
et des problèmes non linéaires**

---

Thèse présentée et soutenue le 2 novembre 2020

Composition du Jury :

Grégory VIAL	Professeur, École Centrale de Lyon	Président
Anthony NOUY	Professeur, École Centrale de Nantes	Rapporteur
Jacques RAPPAZ	Professeur Honoraire, EPFL	Rapporteur
Alexei LOZINSKI	Université de Franche-Comté	Directeur de thèse



# Contents

<b>Introduction</b>	<b>1</b>
<b>1 An overview of global-local numerical methods: Chimera, finite element patches, numerical zoom</b>	<b>5</b>
1.1 Schwarz domain decomposition algorithm or Chimera method	5
1.2 The method of finite element patches . . . . .	7
1.3 Numerical zoom for problems with multiscale data and/or multiscale coefficients . . . . .	8
<b>2 Numerical zoom for elliptic problems on perturbed domains</b>	<b>13</b>
2.1 Presentation of the problem and adaptation of the numerical zoom algorithm . . . . .	13
2.2 Analysis of the algorithm for $\Gamma$ -nested meshes . . . . .	17
2.2.1 The finite element problem: an a priori error estimate .	17
2.2.2 Convergence of the iterative algorithm . . . . .	19
2.3 Analysis of Algorithm 2.1 on non $\Gamma$ -nested meshes . . . . .	23
2.3.1 The finite element problem: an a priori error estimate .	23
2.3.2 Convergence of the iterative algorithm . . . . .	32
2.4 Numerical Zomm with discontinuous Lagrange multipliers for non $\Gamma$ -nested meshes . . . . .	38
2.4.1 The error estimate for Algorithm 2.2 . . . . .	38
2.4.2 Convergence of the iterative algorithm 2.2 . . . . .	44
2.5 A modification of the algorithm for the case of a strongly non conforming interface . . . . .	47
2.5.1 An a priori error estimate for Algorithm 2.3 . . . . .	48
2.5.2 Convergence on iterations in Algorithm 2.3 . . . . .	51
2.6 Numerical tests . . . . .	52
2.6.1 Algorithm 2.1 on $\Gamma$ -nested meshes . . . . .	53
2.6.2 A numerical comparison of Algorithms 2.1–2.3 on general meshes . . . . .	54
<b>3 The approach of matched asymptotic expansions and comparisons with the numerical zoom</b>	<b>61</b>
3.1 The method of matched asymptotic expansions . . . . .	61
3.2 Finite element methods based on asymptotic expansions . . .	64
3.2.1 Superposition method . . . . .	64
3.2.2 A variational method with profiles vanishing on $\partial\Lambda$ .	65
3.2.3 Variational methods with more accurate profiles . . .	65

3.3	Numerical results . . . . .	68
<b>4</b>	<b>Numerical zoom for monotone non linear problems</b>	<b>75</b>
4.1	General properties of monotone operators and applications to PDEs . . . . .	75
4.2	A class of monotone PDEs with localized non-linearity and a Numerical Zoom for it . . . . .	80
4.3	Analysis of Algorithm 4.1 on $\Gamma$ -nested meshes . . . . .	83
4.3.1	The finite element problem: an a priori error estimate . . . . .	84
4.3.2	Convergence of the iterative algorithm for well localized non-linearities . . . . .	85
4.3.3	Convergence of the iterative algorithm for globally Lipschitz non-linearities . . . . .	88
4.4	Numerical tests . . . . .	90

# Introduction

In advanced applications of numerical methods, many models present localized multi-scale features. Some typical engineering problems deal with plastic deformations within a small zone included in a globally linear medium, contact problems on the structural joints in large aircraft assemblies, cracks propagating in elastic bodies, etc. Other examples can be found in computational hydrodynamics, for instance when modelling spread of pollution in the atmosphere, the sources (factories, explosions) can be on much smaller scale than the area where the pollution reaches by advection and diffusion.

The usual approach to solve such problems is of course the adaptive mesh refinement, which may be guided by *a posteriori* error estimators to refine the mesh around the small subregions of the entire computational domain, where some local features should be accurately captured. There is an abundant literature devoted to these techniques and we cite only the classical introductory textbook [41] for a mathematical perspective. While the generation of adapted meshes is far advanced now, it remains a complicated and costly procedure, both in terms of computing resources and of development efforts.

One may look therefore for some alternative approaches. One of the most simple and popular ones consists in superposing two grids, a coarse global one and a fine local one and alternating solutions on these two grids in an iterative manner. One can thus keep a non-adapted coarse grid and perform a multi-scale simulation. This idea appears in the literature under different names, for example the Chimera method [29], the method of finite element patches [20], and numerical zoom [4]. The common feature of all these methods is that the approximate solution is sought as the sum of the global coarse contribution and a local fine one. The coarse part of the overall solution is obtained iteratively from the original governing equations putting the current fine contributions to the right hand side. It is easy to see that such methods are not well suited to the situations where the coefficients in the governing equations are themselves of a localized multi-scale nature, since the finite element stiffness matrices for the coarse problem are then difficult to construct in practice.

To circumvent this drawback, it was proposed in [30] to modify the above cited methods by abandoning the superposition approach. The coarse problem is now constructed using a smoothed version of the original governing model. The local fine model is again introduced on a fine local grid. The coupling between the two grids (and the two models) is achieved by an iterative algorithm alternating the two solvers. Rather than taking the sum of coarse

and fine contributions, we now declare the coarse solution inside the refined zone (the zoom) purely fictitious and we replace it by the fine local solution. The latter is made consistent with the global coarse solution on the boundary of the zoom. The resulting method was baptized “the multi-model numerical zoom” since it couples two (possibly) different models: a global smoothed one and the local refined one.

A very similar approach was also proposed in the computational mechanics community [17–19, 23]. The main motivation of the authors was in developing *non intrusive* coupling methods. Indeed, it often happens that engineers have at their disposal a software that allows them to model e.g. some mechanical structure taken as a whole, but this software is not fine enough at some zones of the structure. This can be caused by a mesh which is too coarse or by neglecting some important physical phenomena. It may be too difficult or even impossible to modify the existing code and one may then want to develop a stand-alone code that provides a refined modeling where needed. One should then couple the global coarse solver with the local fine one so that they interact in an iterative manner, and one seeks for coupling methods that minimize the interactions between the two codes. The methods proposed in the articles cited above, essentially equivalent to the multi-model numerical zoom of [30], are good candidates to achieve this goal and were already tested on “real world” problems.

The methods of the multi-model numerical zoom or non intrusive model coupling have already received some attention in the literature. Apart from the works cited above, basically presenting the methods and discussing the practical issues and the results obtained, there is a mathematical *a posteriori* error analysis in [16, 40]. The works [14, 36] contain proofs of the convergence of iterative algorithms of these methods on the continuous level in the context of [14] to the case of stochastic partial differential equations with localized uncertainties. The work [34] proves the same in the context of monotone partial differential equations (with localized non-linearity). However, apart from the unpublished manuscript [31], there is yet no complete *a priori* error analysis with respect to the discretization, especially when general non-conforming meshes are used. Moreover, the convergence of the iterative algorithm of the method has not been yet investigated on the discrete level, even for simplest possible governing equations.

The goal of the present thesis is to fill to a certain extent the gap in the literature, outlined above. We consider mostly the following simple situation (yet pertinent to some practical application): the Poisson equation in domain containing a small hole. We employ a coarse global mesh that does not see the hole and correct this defect thanks to an additional fine mesh placed over the hole and conforming with it. An iterative algorithm (multi-model numerical zoom or non intrusive model coupling ) is then proposed, solving alternatively the problems on global and local meshes. We introduce a mathematical framework for these methods under very general assumptions on the meshes: the fine mesh may be placed over the coarse one in an arbitrary

---

manner. We perform then a complete theoretical analysis both of the accuracy with respect to a mesh refinement and of the convergence rate of iterations. We also compare this approach with the method of matched asymptotic expansions of [11]. Finally, we adapt our method to monotone problems with localized non-linearities, thus pursuing the work of [34], adapting the convergence proof to the discrete level, and giving an *a priori* error estimate.

The thesis is organized as follows. In the next chapter, we present the existing methods of “numerical zoom” type in more details on the example of a diffusion problem with the diffusion coefficient or the right-hand side exhibiting a localized multi-scale behavior. We also introduce there our “multi-model numerical zoom” method as a modification of the older algorithms. Chapter 2 is devoted to the analysis of the “multi-model numerical zoom” method for the elliptic problem posed in a perforated domain (a small hole inside the domain with Neumann boundary conditions on its boundary). We start the analysis in the case of nested triangulations (in an appropriate sense) and then propose some modifications that can be useful in non-nested settings. We establish optimal *a priori* error estimate and prove the convergence of our iterative algorithms. Chapter 3 is devoted to an alternative method based on matched asymptotic expansions for the same problem as in Chapter 2. We propose several variants of this approach on the discrete level and compare it numerically with the Numerical Zoom. Finally, we turn to monotone non-linear problems in Chapter 4. We are interested there in the case with localized non-linearities, adapting the Numerical Zoom method, the *a priori* error estimate, and the convergence proof to this situation.





## Chapter 1

# An overview of global-local numerical methods: Chimera, finite element patches, numerical zoom

---

We begin by presenting some multi-scale global-local methods on the example of the following classical problem: find a function  $u : \Omega \rightarrow \mathbb{R}$  such that

$$\begin{aligned} -\nabla \cdot (K \nabla u) &= f && \text{in } \Omega, \\ u &= 0 && \text{on } \partial\Omega, \end{aligned} \tag{1.1}$$

Here  $\Omega$  is a bounded domain in  $\mathbb{R}^2$ ,  $f \in L^2(\Omega)$  is a given function and  $K = (K_{ij})$  is a matrix valued function of class  $C^1$  satisfying

$$\alpha |\xi|^2 \leq K(x) \xi \cdot \xi \leq \beta |\xi|^2 \text{ for all } \xi \in \mathbb{R}^2 \text{ and } x \in \Omega$$

with some constants  $0 < \alpha \leq \beta < \infty$ . We are interested in the situation where the right-hand side  $f$  or the coefficients  $K_{ij}$  are highly oscillating in a small subdomain  $\Lambda \subset \Omega$ . We are interested in finite element methods that provide an approximation for the solution  $u$  on a relatively coarse mesh on  $\Omega$ , certainly too coarse to take into account the highly oscillating features inside  $\Lambda$ , and that correct in an iterative manner the numerical solution using another much finer local mesh on  $\Lambda$ .

### 1.1 Schwarz domain decomposition algorithm or Chimera method

One of the possible approaches to achieve the goals above is to use the domain decomposition with overlap and the classical Schwarz alternating method. This idea was introduced in a similar context (originally for nonlinear time dependent problems) by Steger [29] under the name of the Chimera method. The Schwarz method needs two interfaces to pass the information

between the two meshes in both directions (coarse to fine and backwards). One interface is naturally present in the form of the boundary of  $\Lambda$ , which we call here  $S_h$ . In order to provide another interface, one digs a hole  $D$  in the coarse domain strictly inside the zoom region  $\Lambda$ . We consider then the domain  $\Omega_H = \Omega \setminus D$ , denote the new interface  $S_H = \partial D$ , and loop on the two problems: for  $n = 1, 2, \dots$  solve

$$-\nabla \cdot (K \nabla U^n) = f \text{ in } \Omega_H, \quad U^n|_{\partial\Omega} = 0, \quad U^n = u^{n-1} \text{ on } S_H := \partial D,$$

and then

$$-\nabla \cdot (K \nabla u^n) = f \text{ in } \Lambda, \quad u^n = U^n \text{ on } S_h := \partial\Lambda$$

cf. Fig. 1.1.

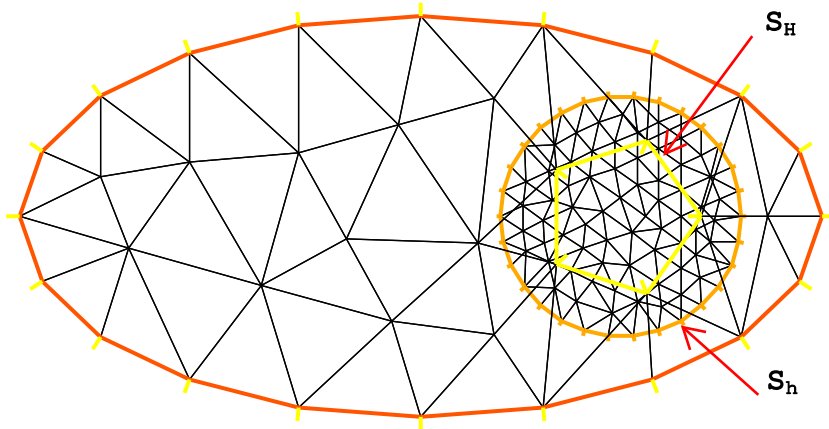


FIGURE 1.1: The drawing shows the fine mesh of the zoom region  $\Lambda$  overlapping the coarse mesh in of  $\Omega_H$  and the interfaces  $S_H, S_h$ .

The problems above are discretized by finite elements using a coarse mesh of size  $H$  on  $\Omega_H$  for  $U^n$  and a fine mesh of size  $h \ll H$  on  $\Lambda$  for  $u^n$ . Although this seems to work fine in most cases, cf. [27, 32], the convergence in the natural energy norm is an open problem, as well as the precision because of the unavoidable interpolation of  $U^n$  on  $\partial\Lambda$  when  $\Lambda$  is not made of elements of the triangulation of  $\Omega$ . Additionally, recalling our initial motivation to devise non-intrusive coupling methods, the necessity to dig a hole  $D$  in the coarse mesh on  $\Omega$  may be seen as a serious drawback: one is led here to change significantly the coarse global problem. Moreover, the rate of convergence of the Schwarz method depends on the width of the overlap between  $S_h$  and  $S_H$ , which should be thus kept sufficiently big. It means that the zoom  $\Lambda$

may have to be chosen artificially large with respect to the size of the zone of multi-scale behavior, which should be concentrated inside  $S_H$  since it cannot be resolved on the coarse mesh on  $\Omega_H$ .

## 1.2 The method of finite element patches

We now present the method of finite element patches [20], closely connected to the numerical zoom approach [4]. The basic idea of this method is to search the approximate multiscale solution as a sum of a global contribution on the coarse mesh and a local correction on the fine mesh. The global coarse contributions are calculated on iterations using the unperturbed coarse problems, thus allowing one to use the "legacy code" without changing it (at least without changing the rigidity matrix).

We now present the method of finite element patches applied to Problem (1.1) on the discrete level. We introduce the following notations: let  $\mathcal{T}_H$  be a triangulation of  $\Omega$  and  $\mathcal{T}_h$  that of  $\Lambda$ . For the sake of simplicity, both domains  $\Omega$  and  $\Lambda$  are supposed polygonal. Both triangulations are supposed regular (with the maximal aspect ratio of the triangles fixed once for all). Their element sizes  $H$  and  $h$  are typically such that  $h \ll H$ . Introduce the finite element spaces

$$V_H = \{v_H \in C^0(\Omega) : v_H|_T \in P_k \forall T \in \mathcal{T}_H, v_H|_{\partial\Omega} = 0\}$$

and

$$V_h^0 = \{v_h \in C^0(\Lambda) : v_h|_T \in P_k \forall T \in \mathcal{T}_h, v_h|_{\partial\Lambda} = 0\}.$$

where  $P_k$  is the set of degree  $k$  polynomials for a given  $k \geq 1$ . The multi-scale finite element approximation is constructed then in the above cited methods by solving the problem: find  $u_{Hh} = u_H + w_h$  with  $u_H \in V_H, w_h \in V_h^0$  such that

$$\int_{\Omega} K \nabla(u_H + w_h) \cdot \nabla(v_H + v_h) = \int_{\Omega} f(v_H + v_h), \quad \forall v_H \in V_H, v_h \in V_h^0. \quad (1.2)$$

Note that the functions in  $V_h^0$  are here assumed to be extended by 0 outside  $\Lambda$ , which makes sense since their traces are 0 on  $\partial\Lambda$  by construction.

As mentioned above, Problem (1.2) is not solved directly but rather by an iterative method, like the following one: find successive approximations  $u_H^n \in V_H, w_h^n \in V_h^0$  satisfying

$$\int_{\Omega} K \nabla u_H^n \cdot \nabla v_H = \int_{\Omega} f v_H - \int_{\Lambda} K \nabla w_h^{n-1} \cdot \nabla v_H, \quad \forall v_H \in V_H \quad (1.3)$$

$$\int_{\Lambda} K \nabla w_h^n \cdot \nabla v_h = \int_{\Lambda} f v_h - \int_{\Lambda} K \nabla u_H^n \cdot \nabla v_h, \quad \forall v_h \in V_h^0. \quad (1.4)$$

It is easy to see that if this iterative method converges, i.e.  $u_H^n \rightarrow u_H, w_h^n \rightarrow w_h$  as  $n \rightarrow \infty$ , then  $u_{Hh} = u_H + w_h$  solves (1.2). The fact that the method is

indeed convergent is proven in [20] where an optimal error estimate is also established for the approximate solution  $u_{Hh}$ .

The method (1.3)–(1.4) thus alternates the solutions of coarse problems on  $\mathcal{T}_H$  with the fine ones on  $\mathcal{T}_h$ . The stiffness matrices of both problems are completely standard and independent from each other. The transfer of information between the two problems is done *via* the mixed terms on the right-hand sides of (1.3)–(1.4). Implementing these terms requires evaluating the integrals on the triangles of  $\mathcal{T}_H$  of functions defined on  $\mathcal{T}_h$  (and vice versa integrals on  $\mathcal{T}_h$  of functions on  $\mathcal{T}_H$ ). Such calculations are not straightforward, but some efficient implementations were proposed in the literature. One can therefore consider that the method works fine, from both theoretical and practical viewpoints, in the case of problems with multi-scale data, i.e. when the right-hand side  $f$  is highly oscillating inside  $\Lambda$ .

We argue however that the method (1.3)–(1.4) is not really suitable for the situations with multi-scale coefficients in the equations. Indeed, if the coefficients  $K_{ij}$  are highly oscillating in  $\Lambda$ , an extra care should be taken in evaluating the integrals  $\int_{\Omega} K \nabla \phi_{H,i} \cdot \nabla \phi_{H,j}$  that form the stiffness matrix of the coarse problem, with  $\phi_{H,i}$  being the finite element basis functions of  $V_H$ . Indeed, one should employ then a very accurate quadrature rule (or possibly a very fine submesh) to calculate the part of these integrals inside  $\Lambda$  because of the oscillations of  $K_{ij}$  there. This comes in contradiction with the usual practice of finite element calculations, in which some standard relatively low-order quadrature rules are used to construct the entries of the stiffness matrix. Inspired by this remark, we want to devise another approach where the coefficients of  $K$  in the coarse finite element sub-problems can be smoothed out inside  $\Lambda$ .

### 1.3 Numerical zoom for problems with multiscale data and/or multiscale coefficients

The core of the difficulties outlined above lies in the reconstruction of the multi-scale solution as a sum of the coarse and fine contributions. We are going therefore to adopt another strategy where the part of the coarse solution inside  $\Lambda$  is finally neglected and the overall solution inside  $\Lambda$  is given by the approximation on the fine mesh  $\mathcal{T}_h$  alone.

First, we restrict ourselves to the special case of nested meshes, i.e. we suppose that  $\mathcal{T}_h$  is formed by a subdivision of the triangles of  $\mathcal{T}_H$  lying inside  $\Lambda$ . In this case, we start by a reformulation of (1.3)–(1.4). Let us introduce the new iterates on the fine mesh as  $u_h^n = u_H^n|_{\Lambda} + w_h^n$ . Note that  $u_h^n$  does no longer vanish on the boundary of  $\Lambda$ . It lies in the space

$$V_h = \{v_h \in C^0(\Lambda) : v_h|_T \in P_k \forall T \in \mathcal{T}_h\} \quad (1.5)$$

i.e. the same fine finite element space as before but without any requirement on the boundary. Rewriting the algorithm with the new variables  $u_H^n \in V_H$ ,

$u_h^n \in V_h$  leads to

$$\begin{aligned} \int_{\Omega} K \nabla u_H^n \cdot \nabla v_H &= \int_{\Omega} f v_H - \int_{\Lambda} K \nabla u_h^{n-1} \cdot \nabla v_H + \int_{\Lambda} K \nabla u_H^{n-1} \cdot \nabla v_H, \quad \forall v_H \in V_H \\ \int_{\Lambda} K \nabla u_h^n \cdot \nabla v_h &= \int_{\Lambda} f v_h, \quad \forall v_h \in V_h^0 \\ u_h^n|_{\partial\Lambda} &= u_H^n|_{\partial\Lambda}. \end{aligned}$$

We can furthermore impose the boundary conditions for  $u_h^n$  on  $\partial\Lambda$  with the help of a Lagrange multiplier. Let us define to this end the finite element space  $M_h$  on  $\partial\Lambda$  as the space of traces of functions in  $V_h$  :

$$M_h = \{\mu_h \in C^0(\partial\Lambda) : \mu_h|_E \in P_k \text{ on every boundary edge } E \text{ of the mesh } \mathcal{T}_h\} \quad (1.6)$$

and rewrite the iterative procedure above as follows: find  $u_H^n \in V_H$ ,  $u_h^n \in V_h$ ,  $\lambda_h^n \in M_h$

$$\begin{aligned} \int_{\Omega} K \nabla u_H^n \cdot \nabla v_H &= \int_{\Omega \setminus \Lambda} f v_H - \int_{\partial\Lambda} \lambda_h^{n-1} v_H \\ &\quad + \int_{\Lambda} K \nabla u_H^{n-1} \cdot \nabla v_H, \quad \forall v_H \in V_H \end{aligned} \quad (1.7)$$

$$\int_{\Lambda} K \nabla u_h^n \cdot \nabla v_h - \int_{\partial\Lambda} \lambda_h^n v_h = \int_{\Lambda} f v_h, \quad \forall v_h \in V_h \quad (1.8)$$

$$\int_{\partial\Lambda} u_h^n \mu_h = \int_{\partial\Lambda} u_H^n \mu_h, \quad \forall \mu_h \in M_h \quad (1.9)$$

Let us emphasize that the last algorithm is equivalent to the original algorithm (1.3)–(1.4) in the case of nested triangulations. We have thus a convergence result for the iterative method and an error estimate for the discretized problem in this particular case.

However, in some applications,  $\Lambda$  is chosen in a manner which may be completely incompatible with the coarse triangulation, for example, to keep the shape of  $\Lambda$  simple in order to use a structured fine mesh on it. For non nested meshes the new method (1.7)–(1.9) together with the definition of the finite element spaces (1.5) and (1.6) makes sense on any meshes  $\mathcal{T}_H$  and  $\mathcal{T}_h$ , but it is no longer equivalent to the method (1.3)–(1.4). The new algorithm has the advantage over the old one in that it reduces the interactions between coarse and fine discretizations. Indeed, the only place where the two discretizations talk to each other is the boundary integrals  $\int_{\partial\Lambda} \lambda_h^{n-1} v_H$  and  $\int_{\partial\Lambda} u_H^n \mu_h$ , in contrast to the mixed terms on the whole of  $\Lambda$  in the method (1.3)–(1.4). This allows us to reduce the computational cost and the programming burden.

More importantly, the new method (1.7)–(1.9) can be slightly modified to be suited to situations where coefficients  $K_{ij}$  are highly oscillating. Indeed, the functions  $u_H^n$  are only relevant outside  $\Lambda$  in the new method. This means that we can modify the coarse problem inside  $\Lambda$  in order to make it smoother

and to facilitate the calculation of the finite element stiffness matrix. We thus introduce coefficients  $\tilde{K} = (\tilde{K}_{ij})$  much smoother than  $K$  in  $\Lambda$  and such that  $\tilde{K}|_{\Omega \setminus \Lambda} = K|_{\Omega \setminus \Lambda}$ . We assume, similarly to the original coefficients  $K$ ,

$$\alpha|\xi|^2 \leq \tilde{K}(x)\xi \cdot \xi \leq \beta|\xi|^2 \text{ for all } \xi \in \mathbb{R}^2 \text{ and } x \in \Omega$$

We can then replace  $K$  by  $\tilde{K}$  in the coarse problem, so that (1.7) becomes

$$\int_{\Omega} \tilde{K} \nabla u_H^n \cdot \nabla v_H = \int_{\Omega \setminus \bar{\Lambda}} f v_H - \int_{\partial \Lambda} \lambda_h^{n-1} v_H + \int_{\Lambda} \tilde{K} \nabla u_H^{n-1} \cdot \nabla v_H, \quad \forall v_H \in V_H \quad (1.10)$$

This does not affect the final solution, provided the iterative process converges. The convergence can be indeed proven, cf. [31], if one adds relaxation to the coarse problem (1.10). We should redefine  $u_H^n$  as the convex combination  $\omega \hat{u}_H^n + (1 - \omega) u_H^{n-1}$ , where  $\omega \in (0, 1]$  is a relaxation parameter. Thus,  $u_H^n \in V_H$  is computed as the solution to

$$\begin{aligned} \int_{\Omega} \tilde{K} \nabla u_H^n \cdot \nabla v_H &= \int_{\Omega} \tilde{K} \nabla u_H^{n-1} \cdot \nabla v_H \\ &+ \omega \left\{ \int_{\Omega \setminus \bar{\Lambda}} f v_H - \int_{\partial \Lambda} \lambda_h^{n-1} v_H - \int_{\Omega \setminus \bar{\Lambda}} \tilde{K} \nabla u_H^{n-1} \cdot \nabla v_H \right\}, \quad \forall v_H \in V_H \end{aligned} \quad (1.11)$$

We refer to the method (1.11)–(1.8)–(1.9) as the multi-model numerical zoom. Indeed, its iterations can be viewed as a coupling of the smooth global model (with  $\tilde{K}$  defined over  $\Omega$ ) and the stiff local one (with  $K$  on  $\Lambda$ ).

Let us reexamine now the non-intrusivity of the algorithm in the sense of [18, 19]. As it is already mentioned, the boundary term in the coarse problem  $\int_{\partial \Lambda} \lambda_h^{n-1} v_H$  should be implemented in a stand-alone software since it contains the fine correction  $\lambda_h$ . Moreover, the term  $\int_{\Lambda} \tilde{K} \nabla u_H^{n-1} \cdot \nabla v_H$  may also need a special treatment outside the coarse solver, although it involves only functions on  $\mathcal{T}_H$ . Here, the integration should be performed on the patch  $\Lambda$  which is not necessarily conforming with  $\mathcal{T}_H$ . The integral  $\int_{\Lambda} \tilde{K} \nabla u_H^{n-1} \cdot \nabla v_H$  will then have to be evaluated outside of the coarse solver. Let us note that latter articles also introduce a closely related method involving Robin conditions on the interface. Such a method is more intrusive because of the modification of the coarse stiffness matrix.

The idea of replacing locally sharp or oscillating coefficient  $K$  with a smoothed version  $\tilde{K}$  can be easily generalized to more complicated settings. We shall consider two of them in the present thesis:

**Chapter 2:** A linear elliptic PDE posed in a perforated domain, namely a domain with a small hole inside it. We shall consider the hole as a perturbation to a simpler problem posed on the whole non-perforated domain and reinterpret our algorithm as coupling between the unperturbed coarse model (approximated on a global coarse mesh that does not see the hole) and the local corrected model (the actual problem on

the patch surrounding the hole). Such a problem can be seen as a prototype of more realistic situations where a coarse solver cannot handle the tiny geometrical details (joints, cracks, etc) and one needs local patches (numerical zooms) to handle them.

**Chapter 4:** Non-linear problems with localized non-linearity (for example, think of plasticity that affects the behaviour of an otherwise linear elastic material only in the vicinity of some critical points). One can then solve the linear global problem on a global coarse mesh, and correct it locally by non-linear solvers on a fine mesh over the patch  $\Lambda$ .





## Chapter 2

# Numerical zoom for elliptic problems on perturbed domains

---

## 2.1 Presentation of the problem and adaptation of the numerical zoom algorithm

Let  $\Omega$  be a bounded domain in  $\mathbb{R}^d$  ( $d = 2$  or  $3$ ) and  $\omega_\varepsilon \subset \Omega$  be a sub-domain of characteristic size  $\varepsilon$  much smaller than the characteristic size of  $\Omega$ , cf. Fig. 2.1 top. We are interested in problems posed on the perturbed domain  $\Omega_\varepsilon = \Omega \setminus \omega_\varepsilon$ . As a typical simple example, we consider specifically the Poisson problem on  $\Omega_\varepsilon$  with Neumann boundary conditions on the boundary of the hole  $\omega_\varepsilon$ : find  $u : \Omega_\varepsilon \rightarrow \mathbb{R}$  such that

$$\begin{aligned} -\Delta u &= f && \text{in } \Omega_\varepsilon, \\ u &= 0 && \text{on } \partial\Omega, \\ \nabla u \cdot n &= 0 && \text{on } \partial\omega_\varepsilon, \end{aligned} \tag{2.1}$$

where  $f \in L^2(\Omega_\varepsilon)$  is a given function. The weak formulation for (2.1) is written as: let

$$V = \{v \in H^1(\Omega_\varepsilon) : v|_{\partial\Omega} = 0\}$$

and find  $u \in V$  such that

$$a(u, v) = \int_{\Omega_\varepsilon} f v, \quad \forall v \in V \tag{2.2}$$

where

$$a(u, v) = \int_{\Omega_\varepsilon} \nabla u \cdot \nabla v. \tag{2.3}$$

We want to devise a finite element method that works on a relatively coarse mesh on  $\Omega$  (the whole non-perforated domain), certainly too coarse

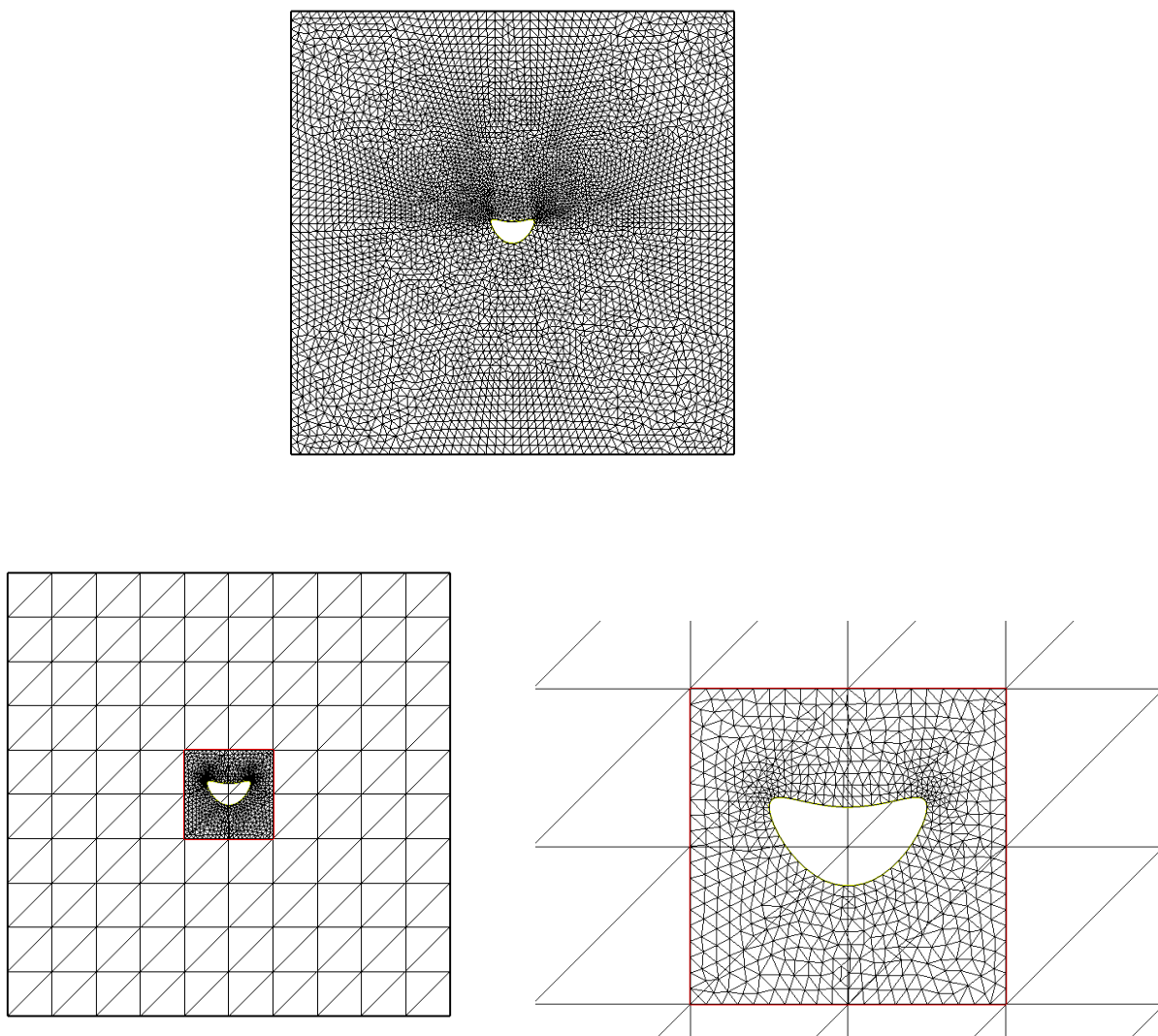


FIGURE 2.1: An example of the perforated domain  $\Omega_\varepsilon = \Omega \setminus \omega_\varepsilon$ . Top:  $\Omega_\varepsilon$  with a fine mesh well resolving  $\omega_\varepsilon$ . Bottom left: The global coarse mesh  $\mathcal{T}_H$  that does not see  $\omega_\varepsilon$  and the fine mesh  $\mathcal{T}_h$  on the patch. Bottom right: same as on the left, zoomed around.

to take into account the small inclusion  $\omega_\varepsilon$ , and then corrects the approximate solution iteratively using another sufficiently fine mesh around  $\omega_\varepsilon$ . We introduce thus the coarse global mesh  $\mathcal{T}_H$  of meshsize  $H$  on  $\Omega$ , with  $H$  typically bigger than  $\varepsilon$ . In addition, we encompass the hole  $\omega_\varepsilon$  into the patch  $\Lambda$ , which is a small sub-domain of  $\Omega$ :  $\omega_\varepsilon \subset \Lambda \subset \Omega$  (with both inclusions being proper). Denote  $\Lambda_\varepsilon = \Lambda \setminus \omega_\varepsilon$  and introduce the fine local mesh  $\mathcal{T}_h$  on  $\Lambda_\varepsilon$  (typically, the meshsize  $h$  is thus much smaller than  $\varepsilon$ ). For the sake of simplicity, both domains  $\Omega$  and  $\Lambda_\varepsilon$  are supposed polygonal and  $\Lambda$  is supposed to lie inside  $\Omega$ , i.e. the boundaries of  $\Lambda$  and  $\Omega$  do not intersect each other. Both meshes  $\mathcal{T}_h$  and  $\mathcal{T}_H$  are supposed regular simplicial triangulations of  $\Omega$  and  $\Lambda_\varepsilon$  respectively, i.e. the maximal aspect ratio of the triangles/tetrahedrons in both these meshes is fixed once for all. An illustration of the meshes is given at Fig. 2.1 bottom.

Introduce the finite element spaces

$$V_H = \{v_H \in C^0(\Omega) : v_H|_T \in P_k \forall T \in \mathcal{T}_H, v_H|_{\partial\Omega} = 0\}$$

and

$$V_h = \{v_h \in C^0(\Lambda_\varepsilon) : v_h|_T \in P_k \forall T \in \mathcal{T}_h\}.$$

where  $P_k$  is the set of polynomials in  $d$  real variables of a given degree  $k \geq 1$ . Let  $\Gamma = \partial\Lambda$ . Note that the boundary of  $\Lambda_\varepsilon$  contains two components:  $\Gamma$  and  $\partial\omega_\varepsilon$ . We shall need a finite element space on  $\Gamma$  to be used for Lagrange multipliers and defined as the space of traces of functions in  $V_h$ :

$$M_h = \{\mu_h \in C^0(\Gamma) : \mu_h|_E \in P_k \text{ on every boundary facet } E \text{ of mesh } \mathcal{T}_h\} \quad (2.4)$$

Our basic algorithm (Algorithm 2.1), inspired by (1.11)–(1.8)–(1.9), is presented on page 16. It starts from an initial coarse approximation  $u_H^0 \in V_H$ , typically the solution to the “unperturbed” problem on the whole domain  $\Omega$  on the coarse mesh without taking into account the hole:

$$\int_{\Omega} \nabla u_H^0 \cdot \nabla v_H = \int_{\Omega} f v_H, \quad \forall v_H \in V_H \quad (2.5)$$

In writing this, we assume  $f \in L^2(\Omega)$  i.e. the right hand side is extended inside the hole  $\omega_\varepsilon$ . The algorithm goes on by correcting this approximation and alternates between the fine problems on  $\Lambda_\varepsilon$  and the coarse problems on the whole  $\Omega$ . Note that the rigidity matrix of these coarse problems is the same as for the original “unperturbed” approximation (2.5).

We note that articles on the original patch algorithm [21, 22, 25] distinguished between the two cases – nested and not nested meshes, and the inherent difficulties were not necessarily the same in the two cases. By the nested meshes, it is understood that every element of the fine mesh  $\mathcal{T}_h$  is included in an element of  $\mathcal{T}_H$ , i.e.  $\mathcal{T}_h$  was formed by splitting the elements of the coarse mesh  $\mathcal{T}_H$  inside the patch  $\Lambda$  in the smaller elements. Obviously, such a notion is not applicable to the case studied here: the coarse mesh is not

Choose an initial guess  $u_H^0 \in V_H$  and the relaxation parameter  $\omega \in (0, 1]$

**for**  $n = 1, 2, 3, \dots$  **do**

Find  $u_h^n \in V_h$  and  $\lambda_h^n \in M_h$  such that

$$\int_{\Lambda_\varepsilon} \nabla u_h^n \cdot \nabla v_h - \int_{\Gamma} \lambda_h^n v_h = \int_{\Lambda_\varepsilon} f v_h, \quad \forall v_h \in V_h$$

$$\int_{\Gamma} u_h^n \mu_h = \int_{\Gamma} u_H^{n-1} \mu_h, \quad \forall \mu_h \in M_h$$

Find  $u_H^n \in V_H$  such that

$$\int_{\Omega} \nabla u_H^n \cdot \nabla v_H = \omega \int_{\Omega \setminus \bar{\Lambda}} f v_H - \omega \int_{\Gamma} \lambda_h^n v_H + \omega \int_{\Lambda} \nabla u_H^{n-1} \cdot \nabla v_H$$

$$+ (1 - \omega) \int_{\Omega} \nabla u_H^{n-1} \cdot \nabla v_H, \quad \forall v_H \in V_H$$

Set

$$u_{Hh}^{n-1/2} = \begin{cases} u_h^n, & \text{in } \Lambda_\varepsilon \\ u_H^{n-1}, & \text{outside } \Lambda \end{cases} \quad u_{Hh}^n = \begin{cases} u_h^n, & \text{in } \Lambda_\varepsilon \\ u_H^n, & \text{outside } \Lambda \end{cases}$$

**end**

**Algorithm 2.1:** Multi-model numerical zoom

conforming with the geometrical features of the small inclusion  $\Omega_\varepsilon$  so that  $\mathcal{T}_h$  which is conforming with  $\Omega_\varepsilon$  cannot be a submesh of  $\mathcal{T}_H$ . We introduce thus the weaker notion of  $\Gamma$ -nested meshes meaning that the boundary  $\Gamma$  of the patch  $\Lambda$  is composed of facets of  $\mathcal{T}_H$  (and thus the patch is formed as a union of certain elements of  $\mathcal{T}_H$ ) and the trace of  $\mathcal{T}_h$  on  $\Gamma$  is obtained by dividing the facets of the coarse mesh into smaller segments/triangles.

In the following section, we analyse the numerical zoom algorithm in the case of  $\Gamma$ -nested meshes. We shall see that this analysis is much easier than in the general case (cf. the subsequent sections). Note that the method is also easier to implement in the  $\Gamma$ -nested case. Indeed, the integrals on  $\Lambda$  in the coarse correction step are then straight-forward to implement since they can be written as the sums of integrals over certain elements of  $\mathcal{T}_H$  unlike the general case where the elements of  $\mathcal{T}_H$  can be arbitrarily cut by  $\Gamma$ . The interpolation operator between  $\mathcal{T}_H$  and  $\mathcal{T}_h$  are also trivial in this case. This is why we think that the case  $\Gamma$ -nested meshes is the most useful one in practice (unless very particular situations where the form of the patch should be fixed by some implementation issues and thus not necessarily conforming with the coarse mesh). Note that the restriction of  $\Gamma$ -nestedness is general enough to allow for an adaptive mesh adaptation of  $\mathcal{T}_h$ , independently from the coarse mesh.

## 2.2 Analysis of the algorithm for $\Gamma$ -nested meshes

As announced above, we assume in this section that the meshes  $\mathcal{T}_H$  and  $\mathcal{T}_h$  are nested on the interface  $\Gamma$ . For future references, we formalize this notion as the following definition

**Definition 2.1.** *The meshes  $\mathcal{T}_h$  and  $\mathcal{T}_H$  are called  $\Gamma$ -nested if the patch  $\Lambda$  is a union of several elements of  $\mathcal{T}_H$  and every boundary facet of the mesh  $\mathcal{T}_h$  lying on  $\Gamma$  is a subset of an internal facet of  $\mathcal{T}_H$ .*

### 2.2.1 The finite element problem: an a priori error estimate

Assume for the moment that Algorithm 2.1 converges (this will be indeed proved in the next subsection). The natural questions are then: how can one characterize the limit of the iterative process in Algorithm 2.1 and what is the precision of this limit with respect to the exact solution of problem (2.1)? Let us suppose thus that  $u_H^n \rightarrow u_H$  on  $\Omega$ ,  $u_h^n \rightarrow u_h$  on  $\Lambda_\varepsilon$ , and  $\lambda_h^n \rightarrow \lambda_h$  on  $\Gamma$  as  $n \rightarrow \infty$ . Passing to the limit in Algorithm 2.1, it is easy to see that the functions  $u_H \in V_H$ ,  $u_h \in V_h$  and  $\lambda_h \in M_h$  satisfy

$$\int_{\Omega \setminus \bar{\Lambda}} \nabla u_H \cdot \nabla v_H + \int_{\Gamma} \lambda_h v_H = \int_{\Omega \setminus \bar{\Lambda}} f v_H, \quad \forall v_H \in V_H \quad (2.6)$$

$$\int_{\Lambda_\varepsilon} \nabla u_h \cdot \nabla v_h - \int_{\Gamma} \lambda_h v_h = \int_{\Lambda_\varepsilon} f v_h, \quad \forall v_h \in V_h \quad (2.7)$$

$$\int_{\Gamma} \mu_h (u_H - u_h) = 0, \quad \forall \mu_h \in M_h. \quad (2.8)$$

We emphasize that  $u_H^n$  survives at the limit  $n \rightarrow \infty$  only outside  $\Lambda$ .

Let us introduce the combined approximation space

$$V_{Hh} = \{v \in C(\bar{\Omega}_\varepsilon) \text{ such that } v = 0 \text{ on } \partial\Omega, v = v_H \text{ on } \Omega \setminus \bar{\Lambda}, v = v_h \text{ on } \Lambda_\varepsilon \\ \text{with some } v_H \in V_H, v_h \in V_h\}$$

and gather  $u_H$  and  $u_h$  into  $u_{Hh} \in V_{Hh}$  such that  $u_{Hh} = u_H$  on  $\Omega \setminus \bar{\Lambda}$  and  $u_{Hh} = u_h$  on  $\Lambda_\varepsilon$ . Note that  $u_{Hh}$  is indeed continuous on  $\Gamma$  thanks to (2.8) which is equivalent to say  $u_H = u_h$  on  $\Gamma$  in the case of  $\Gamma$ -nested meshes. Taking the sum of (2.6) and (2.7) we can easily eliminate  $\lambda_h$  and rewrite this problem in terms of  $u_{Hh}$  alone: find  $u_{Hh} \in V_{Hh}$  such that

$$a(u_{Hh}, v_{Hh}) = \int_{\Omega} f v_{Hh}, \quad \forall v_{Hh} \in V_{Hh}. \quad (2.9)$$

**Theorem 2.1.** *Suppose that the meshes  $\mathcal{T}_h$  and  $\mathcal{T}_H$  are  $\Gamma$ -nested, cf. Definition 2.1. Problem (2.9) admits the unique solution  $u_{Hh} \in V_{Hh}$ . If  $u$ , the exact solution to (2.1), is in  $H^{k+1}(\Omega)$ , we have moreover the following a priori error estimate*

$$\|u_{Hh} - u\|_{1, \Omega_\varepsilon} \leq C (H^k |u|_{k+1, \Omega \setminus \bar{\Lambda}} + h^k |u|_{k+1, \Lambda_\varepsilon}) \quad (2.10)$$

with a constant  $C$  independent of  $H$ ,  $h$  and  $u$ .

*Proof.* The bilinear form  $a$  is coercive on  $V_{Hh} \subset V$  which yields immediately the existence and uniqueness of the solution  $u_{Hh} \in V_{Hh}$  to (2.9). We construct now an appropriate interpolant  $\tilde{u}_{Hh} \in V_{Hh}$  to  $u$ . Let

$$I_H : H^{k+1}(\Omega) \rightarrow V_H \text{ and } I_h : H^{k+1}(\Lambda_\varepsilon) \rightarrow V_h$$

be the standard nodal interpolation operators satisfying

$$|v - I_H v|_{1,T} \leq CH^k |v|_{k+1,T} \text{ for any } v \in H^{k+1}(T), T \in \mathcal{T}_H \quad (2.11)$$

and

$$|v - I_h v|_{1,T} \leq Ch^k |v|_{k+1,T} \text{ for any } v \in H^{k+1}(T), T \in \mathcal{T}_h. \quad (2.12)$$

The constant  $C$  here depends only on the regularity of the meshes.

We note that we cannot define interpolant  $\tilde{u}_{Hh} \in V_{Hh}$  simply by taking  $I_h u$  inside  $\Lambda$  and  $I_H u$  outside  $\Lambda$  since such a function would be discontinuous over  $\Gamma$ . We should thus correct  $I_h u$  inside  $\Lambda$  to restore continuity by adding a finite element function in  $V_h$  equal to  $I_H u - I_h u$  on  $\Gamma$ . Thanks to the trace theorem, there exists

$$r \in H^1(\Lambda) \text{ such that } r = I_H u - I_h u \text{ on } \Gamma \text{ and } \|r\|_{1,\Lambda} \leq C \|r\|_{\frac{1}{2},\Gamma}$$

with a constant  $C > 0$  depending only on  $\Lambda$ . Let  $r_h \in V_h$  be the Scott-Zhang interpolant of  $r$  [37] such that that  $r_h = r$  on  $\Gamma$ . Such a choice is possible if the values of  $r_h$  at the boundary facets of  $\mathcal{T}_h$  on  $\Gamma$  are calculated through the appropriate weighted averages of  $r$  on these facets (recall that the construction of Scott-Zhang allows one to choose either elements or facets of the mesh to construct the interpolant). Since  $r = I_H u - I_h u$  is piecewise polynomial on  $\Gamma$ , such a construction ensures indeed that  $r_h = r$  on  $\Gamma$ . We have moreover

$$\|r_h\|_{1,\Lambda_\varepsilon} \leq C \|r\|_{1,\Lambda_\varepsilon} \leq C \|r\|_{1,\Lambda} \leq C \|r\|_{\frac{1}{2},\Gamma}$$

Combining these estimates and using again the trace theorem we can write

$$\begin{aligned} \|r_h\|_{1,\Lambda_\varepsilon} \leq C \|I_H u - I_h u\|_{\frac{1}{2},\Gamma} &\leq C (\|I_H u - u\|_{\frac{1}{2},\Gamma} + \|I_h u - u\|_{\frac{1}{2},\Gamma}) \\ &\leq C (\|u - I_H u\|_{1,\Omega \setminus \bar{\Lambda}} + \|u - I_h u\|_{1,\Lambda_\varepsilon}) \end{aligned}$$

We now take  $\tilde{u}_{Hh} \in V_{Hh}$  with the components  $\tilde{u}_H \in V_H$  and  $\tilde{u}_h \in V_h$  such that  $\tilde{u}_H = I_H u$  and  $\tilde{u}_h = I_h u + r_h$ . We have thanks to the interpolation estimates mentioned above

$$\begin{aligned} \|u - \tilde{u}_{Hh}\|_{1,\Omega_\varepsilon} &\leq \|u - I_H u\|_{1,\Omega \setminus \bar{\Lambda}} + \|u - I_h u\|_{1,\Lambda_\varepsilon} + \|r_h\|_{1,\Lambda_\varepsilon} \quad (2.13) \\ &\leq C (\|u - I_H u\|_{1,\Omega \setminus \bar{\Lambda}} + \|u - I_h u\|_{1,\Lambda_\varepsilon}) \\ &\leq C (H^k |u|_{k+1,\Omega \setminus \bar{\Lambda}} + h^k |u|_{k+1,\Lambda_\varepsilon}) \end{aligned}$$

In view of (2.9), (2.2) and the fact that  $V_{Hh} \subset V$ , the C ea lemma ensures that  $\|u_{Hh} - u\|_{1,\Omega} \leq C\|\tilde{u}_{Hh} - u\|_{1,\Omega}$  so that (2.13) leads to (2.10).  $\square$

### 2.2.2 Convergence of the iterative algorithm

The proof of the convergence of Algorithm 2.1 will be based on a study of operator  $A_{Hh} : V_H \rightarrow V_H$  defined for fixed  $\mathcal{T}_H$  and  $\mathcal{T}_h$  as follows: for any  $z_H \in V_H$  the function  $A_{Hh}z_H \in V_H$  solves

$$c(A_{Hh}z_H, v_H) = \int_{\Omega \setminus \bar{\Lambda}} \nabla z_H \cdot \nabla v_H + \int_{\Gamma} \nu_h v_H, \quad \forall v_H \in V_H \quad (2.14)$$

where  $c(\cdot, \cdot)$  is the  $H_0^1$  scalar product on  $\Omega$

$$c(u, v) = \int_{\Omega} \nabla u \cdot \nabla v \quad (2.15)$$

and  $\nu_h \in M_h$  together with  $z_h \in V_h$  come as the solution to

$$\int_{\Lambda_\varepsilon} \nabla z_h \cdot \nabla v_h - \int_{\Gamma} \nu_h v_h = 0, \quad \forall v_h \in V_h \quad (2.16)$$

$$\int_{\Gamma} z_h \mu_h = \int_{\Gamma} z_H \mu_h, \quad \forall \mu_h \in M_h. \quad (2.17)$$

To motivate the definition of operator  $A_{Hh}$ , we decompose the iterates  $u_h^n, \lambda_h^n$  from Algorithm 2.1 as

$$u_h^n = y_h + z_h^n, \quad \lambda_h^n = \varphi_h + \nu_h^n$$

where  $(y_h, \varphi_h) \in V_h \times M_h$  is solution to

$$\int_{\Lambda_\varepsilon} \nabla y_h \cdot \nabla v_h - \int_{\Gamma} \varphi_h v_h = \int_{\Lambda_\varepsilon} f v_h, \quad \forall v_h \in V_h \quad (2.18)$$

$$\int_{\Gamma} y_h \mu_h = 0, \quad \forall \mu_h \in M_h$$

and  $(z_h^n, \nu_h^n) \in V_h \times M_h$  solve

$$\int_{\Lambda_\varepsilon} \nabla z_h^n \cdot \nabla v_h - \int_{\Gamma} \nu_h^n v_h = 0, \quad \forall v_h \in V_h$$

$$\int_{\Gamma} z_h^n \mu_h = \int_{\Gamma} u_H^{n-1} \mu_h, \quad \forall \mu_h \in M_h.$$



These are the same equations as (2.16)–(2.17) with  $z_H$  replaced by  $u_H^{n-1}$ . Using these notations, we can rewrite the problem for  $u_H^n$  from Algorithm 2.1 as

$$\begin{aligned} c(u_H^n, v_H) &= c(u_H^{n-1}, v_H) \\ &\quad + \omega \int_{\Omega \setminus \bar{\Lambda}} f v_H - \omega \int_{\Gamma} \varphi_h v_H - \omega \int_{\Gamma} \nu_h^n v_H - \omega \int_{\Omega \setminus \bar{\Lambda}} \nabla u_H^{n-1} \cdot \nabla v_H \\ &= c(u_H^{n-1}, v_H) \\ &\quad + \omega c(F_H, v_H) - \omega \int_{\Gamma} \nu_h^n v_H - \omega \int_{\Omega \setminus \bar{\Lambda}} \nabla u_H^{n-1} \cdot \nabla v_H, \quad \forall v_H \in V_H \end{aligned}$$

where  $F_H \in V_H$  is given by

$$c(F_H, v_H) = \int_{\Omega \setminus \bar{\Lambda}} f v_H - \int_{\Gamma} \varphi_h v_H, \quad \forall v_H \in V_H. \quad (2.19)$$

We see that  $u_H^n$  evolves from one iteration to another as

$$u_H^n = (I - \omega A_{Hh})u_H^{n-1} + \omega F_H. \quad (2.20)$$

It is thus a fixed point algorithm to solve the equation

$$A_{Hh}u_H = F_H \quad (2.21)$$

rewritten as  $u_H = (I - \omega A_{Hh})u_H + \omega F_H$ .

Combining (2.14) and (2.16) we observe  $\forall z_H, v_H \in V_H$

$$c(A_{Hh}z_H, v_H) = \int_{\Omega \setminus \bar{\Lambda}} \nabla z_H \cdot \nabla v_H + \int_{\Lambda_\varepsilon} \nabla z_h \cdot \nabla v_h \quad (2.22)$$

where  $z_h \in V_h$  is the solution to (2.16)–(2.17) and  $v_h$  is any function in  $V_h$  such that  $v_h = v_H$  on  $\Gamma$ . We shall now prove that operator  $A_{Hh}$  is a self-adjoint and coercive with respect to the scalar product  $c$  on a well-chosen subspace of  $V_H$ .

**Lemma 2.2.** *Operator  $A_{Hh}$  is self-adjoint with respect to the scalar product  $c$ , as defined by (2.15):*

$$c(A_{Hh}z_H, z_H^*) = c(z_H, A_{Hh}z_H^*), \quad \forall z_H, z_H^* \in V_H \quad (2.23)$$

*Proof.* Take any  $z_H, z_H^* \in V_H$  and let  $(z_h, \nu_h) \in V_h \times M_h$ , resp.  $(z_h^*, \nu_h^*) \in V_h \times M_h$  be the solutions to (2.16)–(2.17) with  $z_H$ , resp.  $z_H^*$ , in the right hand side of (2.17). By (2.22)

$$c(A_{Hh}z_H, z_H^*) = \int_{\Omega \setminus \bar{\Lambda}} \nabla z_H \cdot \nabla z_H^* + \int_{\Lambda_\varepsilon} \nabla z_h \cdot \nabla z_h^*$$

which entails (2.23). □

We now decompose the finite element space  $V_H$  into the direct sum  $V_H^0 \oplus V_H^1$  where

$$V_H^0 = \{v \in V_H : \text{supp } v \subset \Lambda_\varepsilon\} \quad (2.24)$$

and  $V_H^1$  is the orthogonal complement of  $V_H^0$  with respect to the scalar product (2.15).

**Lemma 2.3.** *The kernel of operator  $A_{Hh}$  coincides with  $V_H^0$  and  $A_{Hh}$  is coercive on its orthogonal complement  $V_H^1$ . More precisely, there exists  $m > 0$  depending only on  $\Lambda_\varepsilon$  and on the regularity of the mesh  $\mathcal{T}_H$  such that*

$$c(A_{Hh}z_H, z_H) \geq m|z_H|_{1,\Omega}^2 \quad \forall z_H \in V_H^1. \quad (2.25)$$

The norm of  $A_{Hh}$  as an operator in the space  $V_H$  equipped with semi-norm of  $H^1(\Omega)$  is bounded by a mesh-independent constant  $M > 0$ .

*Proof.* If  $z_H \in \ker A_{Hh}$ , then  $z_H = 0$  on  $\Omega \setminus \bar{\Lambda}$  as follows from the expression for  $c(A_{Hh}z_H, z_H)$  in (2.22). On the other hand, if  $z_H \in V_H^0$  then  $z_h = 0$  on  $\Lambda_\varepsilon$  and  $z_H = 0$  on  $\Gamma$  so that  $A_{Hh}z_H = 0$ . This entails  $\ker A_{Hh} = V_H^0$ .

In order to prove the coercivity estimate we invoke again (2.22) with  $v_H = z_H \in V_H^1$ , which implies

$$c(A_{Hh}z_H, z_H) \geq \int_{\Omega \setminus \bar{\Lambda}} \nabla z_H \cdot \nabla z_H. \quad (2.26)$$

Let  $v \in H_0^1(\Omega)$  be such that  $v = z_H$  on  $\Omega \setminus \bar{\Lambda}$  and  $v|_\Lambda$  satisfy

$$-\Delta v = 0 \text{ on } \Lambda, \quad v = z_H \text{ on } \Gamma. \quad (2.27)$$

so that

$$\|v\|_{1,\Lambda} \leq C\|z_H\|_{\frac{1}{2},\Gamma}.$$

Let  $R_H : V \rightarrow V_H$  be a Scott-Zhang interpolation operator, cf. [37], chosen so that  $R_H v$  on  $\Omega \setminus \bar{\Lambda}$  (resp. on  $\bar{\Lambda}$ ) is calculated by appropriate averaging of  $v$  on the mesh elements lying in  $\bar{\Omega} \setminus \Lambda$  (resp.  $\bar{\Lambda}$ ). Denoting  $v_H = R_H v$  we observe

$$\|v_H\|_{1,\Lambda} \leq C\|v\|_{1,\Lambda}$$

and, moreover,  $v_H = z_H$  on  $\Omega \setminus \bar{\Lambda}$  since  $v_H = z_H$  on  $\Omega \setminus \bar{\Lambda}$  is already in the finite element space  $V_H$  restricted to  $\Omega \setminus \bar{\Lambda}$ . Hence,  $(v_H - z_H) \in V_H^0$  so that  $c(z_H, v_H - z_H) = 0$  (recall that  $z_H \in V_H^1$ ), which entails by Cauchy-Schwarz inequality

$$|z_H|_{1,\Omega}^2 = c(z_H, z_H) = c(z_H, v_H) \leq |z_H|_{1,\Omega} |v_H|_{1,\Omega}$$

In view of the properties of the interpolation operator mentioned above, we have thus

$$\begin{aligned} |z_H|_{1,\Omega}^2 &\leq |v_H|_{1,\Omega}^2 \leq (C\|v\|_{1,\Lambda}^2 + |z_H|_{1,\Omega \setminus \bar{\Lambda}}^2) \\ &\leq (C\|z_H\|_{\frac{1}{2},\Gamma}^2 + |z_H|_{1,\Omega \setminus \bar{\Lambda}}^2) \leq C|z_H|_{1,\Omega \setminus \bar{\Lambda}}^2 \end{aligned} \quad (2.28)$$

Combining (2.26) with (2.28), we obtain  $c(A_{Hh}z_H, z_H) \geq \frac{1}{C}|z_H|_{1,\Omega}^2$  so that (2.25) is established.

The last statement of the Lemma concerns the norm of operator  $A_{Hh}$ . In order to prove it, we recall problem (2.16), reintroduce  $v \in H^1(\Lambda)$  as the solution to (2.27), and construct  $v_h \in V_h$  as a Scott-Zhang interpolation of  $v$  being a projection on the finite element trace space on  $\Gamma$ . We have thus  $v_h = z_H$  on  $\Gamma$  so that  $\int_{\Lambda_\varepsilon} \nabla z_h \cdot \nabla(z_h - v_h) = 0$  and

$$\|z_h\|_{1,\Lambda_\varepsilon} \leq \|v_h\|_{1,\Lambda_\varepsilon} \leq C\|v\|_{1,\Lambda} \leq C\|z_H\|_{\frac{1}{2},\Gamma} \leq C\|z_H\|_{1,\Omega \setminus \bar{\Lambda}}$$

with a constant that depends only on  $\Lambda$ . We have thus using (2.22) and taking an appropriate  $v_h \in V_h$  (constructed from  $v_H \in V_H$  in a similar manner to  $z_h, z_H$  above)

$$\begin{aligned} c(A_{Hh}z_H, v_H) &\leq C(|z_H|_{1,\Omega \setminus \bar{\Lambda}}|v_H|_{1,\Omega \setminus \bar{\Lambda}} + |z_h|_{1,\Lambda_\varepsilon}|v_h|_{1,\Lambda_\varepsilon}) \\ &\leq M|z_H|_{1,\Omega}|v_H|_{1,\Omega} \end{aligned}$$

where  $C$  and  $M$  denote the mesh-independent constants. Taking  $v_H = A_{Hh}z_H$  gives

$$|A_{Hh}z_H|_{1,\Omega} \leq M|z_H|_{1,\Omega}$$

i.e.  $\|A_{Hh}\| \leq M$  where  $\|\cdot\|$  means the operator norm in the space  $V_H$  equipped with the  $H^1(\Omega)$  semi-norm.  $\square$

**Theorem 2.4.** *Suppose that the meshes  $\mathcal{T}_h$  and  $\mathcal{T}_H$  are  $\Gamma$ -nested, cf. Definition 2.1. Algorithm 2.1 converges to the solution of (2.9) provided  $0 < \omega < \omega^*$  where  $\omega^*$  is a mesh-independent constant, i.e.  $u_{Hh}^{n-1/2} \rightarrow u_{Hh}$  and  $u_{Hh}^n \rightarrow u_{Hh}$  as  $n \rightarrow \infty$  where  $u_{Hh} \in V_{Hh}$  is the unique solution of (2.9). The convergence rate depends only on the regularity of  $\mathcal{T}_H$  and on  $\Lambda_\varepsilon$ .*

*Proof.* We decompose each iterate of Algorithm 2.1 as  $u_H^n = u_H^{n,0} + u_H^{n,1}$  with  $u_H^{n,0} \in V_H^0$  and  $u_H^{n,1} \in V_H^1$ . Using the facts that  $\ker A_{Hh} = V_H^0$  and  $F_H \in \text{Im } A_{Hh} = (\ker A_{Hh})^\perp = V_H^1$ , equation (2.20) can be decomposed in separate equations on  $V_H^0$  and  $V_H^1$ :

$$\begin{aligned} u_H^{n,0} &= u_H^{n-1,0} \\ u_H^{n,1} &= (I - \omega A_{Hh})u_H^{n-1,1} + \omega F_H \end{aligned}$$

As proved in the two preceding lemmas, the restriction of  $A_{Hh}$  to  $V_H^1$  is a symmetric and positive definite operator. Its spectrum is thus real and lies in the interval  $[m, M]$ ,  $m$  being a lower bound for the coercivity constant of  $A_{Hh}$  on  $V_H^1$  and  $M$  being an upper bound for its norm. It follows that the operator  $(I - \omega A_{Hh})$  is a contraction provided  $\omega < 2/M$ . This shows the convergence of the sequence  $\{u_H^{n,1}\}$ . The iterates  $u_h^n$  are uniquely determined by the traces of  $\{u_H^n\}$  on  $\Gamma$  which coincide with those of  $u_H^{n,1}$ . We see thus that the sequence  $\{u_h^n\}$  is also convergent, as are the sequences  $\{u_{Hh}^{n-1/2}\}$ ,  $\{u_{Hh}^n\}$  since  $u_{Hh}^n = u_H^{n,1}$  on  $\Omega \setminus \bar{\Lambda}$  and  $u_{Hh}^n = u_H^n$ ,  $u_{Hh}^{n-1/2} = u_H^{n-1}$  on  $\Lambda_\varepsilon$ .  $\square$

## 2.3 Analysis of Algorithm 2.1 on non $\Gamma$ -nested meshes

We want now to abandon the Assumption of  $\Gamma$ -nested meshes (Definition 2.1). We shall see that the *a priori* error analysis of the general case reveals potentially larger errors in the general case, although it is not usually seen in the numerical experiments. Moreover, the iterative algorithm 2.1 can suffer from slow convergence unless we are in a situation of a conforming interface, as announced in the definition below, or close to it, in an appropriate sense as will be seen in the convergence analysis below.

**Definition 2.2.** *We say that the meshes  $\mathcal{T}_h$  and  $\mathcal{T}_H$  have a conforming interface if the boundary of the zoom  $\Lambda$  is composed of the facets of  $\mathcal{T}_H$ .*

This is thus a generalization of Definition 2.1. Note that the issue of possibly slow convergence was already recognized in the literature on the original patches algorithm [20]. A possible remedy was proposed in [25] under the name of the method of harmonic patches. Only the triangulations with conforming interface were studied theoretically in [25]. In the current Section, contrary to this article, we do not assume the conforming interface and we keep our assumption on the meshes quite general, although we shall recognize that the case of a conforming interface is the most beneficial with respect to the rate of convergence.

### 2.3.1 The finite element problem: an a priori error estimate

Let us admit for the moment that Algorithm 2.1 converges (this will be indeed proved in the next section). Here, we are going to characterize the limit of the iterative process in Algorithm 2.1 and to examine the precision of this limit with respect to the exact solution of problem (2.1). We suppose thus that  $u_H^n \rightarrow u_H$ ,  $u_h^n \rightarrow u_h$  on  $\Omega$  and  $\lambda_h^n \rightarrow \lambda_h$  on  $\Gamma$  as  $n \rightarrow \infty$ . It is easy to see that the functions  $u_H \in V_H$ ,  $u_h \in V_h$  and  $\lambda_h \in M_h$  satisfy

$$\int_{\Omega \setminus \bar{\Lambda}} \nabla u_H \cdot \nabla v_H + \int_{\Gamma} \lambda_h v_H = \int_{\Omega \setminus \Lambda} f v_H, \quad \forall v_H \in V_H \quad (2.29)$$

$$\int_{\Lambda_\varepsilon} \nabla u_h \cdot \nabla v_h - \int_{\Gamma} \lambda_h v_h = \int_{\Lambda_\varepsilon} f v_h, \quad \forall v_h \in V_h \quad (2.30)$$

$$\int_{\Gamma} \mu_h (u_H - u_h) = 0, \quad \forall \mu_h \in M_h. \quad (2.31)$$

These are of course the same as Equations (2.6)–(2.8) but we prefer to write them once more to emphasize the difference with the previously studied case of  $\Gamma$ -nested meshes: we no longer have  $u_h = u_H$  on  $\Gamma$  and it is no longer possible to exclude the Lagrange multiplier simply as before.

To compress the notations, we introduce the combined approximation space

$$V_{Hh}^d = \{v : \Omega \rightarrow \mathbb{R} \text{ such that } v = v_H \text{ on } \Omega \setminus \bar{\Lambda}, v = v_h \text{ on } \Lambda_\varepsilon \quad (2.32)$$

with some  $v_H \in V_H, v_h \in V_h\}$

and gather  $u_H$  and  $u_h$  into  $u_{Hh} \in V_{Hh}^d$  such that  $u_{Hh} = u_H$  on  $\Omega \setminus \bar{\Lambda}$  and  $u_{Hh} = u_h$  on  $\Lambda_\varepsilon$ . The problem (2.29)–(2.31) can be rewritten in terms of  $u_{Hh}$  and  $\lambda_h$  as

$$\begin{aligned} a(u_{Hh}, v) + b(v, \lambda_h) &= L(v), \quad \forall v \in V_{Hh}^d \\ b(u_{Hh}, \mu) &= 0, \quad \forall \mu \in M_h \end{aligned} \quad (2.33)$$

where

$$a(u, v) = \int_{\Omega \setminus \bar{\Lambda}} \nabla u \cdot \nabla v + \int_{\Lambda_\varepsilon} \nabla u \cdot \nabla v \quad (2.34)$$

$$b(v, \mu) = \int_{\Gamma} [v] \mu \quad (2.35)$$

$$L(v) = \int_{\Omega} f v \quad (2.36)$$

and  $[v] = v|_{\Omega \setminus \bar{\Lambda}} - v|_{\Lambda}$  denotes the jump of  $v$  on the interface  $\Gamma$ . Note that no continuity on  $\Gamma$  of functions in  $V_{Hh}^d$  is imposed, unlike the  $\Gamma$ -nested case. The approximate continuity of  $u_{Hh}$  is now ensured by the finite element problem, i.e. the second equation in (2.33). Our a priori error estimates will be derived directly from the mixed problem (2.33) without trying to eliminate the Lagrange multiplier  $\lambda_h$  from the equations (cf. however Remark 2.1 with an alternative route of the proof using a subspace of weakly continuous functions). We shall face the problem of the lack of regularity of  $\nabla u \cdot n$  at the corners (edges) of  $\Lambda$ , which will prevent us from giving completely satisfactory theoretical error estimates, cf. the forthcoming Lemma 2.8.

We start by rewriting the continuous problem (2.1) for  $u$  in the mixed form similar to (2.33). To this end, we introduce the functional space

$$V^d = \{v : \Omega_\varepsilon \rightarrow \mathbb{R} \text{ such that } v|_{\Lambda_\varepsilon} \in H^1(\Lambda_\varepsilon), v|_{\Omega \setminus \bar{\Lambda}} \in H^1(\Omega \setminus \bar{\Lambda}) \text{ and } v|_{\partial\Omega} = 0\}$$

equipped with the norm

$$\|v\|_V = \left( \|v\|_{1, \Omega \setminus \bar{\Lambda}}^2 + \|v\|_{1, \Lambda_\varepsilon}^2 \right)^{1/2}.$$

We also set  $M = H^{-1/2}(\Gamma)$ . Obviously,  $u \in H_0^1(\Omega) \subset V^d$  so that problem (2.1) can be rewritten as: find  $u \in V^d$  and  $\lambda \in M$  (the Lagrange multiplier

corresponding to the constraint  $[u] = 0$  on  $\Gamma$ ) such that

$$\begin{aligned} a(u, v) + b(v, \lambda) &= L(v) \quad \forall v \in V \\ b(u, \mu) &= 0 \quad \forall \mu \in M \end{aligned} \quad (2.37)$$

This problem is well-posed. Indeed, if  $(u, \lambda) \in V \times M$  is a solution to (2.37), then the second equation in (2.37) implies that  $u \in H_0^1(\Omega)$  and restricting the test functions in the first equation to  $H_0^1(\Omega)$  shows that  $u$  is in fact the unique solution to (2.1). An integration by parts allows us to identify then  $\lambda \in M$  with  $(\nabla u \cdot n)|_\Gamma$  where  $n$  is the unit normal vector on  $\Gamma$  looking outwards from  $\Lambda$ .

We can now prove an error estimate for problem (2.33) as an approximation to problem (2.37) using the theory of approximations to mixed problems [12]. The main ingredients to this proof are the two lemmas below proving the coerciveness of the form  $a$  on the kernel of the operator associated to the form  $b$  on both continuous and finite element levels, as well as the inf-sup property for  $b$ . We follow essentially [13] where the analogous results are proven in a slightly different context.

Let  $\mathcal{B} : V \rightarrow M' = H^{1/2}(\Gamma)$  be the operator associated to the bilinear form  $b$  by

$$\langle \mathcal{B}v, \mu \rangle_{M', M} = b(v, \mu) \quad \forall v \in V, \mu \in M$$

and let  $\mathcal{B}_{Hh} : V_{Hh}^d \rightarrow M'_h$  be its discrete counterpart defined by

$$\langle \mathcal{B}_{Hh}v_{Hh}, \mu_h \rangle_{M', M} = b(v_{Hh}, \mu_h) \quad \forall v_{Hh} \in V_{Hh}^d, \mu_h \in M_h.$$

**Lemma 2.5.** *The bilinear form  $a$  is coercive on  $\ker \mathcal{B} \cup \ker \mathcal{B}_{Hh}$ , i.e. there is a constant  $\gamma_0 > 0$  independent of  $H, h$  such that*

$$a(v, v) \geq \gamma_0 \|v\|_V^2 \quad \forall v \in \ker \mathcal{B} \cup \ker \mathcal{B}_{Hh} \quad (2.38)$$

*Proof.* Consider the following subspace of  $V$

$$V_0 = \{v \in V^d : \int_\Gamma [v] = 0\}.$$

Inequality (2.38) is satisfied for all  $v \in V_0$  with some constant  $\gamma_0$  that depends only on  $\Omega, \Lambda$  and the coefficients  $K$ . This follows from the Peetre-Tartar lemma [39], since the inclusion of  $V$  into  $L^2(\Omega)$  is compact and

$$a(v, v) = 0 \text{ and } \int_\Gamma [v] = 0 \implies v = 0.$$

Indeed, if  $a(v, v) = 0$  for some  $v \in V$ , then  $\nabla v = 0$  on  $\Lambda$  and on  $\Omega \setminus \bar{\Lambda}$  so that  $v = c = \text{const}$  on  $\Lambda$  and  $v = 0$  on  $\Omega \setminus \bar{\Lambda}$  since moreover  $v|_{\partial\Omega} = 0$ . If we also suppose that  $\int_\Gamma [v] = 0$  then  $c = 0$  so that  $v = 0$  on  $\Omega$ .

It is easy to see that  $\mathcal{B}v = [v]_\Gamma$  and consequently  $\ker \mathcal{B} = H_0^1(\Omega) \subset V_0$ . On the discrete level, we observe that  $\ker \mathcal{B}_{Hh} = \{v \in V_{Hh}^d : \int_\Gamma [v]\mu = 0, \forall \mu \in$

$M_h\} \subset V_0$  since  $1 \in M_h$ . Thus  $\ker \mathcal{B} \cup \ker \mathcal{B}_{Hh} \subset V_0$ , consequently (2.38) is satisfied for all  $v \in \ker \mathcal{B} \cup \ker \mathcal{B}_{Hh}$ .  $\square$

**Lemma 2.6.** *There exists  $\delta > 0$  depending only on  $\Omega$  and  $\Lambda$  such that*

$$\inf_{\lambda \in M} \sup_{v \in V^d} \frac{b(v, \lambda)}{\|v\|_V \|\lambda\|_M} \geq \delta \quad (2.39)$$

and

$$\inf_{\lambda_h \in M_h} \sup_{v_{Hh} \in V_{Hh}^d} \frac{b(v_{Hh}, \lambda_h)}{\|v_{Hh}\|_V \|\lambda_h\|_M} \geq \delta. \quad (2.40)$$

*Proof.* The continuous inf-sup property (2.39) follows from the following inequalities, valid for any  $\lambda \in M$

$$\begin{aligned} \|\lambda\|_M &= \|\lambda\|_{-1/2, \Gamma} = \sup_{\mu \in H^{1/2}(\Gamma)} \frac{\int_{\Gamma} \lambda \mu}{\|\mu\|_{1/2, \Gamma}} \\ &\leq C \sup_{w \in H^1(\Lambda_\varepsilon)} \frac{\int_{\Gamma} \lambda w}{\|w\|_{1, \Lambda_\varepsilon}} \\ &\quad (\text{since } \forall \mu \in H^{1/2}(\Gamma), \exists w \in H^1(\Lambda_\varepsilon) \text{ such that } w = \mu \text{ on } \partial\Lambda_\varepsilon \text{ and } \|w\|_{1, \Lambda_\varepsilon} \leq C \|\mu\|_{1/2, \Gamma} \\ &\quad \text{with a constant } C \text{ that depends only on } \Lambda_\varepsilon) \\ &\leq C \sup_{v \in V^d} \frac{b(v, \lambda)}{\|v\|_V} \\ &\quad (\text{since one can always take } v \in V^d \text{ as } v = -w \text{ on } \Lambda_\varepsilon \text{ and } v = 0 \text{ on } \Omega \setminus \bar{\Lambda}_\varepsilon) \end{aligned}$$

To reproduce this proof on the discrete level, we borrow from [6] the following result: for all  $\lambda_h \in M_h$  there exists  $v_h \in V_h$  such that

$$\frac{\int_{\Gamma} v_h \lambda_h}{\|v_h\|_{1, \Lambda} \|\lambda_h\|_{-\frac{1}{2}, \Gamma}} \geq \delta. \quad (2.41)$$

Note that this estimate is announced in [6] only for  $P_1$  finite elements, but we can easily prove it for  $P_k$  elements with any  $k \geq 1$ . To this end, we start by the definition of the  $H^{-\frac{1}{2}}$  norm

$$\|\lambda_h\|_{-\frac{1}{2}, \Gamma} = \sup_{v \in H^{\frac{1}{2}}(\Gamma)} \frac{\int_{\Gamma} v \lambda_h}{\|v\|_{\frac{1}{2}, \Gamma}} \leq C \sup_{v \in H^1(\Lambda)} \frac{\int_{\Gamma} v \lambda_h}{\|v\|_{1, \Lambda}} \quad (2.42)$$

Let  $\tilde{I}_h : H^1(\Lambda_\varepsilon) \rightarrow V_h$  be the Scott-Zhang interpolator satisfying

$$|\tilde{I}_h v|_{1, \Lambda_\varepsilon} \leq C |v|_{1, \Lambda_\varepsilon}, \quad \|v - \tilde{I}_h v\|_{0, \Lambda_\varepsilon} \leq Ch |v|_{1, \Lambda_\varepsilon}, \quad \|v - \tilde{I}_h v\|_{0, \Gamma} \leq C\sqrt{h} |v|_{1, \Lambda_\varepsilon},$$

for any  $v \in H^1(\Lambda_\varepsilon)$ . Now, take any  $v \in H^1(\Lambda_\varepsilon)$  and construct  $v_h \in V_h$  to be equal to  $\tilde{I}_h v$  on the internal degrees of freedom inside  $\Lambda_\varepsilon$  and to be the  $L^2(\Gamma)$

orthogonal projection of  $v$  on  $M_h$ . We have thus

$$\|v_h - \tilde{I}_h v\|_{0,\Gamma} \leq \|v - \tilde{I}_h v\|_{0,\Gamma} + \|v - v_h\|_{0,\Gamma} \leq 2\|v - \tilde{I}_h v\|_{0,\Gamma}$$

Owing to the fact that  $v_h$  and  $\tilde{I}_h v$  differ only at the boundary  $\Gamma$ , one can prove (see the details in Lemma 2.7 below)

$$\|v_h - \tilde{I}_h v\|_{0,\Lambda_\varepsilon} \leq C\sqrt{h}\|v_h - \tilde{I}_h v\|_{0,\Gamma} \quad \text{and} \quad |v_h - \tilde{I}_h v|_{1,\Lambda_\varepsilon} \leq \frac{C}{\sqrt{h}}\|v_h - \tilde{I}_h v\|_{0,\Gamma}$$

Putting all these estimates together gives

$$\|v_h\|_{0,\Lambda_\varepsilon} \leq \|v_h - \tilde{I}_h v\|_{0,\Lambda_\varepsilon} + \|v - \tilde{I}_h v\|_{0,\Lambda_\varepsilon} + \|v\|_{0,\Lambda_\varepsilon} \leq Ch|v|_{1,\Lambda_\varepsilon} + \|v\|_{0,\Lambda_\varepsilon}$$

and

$$|v_h|_{1,\Lambda_\varepsilon} \leq |v_h - \tilde{I}_h v|_{1,\Lambda_\varepsilon} + |\tilde{I}_h v|_{1,\Lambda_\varepsilon} \leq C|v|_{1,\Lambda_\varepsilon}$$

This means  $\|v_h\|_{1,\Lambda_\varepsilon} \leq C\|v\|_{1,\Lambda_\varepsilon}$ , so that we can continue the calculation in (2.42) using for any  $v \in H^1(\Lambda_\varepsilon)$  the corresponding  $v_h \in V_h$  constructed as above and recalling that  $v_h$  is the  $L^2(\Gamma)$ -orthogonal projection of  $v$  on  $\Gamma$

$$\|\lambda_h\|_{-\frac{1}{2},\Gamma} \leq C \sup_{v \in H^1(\Lambda_\varepsilon)} \frac{\int_\Gamma v \lambda_h}{\|v\|_{1,\Lambda_\varepsilon}} = C \sup_{v \in H^1(\Lambda_\varepsilon)} \frac{\int_\Gamma v_h \lambda_h}{\|v\|_{1,\Lambda_\varepsilon}} \leq C \sup_{v_h \in V_h} \frac{\int_\Gamma v_h \lambda_h}{\|v_h\|_{1,\Lambda_\varepsilon}}$$

which is equivalent to (2.41).

Returning to the proof of the discrete inf-sup (2.40), for any  $\lambda_h \in M_h$ , we can thus take  $v_{Hh} \in V_{Hh}^d$  as  $v_{Hh}|_{\Omega \setminus \bar{\Lambda}} = 0$  and  $v_{Hh}|_{\Lambda_\varepsilon} = -v_h$ , with  $v_h \in V_h$  given by (2.41), so that  $[v_{Hh}] = v_h$  on  $\Gamma$ . Observing that  $\|v_{Hh}\|_V = \|v_h\|_{1,\Lambda_\varepsilon}$  and  $\|\lambda_h\|_M = \|\lambda_h\|_{-\frac{1}{2},\Gamma}$  we conclude that (2.41) implies (2.40).  $\square$

We provide in the following Lemma some technicalities which were used in the previous one.

**Lemma 2.7.** *Let  $v_h \in V_h$  be such that all its degrees of freedom (in the sense of [15]) vanish except those on the boundary  $\Gamma$  (i.e.  $v_h$  vanishes at all the interior nodes of  $\mathcal{T}_h$ , at all the degrees of freedom inside the internal facets of  $\mathcal{T}_h$  and on the boundary facets on  $\partial\Omega_\varepsilon$ , and at all the degrees of freedom inside the elements of  $\mathcal{T}_h$ ). Then,*

$$\|v_h\|_{0,\Lambda_\varepsilon} \leq C\sqrt{h}\|v_h\|_{0,\Gamma} \quad \text{and} \quad |v_h|_{1,\Lambda_\varepsilon} \leq \frac{C}{\sqrt{h}}\|v_h\|_{0,\Gamma}$$

*Proof.* The function  $v_h \in V_h$  satisfying the hypotheses of the Lemma is non-zero only on the mesh elements touching the boundary  $\Gamma$ . Let  $T \in \mathcal{T}_h$  be such an element such that one of its faces  $F$  lies on  $\Gamma$ . Mapping  $v_h|_T$  to the reference element and using the equivalence of norms we see that

$$\|v_h\|_{0,T} \leq C\sqrt{h}\|v_h\|_{0,F}$$



Consider now  $T \in \mathcal{T}_h$  such that it touches  $\Gamma$  at only one node  $x$ . Let us choose a boundary mesh facet  $F \subset \Gamma$  such that  $x$  is a vertex of  $F$ . Again, by mapping to the reference element and the equivalence of norms we see that

$$\|v_h\|_{0,T} \leq Ch^{\frac{d}{2}} |v_h(x)| \leq Ch^{\frac{d}{2}} \times \frac{1}{h^{\frac{d-1}{2}}} \|v_h\|_{0,F} \leq C\sqrt{h} \|v_h\|_{0,F}$$

In 3D, there is also the case of tetrahedrons  $T \in \mathcal{T}_h$  touching  $\Gamma$  at an edge  $E$ . Choosing a boundary mesh face  $F \subset \Gamma$  such that  $E$  is a side of  $F$ , we get by similar reasoning as above

$$\|v_h\|_{0,T} \leq C\sqrt{h} \|v_h\|_{0,F}$$

Denoting by  $\mathcal{T}_h^\Gamma$  the ensemble of mesh elements  $T \in \mathcal{T}_h$  touching  $\Gamma$ , and by  $F(T)$  the boundary facet on  $\Gamma$  chosen for any  $T \in \mathcal{T}_h^\Gamma$  as above, we get

$$\|v_h\|_{0,\Lambda_\varepsilon} = \left( \sum_{T \in \mathcal{T}_h^\Gamma} \|v_h\|_{0,T}^2 \right)^{\frac{1}{2}} \leq C \left( \sum_{T \in \mathcal{T}_h^\Gamma} h \|v_h\|_{0,F(T)}^2 \right)^{\frac{1}{2}} \leq C\sqrt{h} \|v_h\|_{0,\Gamma}$$

This is the announced estimate in  $L^2(L_\varepsilon)$ . The estimate in  $H^1(L_\varepsilon)$  is derived by the usual inverse inequality.  $\square$

The following Lemma provides an interpolation estimate for the Lagrange multiplier  $\lambda = \nabla u \cdot n$  and is thus crucial for establishing the a priori error estimate for (2.33). We note that it is optimal only if  $k = 1$ , and even in this case the result is not completely satisfactory since it requires more than  $H^2$  regularity of  $u$ .

**Lemma 2.8.** *Let  $P_h$  be the projector on  $M_h$  orthogonal in  $L^2(\Gamma)$ . Then, for any  $u \in H^{k+1}(\Lambda_\varepsilon)$  with  $\nabla u \in L^\infty(\Gamma)$ , setting  $\lambda = \nabla u \cdot n$  on  $\Gamma$ , it holds*

$$\|\lambda - P_h \lambda\|_{-1/2,\Gamma} \leq Ch^k |u|_{k+1,\Lambda_\varepsilon} + Ch^{\frac{3}{2}} \|\nabla u\|_{L^\infty(\Gamma)} \quad (2.43)$$

with constant  $C > 0$  depending only on the mesh regularity and on  $\Lambda$ .

*Proof.* Let  $\Gamma_1, \dots, \Gamma_N$  be the sides (segments in 2D, polygons in 3D) composing the boundary of the polygon (polyhedron)  $\Lambda$ . Denoting by  $I_h$  the usual nodal interpolator to  $V_h$  (or a Scott-Zhang interpolator, if appropriate) we observe on any side  $\Gamma_s$

$$\left\| \frac{\partial u}{\partial x_i} - I_h \frac{\partial u}{\partial x_i} \right\|_{0,\Gamma_s} \leq Ch^{k-\frac{1}{2}} \left| \frac{\partial u}{\partial x_i} \right|_{k,\Lambda_\varepsilon}$$

Let  $n^{(s)} = (n_1^{(s)}, \dots, n_d^{(s)})$  be the external unit normal on  $\Gamma_s$  and set  $\lambda_h^{(s)} = \sum_{i=1}^d n_i^{(s)} I_h \frac{\partial u}{\partial x_i}$ . Then,

$$\|n^{(s)} \cdot \nabla u - \lambda_h^{(s)}\|_{0,\Gamma_s} \leq Ch^{k-\frac{1}{2}} |u|_{k+1,\Lambda_\varepsilon}$$

Let us glue  $\lambda_h^{(1)}, \dots, \lambda_h^{(N)}$  into a function  $\lambda_h^d$  defined on  $\Gamma$  by  $\lambda_h^d|_{\Gamma_s} = \lambda_h^{(s)}|_{\Gamma_s}$ ,  $s = 1, \dots, N$ . Recalling that  $\lambda = \nabla u \cdot n$  on  $\Gamma$ , we have

$$\|\lambda - \lambda_h^d\|_{0,\Gamma} \leq Ch^{k-\frac{1}{2}}|u|_{k+1,\Lambda_\varepsilon}$$

The function  $\lambda_h^d$  is piecewise polynomial (of degree  $k$ ) and continuous on every side  $\Gamma_s$ . However, in general, it is discontinuous on  $\Gamma$  since the normal  $n$  jumps over the corners (edges) of the polygon (polyhedron)  $\Gamma$ . We now construct a continuous ‘‘correction’’  $\lambda_h \in M_h$  of  $\lambda_h^d$  by setting  $\lambda_h = \lambda_h^d$  at all the internal degrees of freedom on every side  $\Gamma_s$  and setting  $\lambda_h = 0$  at the corners of  $\Gamma$  (or the degrees of freedom on the edges in the 3D case).

Let us denote  $\mathcal{C}_h$  the ensemble of triangles of  $\mathcal{T}_h$  adjacent to the corners of  $\Gamma$  in 2D (or the ensemble of tetrahedrons of  $\mathcal{T}_h$  adjacent to the edges of  $\Gamma$  in 3D). By construction,  $\lambda_h$  coincide with  $\lambda_h^d$  on  $\Gamma$  outside  $\mathcal{C}_h$  so that

$$\|\lambda_h - \lambda_h^d\|_{0,\Gamma} \leq C\|\lambda_h^d\|_{L^\infty(\Gamma)}\sqrt{|\mathcal{C}_h|}$$

By construction,  $\lambda_h^d$  is uniformly bounded by the maximum of  $|\nabla u|$  on  $\Gamma$  (eventually, multiplied by a constant that depends only on the degree  $k$ ). It is also easy to see that  $|\mathcal{C}_h| \leq Ch^2$  with the constant  $C$  depending only on  $\Lambda$ . Thus,

$$\|\lambda_h - \lambda_h^d\|_{0,\Gamma} \leq Ch\|\nabla u\|_{L^\infty(\Gamma)}$$

Recalling that  $P_h$  is the  $L^2(\Gamma)$ -orthogonal projection on  $M_h$  and  $\lambda_h \in M_h$ , we see

$$\begin{aligned} \|\lambda - P_h\lambda\|_{0,\Gamma} &\leq \|\lambda - \lambda_h\|_{0,\Gamma} \leq \|\lambda - \lambda_h^d\|_{0,\Gamma} + \|\lambda_h - \lambda_h^d\|_{0,\Gamma} \\ &\leq Ch^{k-\frac{1}{2}}|u|_{k+1,\Lambda_\varepsilon} + Ch\|\nabla u\|_{L^\infty(\Gamma)}. \end{aligned}$$

We now can also bound the  $H^{-\frac{1}{2}}$  norm

$$\begin{aligned} \|\lambda - P_h\lambda\|_{-1/2,\Gamma} &= \sup_{v \in H^{1/2}(\Gamma)} \frac{(\lambda - P_h\lambda, v)_{L^2(\Gamma)}}{\|v\|_{1/2,\Gamma}} = \sup_{v \in H^{1/2}(\Gamma)} \frac{(\lambda - P_h\lambda, v - I_h v)_{L^2(\Gamma)}}{\|v\|_{1/2,\Gamma}} \\ &\leq \left( Ch^{k-\frac{1}{2}}|u|_{k+1,\Lambda_\varepsilon} + Ch\|\nabla u\|_{L^\infty(\Gamma)} \right) \times \sqrt{h} \end{aligned}$$

since  $\|v - I_h v\|_{0,\Gamma} \leq C\sqrt{h}|v|_{1,\Lambda_\varepsilon} \leq C\sqrt{h}\|v\|_{1/2,\Gamma}$  assuming that  $v$  is extended to  $\Lambda_\varepsilon$  as a harmonic function.  $\square$

**Theorem 2.9.** *Problem (2.33) admits a unique solution  $(u_{Hh}, \lambda_h) \in V_{Hh}^d \times M_h$ . Provided  $u \in H^{k+1}(\Omega)$  and  $\nabla u \in L^\infty(\Gamma)$ , we have moreover the following a priori error estimate*

$$\|u_{Hh} - u\|_V \leq C \left( H^k|u|_{k+1,\Omega \setminus \bar{\Lambda}} + h^k|u|_{k+1,\Lambda_\varepsilon} + Ch^{\frac{3}{2}}\|\nabla u\|_{L^\infty(\Gamma)} \right) \quad (2.44)$$

with constant  $C > 0$  depending only on the mesh regularity and on  $\Lambda$ .

*Proof.* The bilinear form  $a$  is uniformly coercive on  $\ker \mathcal{B}_{Hh}$  (Lemma 2.5) and form  $b$  satisfies the uniform inf-sup condition on  $V_{Hh}^d \times M_h$  with a mesh-independent constant (Lemma 2.6). It implies by the approximation theory of mixed problems [12] that the discrete problem (2.33) is well-posed. Moreover, analogous properties hold on the continuous level. This entails that the unique solution  $(u_{Hh}, \lambda_h)$  to (2.33) satisfies the error bound

$$\|u - u_{Hh}\|_V + \|\lambda - \lambda_h\|_M \leq C \left( \min_{v_{Hh} \in V_{Hh}^d} \|u - v_{Hh}\|_V + \min_{\mu_h \in M_h} \|\lambda - \mu_h\|_M \right). \quad (2.45)$$

It remains thus to find the interpolants  $v_{Hh}$  and  $\mu_h$  to  $u$  and  $\lambda$  respectively that provide the optimal error estimate in the sense of inequality (2.44). We begin by constructing the appropriate  $v_{Hh}$ . Let  $\tilde{u} \in H^{k+1}(\Omega)$  be the extension of  $u$  from  $\Omega \setminus \bar{\Lambda}$  to the whole of  $\Omega$ , i.e.  $\tilde{u} = u$  on  $\Omega \setminus \bar{\Lambda}$ . By the extension theorem for Sobolev spaces [1], we can construct  $\tilde{u}$  so that  $\|\tilde{u}\|_{k+1,\Omega} \leq C\|u\|_{k+1,\Omega \setminus \bar{\Lambda}}$  where  $C$  is a constant that depends only on  $\Omega$  and  $\Lambda$ . Let  $I_H : H^{k+1}(\Omega) \rightarrow V_H$  and  $I_h : H^{k+1}(\Lambda) \rightarrow V_h$  be the standard interpolation operators satisfying  $|v - I_H v|_{1,\Omega} \leq CH^k |v|_{k+1,\Omega}$  for any  $v \in H^{k+1}(\Lambda_\varepsilon)$  and  $|v - I_h v|_{1,\Lambda_\varepsilon} \leq Ch^k |v|_{k+1,\Lambda_\varepsilon}$  for any  $v \in H^{k+1}(\Lambda_\varepsilon)$  where the constant  $C$  depends only on the regularity of the meshes. We choose then  $v_{Hh} \in V_{Hh}^d$  as follows:  $v_{Hh} = I_H \tilde{u}$  on  $\Omega \setminus \bar{\Lambda}$  and  $v_{Hh} = I_h u$  on  $\Lambda$ . The function satisfies

$$\begin{aligned} \|u - v_{Hh}\|_V &\leq C(|u - I_H \tilde{u}|_{1,\Omega} + |u - I_h u|_{1,\Lambda_\varepsilon}) \\ &\leq C(H^k |\tilde{u}|_{k+1,\Omega} + h^k |u|_{k+1,\Lambda_\varepsilon}) \end{aligned} \quad (2.46)$$

We now recall  $\lambda = (\nabla u \cdot n)$  on  $\Gamma$  and take  $\mu_h \in M_h$  as the orthogonal projection  $\mu_h = P_h \mu$ . Combining (2.43) with (2.46) and substituting into (2.45) gives the announced error estimate (2.44).  $\square$

**Remark 2.1.** *As an alternative to error estimate derivation based on the mixed formulation as above, one can try a more direct approach by eliminating the Lagrange multiplier  $\lambda_h$  from (2.33).*

*We start by introducing the space of functions satisfying the constraint in (2.33):*

$$V_{Hh}^{wc} = \{v \in V_{Hh}^d \text{ such that } b(v, \mu) = 0 \quad \forall \mu \in M_h\}$$

*The function in  $V_{Hh}^{wc}$  are “weakly continuous” in the sense of a natural finite element approximation of the condition  $[v] = 0$  on  $\Gamma$ . We can now rewrite problem (2.33) as: find  $u_{Hh} \in V_{Hh}^{wc}$  such that*

$$a(u_{Hh}, v) = L(v), \quad \forall v \in V_{Hh}^{wc} \quad (2.47)$$

*It is possible to construct an optimal interpolant  $\tilde{u}_{Hh} \in V_{Hh}^{wc}$  to  $u$ . Let  $I_H : H^{k+1}(\Omega) \rightarrow V_H$  and  $I_h : H^{k+1}(\Lambda_\varepsilon) \rightarrow V_h$  be the standard nodal interpolation operators satisfying (2.11)–(2.12) and*

$$|v - I_H v|_{1,E} \leq CH^{k-\frac{1}{2}} |v|_{k+1,T} \text{ for any } v \in H^{k+1}(T), T \in \mathcal{T}_H, E \in \partial T$$

and

$$|v - I_h v|_{1,E} \leq Ch^{k-\frac{1}{2}} |v|_{k+1,T} \text{ for any } v \in H^{k+1}(T), T \in \mathcal{T}_h, E \in \partial T$$

with  $E$  representing any side of  $T$ .

As in the proofs above, we start to define the interpolant  $\tilde{u}_{Hh} \in V_{Hh}^{wc}$  by taking  $I_H \tilde{u}$  outside  $\Lambda$  where  $\tilde{u}$  is an extension of  $u$  from  $\Omega \setminus \bar{\Lambda}$  to the whole  $\Omega$ . We cannot take  $\tilde{u}_{Hh}$  simply as  $I_h u$  inside  $\Lambda$  since such a function would not satisfy the weak continuity constraint over  $\Gamma$ . We should thus correct  $I_h u$  inside  $\Lambda$  to restore the weak continuity by adding an appropriate finite element function  $r_h \in V_h$  equal to  $P_h(I_H \tilde{u}) - I_h u$  on  $\Gamma$ . We introduce  $r \in H^1(\Lambda)$  such that  $r = I_H \tilde{u} - I_h u$  on  $\Gamma$  and  $\|r\|_{1,\Lambda} \leq C \|r\|_{\frac{1}{2},\Gamma}$  with a constant  $C > 0$  depending only on  $\Lambda$ . Moreover, let  $\tilde{I}_h : H^1(\Lambda_\varepsilon) \rightarrow V_h$  be the Scott-Zhang interpolant satisfying

$$\|r - \tilde{I}_h r\|_{0,\Gamma} \leq Ch |r|_{1,\Gamma} \text{ and } \|\tilde{I}_h r\|_{1,\Lambda_\varepsilon} \leq C \|r\|_{1,\Lambda_\varepsilon}$$

We have thus

$$\begin{aligned} \|\tilde{I}_h r\|_{1,\Lambda_\varepsilon} &\leq C \|r\|_{1,\Lambda_\varepsilon} \leq C \|r\|_{1,\Lambda} \leq C \|r\|_{\frac{1}{2},\Gamma} \\ &= C \|I_H \tilde{u} - I_h u\|_{\frac{1}{2},\Gamma} \leq C (\|I_H \tilde{u} - u\|_{\frac{1}{2},\Gamma} + \|I_h u - u\|_{\frac{1}{2},\Gamma}) \\ &\leq C (\|u - I_H \tilde{u}\|_{1,\Omega \setminus \bar{\Lambda}} + \|u - I_h u\|_{1,\Lambda_\varepsilon}) \end{aligned}$$

Let  $r_h \in V_h$  coincide with  $\tilde{I}_h r$  at all the internal degrees of freedom of the mesh  $\mathcal{T}_h$  and be defined on  $\Gamma$  by  $r_h = P_h r = P_h(I_H \tilde{u}) - I_h u$ . Invoking Lemma 2.7 and the estimates on the interpolator  $\tilde{I}_h$ , we obtain

$$\begin{aligned} \|r_h - \tilde{I}_h r\|_{1,\Lambda_\varepsilon} &\leq \frac{C}{\sqrt{h}} \|r_h - \tilde{I}_h r\|_{0,\Gamma} \leq \frac{C}{\sqrt{h}} (\|r - P_h r\|_{0,\Gamma} + \|r - \tilde{I}_h r\|_{0,\Gamma}) \\ &\leq \frac{C}{\sqrt{h}} \|r - \tilde{I}_h r\|_{0,\Gamma} \leq C \sqrt{h} |r|_{1,\Gamma} \leq C \sqrt{h} (\|u - I_H \tilde{u}\|_{1,\Gamma} + \|u - I_h u\|_{1,\Gamma}) \end{aligned}$$

We now take  $\tilde{u}_{Hh} \in V_{Hh}^{wc}$  with the components  $\tilde{u}_H \in V_H$  and  $\tilde{u}_h \in V_h$  such that  $\tilde{u}_H = I_H \tilde{u}$  and  $\tilde{u}_h = I_h u + r_h$ . We have thanks to the interpolation estimates mentioned above

$$\begin{aligned} \|u - \tilde{u}_{Hh}\|_{1,\Omega_\varepsilon} &\leq \|u - I_H \tilde{u}\|_{1,\Omega \setminus \bar{\Lambda}} + \|u - I_h u\|_{1,\Lambda_\varepsilon} + \|\tilde{I}_h r\|_{1,\Lambda_\varepsilon} + \|r_h - \tilde{I}_h r\|_{1,\Lambda_\varepsilon} \\ &\leq C (\|u - I_H \tilde{u}\|_{1,\Omega \setminus \bar{\Lambda}} + \|u - I_h u\|_{1,\Lambda_\varepsilon}) \\ &\quad + C \sqrt{h} (\|u - I_H \tilde{u}\|_{1,\Gamma} + \|u - I_h u\|_{1,\Gamma}) \\ &\leq C (H^k |u|_{k+1,\Omega \setminus \bar{\Lambda}} + h^k |u|_{k+1,\Lambda_\varepsilon}) \\ &\quad + C \sqrt{h} (H^{k-\frac{1}{2}} |u|_{k+1,\Omega \setminus \bar{\Lambda}} + h^{k-\frac{1}{2}} |u|_{k+1,\Lambda_\varepsilon}) \\ &\leq C (H^k |u|_{k+1,\Omega \setminus \bar{\Lambda}} + h^k |u|_{k+1,\Lambda_\varepsilon}) \end{aligned}$$

We have thus constructed an optimal interpolant  $\tilde{u}_{Hh} \in V_{Hh}^{wc}$  for  $u$ , as in the  $\Gamma$ -nested case, cf. the proof of Theorem 2.1. Unfortunately, this does not leave to an a priori error estimate for the solution of Problem (2.47). Indeed, this discretization is non-conforming: substituting the exact solution  $u$  there gives

$$a(u_{Hh}, v) = L(v) + b(v, \lambda), \quad \forall v \in V_{Hh}^{wc}$$

with the  $b$ -term which cannot be neglected. Dealing with it by a Strang lemma leads again to the possibly sub-optimal estimate of Theorem 2.9.

### 2.3.2 Convergence of the iterative algorithm

The proof of the convergence of Algorithm 2.1 in the present general case starts in the same manner as that in the  $\Gamma$ -dependent case in Subsection 2.2.2: we introduce the operator  $A_{Hh} : V_H \rightarrow V_H$  by (2.14) and recall the scalar product (2.15). As in Section 2.2.2, we verify that the iterates  $u_H^n$  evolve from one iteration to another as

$$u_H^n = (I - \omega A_{Hh})u_H^{n-1} + \omega F_H. \quad (2.48)$$

with  $F_H$  defined by (2.19) and (2.18). We can again prove that operator  $A_{Hh}$  is self-adjoint and coercive with respect to the scalar product (2.15), cf. (2.23) in Lemma 2.2. The expression (2.22) for  $A_{Hh}$  remains also valid.

In what follows we shall work with the ensemble of the triangles from the coarse mesh that lie inside  $\Lambda$  (in contrast with the  $\Gamma$ -nested case, this ensemble does not necessarily coincide with  $\Lambda$ ) and we shall need to introduce some assumptions about this set:

**Definition 2.3.** Let  $\Lambda_H \subset \Lambda$  be defined as the interior of the union of all the cells  $T \in \mathcal{T}_H$  that lie inside  $\bar{\Lambda}$  (we suppose here that  $\Lambda$  is an open set and the cells  $T$  are closed). Thus,  $\Lambda_H = (\cup_{T \in \mathcal{T}_H, T \subset \bar{\Lambda}} T)^\circ$ . We also denote  $\Gamma_H = \partial \Lambda_H$

**Definition 2.4.** Using the notation  $\Lambda_H \subset \Lambda$  from the previous definition, we introduce the patch conformity parameter  $\kappa_H$  as  $\kappa_H = \min_{T \in \mathcal{T}_H} \kappa(T)$  with

$$\kappa(T) = \begin{cases} +\infty, & \text{if } T \subset \bar{\Lambda} \\ \frac{|T \setminus \bar{\Lambda}|}{|T|}, & \text{otherwise} \end{cases}$$

for any cell  $T \in \mathcal{T}_H$ . The patch  $\Lambda$  is said to be geometrically conforming with the coarse mesh  $\mathcal{T}_H$  if  $\kappa_H = 1$ .

We observe that the patch conformity parameter is necessarily a number in  $(0, 1]$ . Indeed, there are necessarily some mesh cells  $T \in \mathcal{T}_H$  such that  $T \not\subset \bar{\Lambda}$  (otherwise, the patch  $\Lambda$  would coincide with  $\Omega$ , which is excluded by our general assumptions) and  $\kappa(T) \in (0, 1]$  for any such cell  $T$ . The case of a conforming interface, as in Definition 2.2 corresponds to  $\kappa_H = 1$ . On the other side of the spectrum,  $\kappa_H \ll 1$  indicates the presence of mesh cells

$T \in \mathcal{T}_H$  that are almost, but not entirely, covered by  $\Lambda$ . Such situations are maleficent for the convergence of the iterative Algorithm 2.1, as will be seen below.

We shall also need a rather technical assumption on  $\Lambda$  and  $\Lambda_H$ , as stated in the Definition below. We choose to write this out only in the case  $d = 2$ , but the case  $d = 3$  can be treated similarly modulo some more tedious notations.

**Definition 2.5.** *The patch  $\Lambda$  will be called regular with respect to the mesh  $\mathcal{T}_H$  if the boundary of the corresponding subdomain  $\Lambda_H$  can be covered by a finite number of open sets  $U_1, U_2, \dots$  so that*

1. *The number of sets  $U_i$  is not greater than  $N$ ;*
2. *Any point  $x \in \Gamma_H$  belongs to at least one set  $U_i$  together with the ball  $B(x, \varepsilon)$  of center  $x$  and radius  $\varepsilon$ ;*
3. *The intersection of  $\Gamma_H$  with each  $U_i$  can be represented as the graph of a Lipschitz function with Lipschitz constant  $\leq M$ , i.e. for each  $U_i$  there exist some Cartesian coordinates  $\xi_1, \xi_2$  and a function  $\phi_i : \mathbb{R} \rightarrow \mathbb{R}$  such that*

$$\Lambda_H \cup U_i = \{(\xi_1, \xi_2) \in \Lambda_H \mid \xi_2 > \phi_i(\xi_1)\}$$

and

$$|\phi_i(x) - \phi_i(y)| \leq M|x - y|, \quad \forall x, y \in \mathbb{R}.$$

We will also assume that  $\Lambda$  is a polygon and

4. *The intersection of  $\Gamma$  with any cell  $T \in \mathcal{T}_H$  consists of at most  $K$  straight segments (planar faces).*

The positive constants  $M, \varepsilon$  and the integers  $N, K$  should be chosen independently of the meshes  $\mathcal{T}_H$  and  $\mathcal{T}_h$ . They will be referred to as the regularity parameters of  $\Lambda$  with respect to  $\mathcal{T}_H$ .

The regularity assumptions 1–3 are introduced in the book [38] to characterize *minimally smooth* domains for which it is possible to construct the extension operators for the Sobolev spaces.<sup>1</sup> In our analysis below, we shall not only need that the regularity parameters  $M, \varepsilon$  and  $N$  exist but also that they are independent of  $\mathcal{T}_H$  in the considered class of meshes. While it is not entirely clear what restrictions do we need to impose on the meshes  $\mathcal{T}_H$  in order to satisfy such an assumption, it does not seem too restrictive. Indeed, in the 2D case, for any polygonal patch  $\Lambda$  and any regular family of coarse meshes with non-obtuse cells, the angle between any edge of  $\mathcal{T}_H$  on  $\Gamma_H$  and the nearest edge of  $\Lambda$  will be less than some maximal angle  $\alpha_{\max} < \frac{\pi}{2}$ . One can thus see that the portion of  $\Gamma_H$  that goes along an edge of  $\Lambda$  can be parametrized by a function with the Lipschitz constant that depends only on  $\alpha_{\max}$ . Similar considerations are also valid in the 3D case.

<sup>1</sup>In fact, the definition in [38] is more general as it allows for an infinite sequence of open sets  $\{U_i\}$  such that no point of  $\mathbb{R}^2$  is contained in more than  $N$  of the  $U_i$ 's, but this subtlety is not important in our context.

**Lemma 2.10.** *Suppose that the patch  $\Lambda$  is regular with respect to the mesh  $\mathcal{T}_H$  and recall the patch conformity parameter  $\kappa_H$  from Definition 2.4. There exists  $\delta > 0$  which depends only on  $\kappa_H$  and on the regularity of  $\mathcal{T}_H$  and of  $\Lambda$ , such that*

$$\int_{T \setminus \bar{\Lambda}} |\nabla u_H|^2 \geq \delta \int_T |\nabla u_H|^2, \quad \forall u_H \in V_H \text{ and } \forall T \in \mathcal{T}_H.$$

*Proof.* We give the proof only in the 2D case to ease the notations. We want to prove that the quantity

$$\mathcal{F}(T, \Lambda, u_H) = \frac{\int_{T \setminus \bar{\Lambda}} |\nabla u_H|^2}{\int_T |\nabla u_H|^2}$$

is bounded from below by a positive constant for all admissible  $T, \Lambda$  and for all polynomials  $u_H \neq 0$  of degree  $\leq k$ .  $\mathcal{F}(T, \Lambda, u_H)$  is invariant under the following types of coordinate change: shift of the origin, rotation and homothety  $x \mapsto \lambda x$  ( $\lambda \in \mathbb{R}$ ). It is thus sufficient to bound this quantity under the following geometrical assumption: the triangle  $T$  has the vertices  $A, B, C$  with  $A = (0, 0)$ ,  $B = (0, 1)$  and  $C = (x_C, y_C)$  with some  $x_C, y_C$  bounded by the regularity parameter of the mesh. The curve  $\Gamma \cap T$  is the union of at most  $K$  segments. Thus the geometry of  $T$  and  $T \setminus \bar{\Lambda}$  is determined by  $2(K + 1)$  real parameters which are the coordinates of  $C$  and the end points of the segments in  $\Gamma \cap T$ . All these parameters are uniformly bounded.  $\mathcal{F}(T, \Lambda, u_H)$  does not change if we multiply the polynomial  $u_H$  by any real number, so that we can assume that all the coefficients of  $u_H$  are bounded by 1 in absolute value. Thus, the problem of finding  $\delta = \inf \mathcal{F}(T, \Lambda, u_H)$  under the restrictions on  $T, \Lambda, u_H$  described above is a minimization problem for a continuous function that depends on a finite number of parameters and all these parameters are bounded. This problem admits therefore a minimizer, i.e. there exist  $T, \Lambda, u_H$  such that  $\delta = \mathcal{F}(T, \Lambda, u_H)$ . It remains to verify that  $\delta > 0$ . Supposing that it's not true, i.e.  $\delta = 0$ , implies  $\int_{T \setminus \bar{\Lambda}} |\nabla u_H|^2 = 0$  which is only possible if  $\text{meas}(T \setminus \bar{\Lambda}) = 0$ . But this contradicts the assumption  $\text{meas}(T \setminus \bar{\Lambda}) \geq \kappa_H \text{meas}(T)$ .  $\square$

**Remark 2.2.** *The estimate of the lemma above is trivial for  $P_1$  finite elements and we can take  $\delta = \kappa_H$  in this case. Indeed, for any cell  $T \in \mathcal{T}_H, T \not\subset \Lambda$*

$$\int_{T \setminus \bar{\Lambda}} |\nabla u_H|^2 = \frac{|T \setminus \bar{\Lambda}|}{|T|} \int_T |\nabla u_H|^2 \geq \kappa_H \int_T |\nabla u_H|^2$$

since  $|\nabla u_H| = \text{const}$  on  $T$ .

**Lemma 2.11.** *The kernel of operator  $A_{Hh}$  coincides with  $V_H^0$ , as defined by (2.24), and  $A_{Hh}$  is coercive on its orthogonal complement  $V_H^1$ . More precisely, assuming that  $\Lambda$  is regular with respect to  $\mathcal{T}_H$ , there exists  $m > 0$  depending only on the regularity parameters of  $\Lambda$  with respect to  $\mathcal{T}_H$ , on the parameter  $\kappa_H \in (0, 1]$  from*

Definition 2.4, and on the regularity parameters of  $\mathcal{T}_H$  itself, such that

$$(A_{Hh}v_H, v_H) \geq m|v_H|_{1,\Omega}^2 \quad \forall v_H \in V_H^1 \quad (2.49)$$

The norm of  $A_{Hh}$  as an operator in the Hilbert space  $H_0^1(\Omega)$  equipped with the scalar product (2.15) is bounded by a mesh-independent constant.

*Proof.* Let us first prove that  $\ker A_{Hh} \subset V_H^0$ . If  $u_H \in \ker A_{Hh}$ , then  $u_H = 0$  on  $\Omega \setminus \bar{\Lambda}$  as follows from the expression for  $(A_{Hh}u_H, u_H)$  in (2.22). This means that  $u_H = 0$  on every cell  $T \in \mathcal{T}_H$  which is not entirely inside  $\Lambda$ , since  $u_H$  is a polynomial. We have thus  $u_H = 0$  on  $\Omega \setminus \bar{\Lambda}_H$ . On the other hand, if  $u_H \in V_H^0$  then  $z_h = 0$  on  $\Lambda$  and  $v_h = 0$  on  $\Gamma$  so that  $A_{Hh}u_H = 0$ . This entails  $\ker A_{Hh} = V_H^0$ .

In order to prove the coercivity estimate we invoke again (2.22) with  $z_H = u_H \in V_H^1$ , which implies

$$(A_{Hh}u_H, u_H) \geq \int_{\Omega \setminus \bar{\Lambda}} \nabla u_H \cdot \nabla u_H \geq \sum_{T \in \mathcal{T}_H} \int_{T \setminus \bar{\Lambda}} |\nabla u_H|^2 \geq \delta \int_{\Omega \setminus \bar{\Lambda}_H} |\nabla u_H|^2 \quad (2.50)$$

with  $\delta > 0$  from Lemma 2.10.

Let  $E$  be the Stein's extension operator [38] that maps any integrable function  $u : \Omega \setminus \bar{\Lambda}_H \rightarrow \mathbb{R}$  to the function  $Eu : \Omega \rightarrow \mathbb{R}$  so that  $Eu = u$  on  $\Omega \setminus \bar{\Lambda}_H$ . In particular,  $E$  maps  $H^1(\Omega \setminus \bar{\Lambda}_H)$  to  $H^1(\Omega)$ . By construction, described in detail in [38], the norm of  $E$  in these spaces depends only on the regularity constants of  $\Lambda$  with respect to  $\mathcal{T}_H$ , cf. Definition 2.5. Now, let  $R_H$  be a Clément type interpolation operator acting on functions in  $H^1(\Lambda_H)$  and producing piecewise polynomial (of degree  $k$ ) finite element functions on the part of the coarse mesh  $\mathcal{T}_H$  inside  $\Lambda_H$ . One can assume that  $R_H u = u$  on  $\partial\Lambda_H$  provided  $u$  is piecewise polynomial (of degree  $k$ ) there [7]. The norm of  $R_H$  in  $H^1(\Lambda_H)$  depends only on the regularity of  $\mathcal{T}_H$ . Taking any  $u_H \in V_H^1$ , we can thus construct  $v_H \in V_H$  such that

$$v_H = \begin{cases} u_H, & \text{on } \Omega \setminus \bar{\Lambda}_H \\ R_H E u_H, & \text{on } \Lambda_H \end{cases}$$

By definition of  $V_H^1$ , we have  $c(u_H, v_H - u_H) = 0$  which entails  $|u_H|_{1,\Omega} \leq |v_H|_{1,\Omega}$  so that

$$\begin{aligned} |u_H|_{1,\Omega}^2 &\leq \|R_{H,\Lambda_H}\|^2 \|E u_H\|_{H^1(\Lambda_H)}^2 + \|u_H\|_{H^1(\Omega \setminus \Lambda_H)}^2 \\ &\leq (\|R_H\|^2 \|E\|^2 + 1) \|u_H\|_{H^1(\Omega \setminus \Lambda_H)}^2 \\ &\leq (\|R_H\|^2 \|E\|^2 + 1) C_P |u_H|_{1,\Omega \setminus \bar{\Lambda}_H}^2. \end{aligned} \quad (2.51)$$

$C_P$  in the last line stands for the constant in a Poincaré type inequality, which is valid since  $u_H$  vanishes on  $\partial\Omega$ . Combining (2.50) with (2.51), we see that

$$(A_{Hh}u_H, u_H) \geq \frac{\delta}{(\|R_H\|^2 \|E\|^2 + 1) C_P} |u_H|_{1,\Omega}^2, \quad (2.52)$$



which is equivalent to (2.49).

The last statement of the Lemma concerns the norm of operator  $A_{Hh}$ . In order to prove it, we first observe that by the standard theory of the finite element approximations to the mixed problems [12], the solution  $(z_h, \nu_h)$  to problem (2.16) satisfies

$$\|z_h\|_{1,\Lambda} + \|\nu_h\|_{-\frac{1}{2},\Gamma} \leq C \|z_H\|_{\frac{1}{2},\Gamma}$$

with a constant that depends only on  $\Lambda$ . The definition of operator  $A_{Hh}$  now gives  $\forall z_H, v_H \in V_H$

$$\begin{aligned} (A_{Hh}z_H, v_H) &\leq \int_{\Omega \setminus \bar{\Lambda}} \nabla z_H \cdot \nabla v_H + \|\nu_h\|_{-\frac{1}{2},\Gamma} \|v_H\|_{\frac{1}{2},\Gamma} \\ &\leq \int_{\Omega \setminus \bar{\Lambda}} \nabla z_H \cdot \nabla v_H + C \|z_H\|_{\frac{1}{2},\Gamma} \|v_H\|_{\frac{1}{2},\Gamma} \\ &\leq M \|z_H\|_{1,\Omega} \|v_H\|_{1,\Omega} \end{aligned}$$

where  $C, M$  denote the mesh-independent constants. Thus  $\|A_{Hh}\| \leq M$ .  $\square$

**Theorem 2.12.** *Assume that  $\Lambda$  is regular with respect to  $\mathcal{T}_H$ , cf. Definitions 2.5 and 2.3. Algorithm 2.1 converges to the solution to (2.33) provided  $0 < \omega < \omega^*$  where  $\omega^*$  is a mesh-independent constant. This means that  $u_{Hh}^n \rightarrow u_{Hh}$  and  $\lambda_h^n \rightarrow \lambda_h$  as  $n \rightarrow \infty$  where  $(u_{Hh}, \lambda_h) \in V_{Hh}^d \times M_h$  is solution to (2.33). The convergence rate depends on the regularity of  $\mathcal{T}_H$ , on  $\Lambda$  and on its regularity with respect to  $\mathcal{T}_H$  and also on the parameter  $\kappa_H$  introduced in Definition 2.4.*

We skip the proof of this Theorem since it goes along literally the same line as that of its analogue in the  $\Gamma$ -nested case (Theorem 2.4). Note that  $\omega^*$  can be chosen indeed independent of  $\kappa_H$  since it depends essentially on the continuity constant (the norm) of operator  $A_{Hh}$ , which is not affected by  $\kappa_H$ . However, the patch conformity parameter  $\kappa_H$  has a crucial role, at least in theory. Indeed, the convergence rate of the algorithm is essentially determined by the coercitivity constant of operator  $A_{Hh}$  which, according to (2.52), is essentially of the order of  $\kappa_H$ . Thus, the convergence of the iterations can be very slow if the patch is badly positioned on the coarse mesh so that  $\kappa_H \ll 1$ .

**Remark 2.3.** *In the general case of two arbitrary meshes  $\mathcal{T}_H$  and  $\mathcal{T}_h$ ,  $\kappa_H$  can be extremely small if some cells of  $\mathcal{T}_H$  are cut by the boundary of  $\Lambda$  so that only a tiny portion of them rests outside  $\Lambda$ . Thus, the convergence of Algorithm 2.1 can be arbitrarily slow. We stress that this observation is not an artifact of possibly non optimal estimates in the proof of our lemmas. It reflects the real behavior of Algorithm 2.1 on general meshes as can be seen on the following simple example in 1D: let  $\Omega = (0, 1)$  and consider the problem*

$$-u'' = f \text{ on } \Omega, \quad u(0) = u(1) = 1.$$

We take the patch  $\Lambda = (a, b)$  and suppose that it is placed symmetrically, i.e.  $a + b = 1$ . We choose a uniform coarse grid of step  $H$  on  $\Omega$  and introduce the piecewise linear finite element space  $V_H$  on it. We also introduce a fine mesh  $\mathcal{T}_h$  on  $\Lambda$  and the fine finite element space  $V_h$ .

We now apply Algorithm 2.1 to this problem in the trivial case  $u = f = 0$  starting from some non-zero initial approximation  $u_H^0$  (there is no hole  $\Omega_\varepsilon$  in this simple example so that  $\Lambda_\varepsilon = \Lambda$ ). We take  $\omega = 1$  (relaxation, i.e. taking  $\omega < 1$  would make the convergence even slower in this case). The coarse problem is

$$\int_0^1 (u_H^n)' v_H' = -\lambda_h^{n-1}(a) v_H(a) - \lambda_h^{n-1}(b) v_H(b) + \int_a^b (u_H^{n-1})' v_H', \quad \forall v_H \in V_H$$

The point  $a$  is inside the coarse mesh interval, say  $[i_0 H, (i_0 + 1)H)$ , for some integer  $i_0$ . We have thus  $a = (i_0 + \kappa_H)H$ . By symmetry  $b = (i_1 - \kappa_H)H$  for some  $i_1 > i_0$ . If the initial approximation is symmetric, so are all the iterates. Then  $u_h^n(x) = u_H^n(a)$  for all  $x \in (a, b)$  and  $\lambda_h^n = 0$  so that the coarse problem is simplified to

$$\int_0^1 (u_H^n)' v_H' = \int_a^b (u_H^{n-1})' v_H', \quad \forall v_H \in V_H$$

This equation has a simple explicit solution if we take  $u_H^0$  such that  $u_H^0(x) = 0$  for  $x \in [0, i_0 H] \cap [i_1 H, 1]$  and  $u_H^0(x) = 1$  for  $x \in [(i_0 + 1)H, (i_1 - 1)H]$ . We have then (recall that both  $V_H$  and  $V_h$  are supposed to be the spaces of piecewise linear functions on the corresponding meshes)

$$u_H^n = (1 - \kappa_H)^n u_H^0.$$

This proves that Algorithm 2.1 can indeed converge very slowly if  $\kappa_H \ll 1$ .

This being said, the numerical tests usually demonstrate that Algorithm 2.1 converges rapidly even on “bad” meshes, more precisely the slow convergence is observed in practice only when we measure the error between the iterates  $u_{Hh}^n$  and the converged numerical solution  $u_{Hh}$ , but not for the error between  $u_{Hh}^n$  and the exact solution  $u$ , which is ultimately the only quantity of practical interest. We do not have a theoretical justification of this phenomenon, neither can we assure its generality. We can conjecture, however, the following scenario that may be quite common: the error on each iteration ( $u_{Hh}^n - u_{Hh}$ ) can be decomposed into the sum of “fast” modes (the convergence on these is not affected by the possible smallness of  $\kappa_H$ ) and “slow” ones which are diminished by the algorithm at the rate proportional to  $\kappa_H$ , as in the 1D example above. This example suggests also that the slow modes are somewhat “pathological”, in the sense that they are finite element approximations of some discontinuous functions. The contribution of such modes is small already in the initial approximation ( $u_{Hh}^0 - u_{Hh}$ ) if one constructs  $u_{Hh}^0$  properly, for example as the numerical solution on the coarse mesh. The part of the error on the “slow” modes is thus masked out by the discretization error ( $u_{Hh} - u$ ). The possible slow convergence on general meshes remains nevertheless an undesirable feature of Algorithm 2.1. In the next section, we propose a modification of this algorithms to get rid

of the dependence on  $\kappa_H$ .

## 2.4 Numerical Zomm with discontinuous Lagrange multipliers for non $\Gamma$ -nested meshes

Algorithm 2.1 is not completely satisfactory if one wants to deal with arbitrary, not necessarily  $\Gamma$ -nested triangulations  $\mathcal{T}_H$  and  $\mathcal{T}_h$ . Indeed, one cannot guarantee then the optimal a priori estimate as in Theorem 2.1. The main trouble is in the choice of continuous finite elements as the space  $M_h$  for the Lagrange multiplier  $\lambda_h$ . This quantity can be interpreted as an approximation to the normal flux  $\lambda = n \cdot \nabla u|_\Gamma$  which is discontinuous at the corners of  $\Gamma$ . The error  $\lambda_h - \lambda$  cannot thus be of the optimal order. This does not affect the error  $u_{Hh} - u$  (the only quantity of interest for us) in the case of  $\Gamma$ -nested meshes since  $\lambda_h$  can be then essentially eliminated from the system, cf. the proof of Theorem 2.1. However, this will not be necessarily the case if one works on non  $\Gamma$ -nested meshes. We propose therefore to replace the continuous finite element space  $M_h$  by the discontinuous one

$$M_h^d = \{ \mu_h \in L^2(\Gamma) : \mu_h|_E \in P_{k-1} \text{ on every boundary edge } E \text{ of the mesh } \mathcal{T}_h \text{ inside } \Gamma \} \quad (2.53)$$

The pair of spaces  $V_h \times M_h^d$  does no longer enjoy the infsup property with respect to the bilinear form  $\int_\Gamma \mu_h [v_{Hh}]$ . We introduce therefore a Barbosa-Hughes stabilization in the fine problem for  $(u_h^n, \lambda_h^n)$  as in [5, 24]. This gives Algorithm 2.2.

In this Subsection, we shall investigate the precision and the convergence of this Algorithm. As expected, an optimal *a priori* error estimates will be established. On the other hand, Algorithm 2.2 can still suffer from slow convergence if the meshes do not present a conforming interface (Definition 2.2).

### 2.4.1 The error estimate for Algorithm 2.2

The first thing to check about this algorithm is whether each iteration of it is well defined. In particular, it is not immediate to see if the fine problem for  $(u_h^n, \lambda_h^n)$  admits a unique solution in  $V_h \times M_h^d$ . In order to see it, we note that this problem can be rewritten in a compact form as: find  $(u_h^n, \lambda_h^n) \in V_h \times M_h^d$  such that

$$\mathcal{B}_{\Lambda_\varepsilon}((u_h^n, \lambda_h^n), (v_h, \mu_h)) = \int_{\Lambda_\varepsilon} f v_h - \int_\Gamma u_H^n \mu_h, \quad \forall (v_h, \mu_h) \in V_h \times M_h^d$$

where

$$\mathcal{B}_{\Lambda_\varepsilon}((u, \lambda), (v, \mu)) = \int_{\Lambda_\varepsilon} \nabla u \cdot \nabla v - \int_\Gamma \lambda v - \int_\Gamma \mu u - \sigma h \int_\Gamma (\lambda - n \cdot \nabla u)(\mu - n \cdot \nabla v)$$

Choose an initial guess  $u_H^0 \in V_H$  and the parameters  $\omega \in (0, 1]$ ,  $\sigma > 0$   
**for**  $n = 1, 2, 3, \dots$  **do**  
    Find  $u_h^n \in V_h$  and  $\lambda_h^n \in M_h^d$  such that

$$\begin{aligned} \int_{\Lambda_\varepsilon} \nabla u_h^n \cdot \nabla v_h - \int_\Gamma \lambda_h^n v_h + \sigma h \int_\Gamma (\lambda_h^n - n \cdot \nabla u_h^n) n \cdot \nabla v_h \\ = \int_{\Lambda_\varepsilon} f v_h, \quad \forall v_h \in V_h \\ - \int_\Gamma u_h^n \mu_h - \sigma h \int_\Gamma (\lambda_h^n - n \cdot \nabla u_h^n) \mu_h \\ = - \int_\Gamma u_H^{n-1} \mu_h, \quad \forall \mu_h \in M_h^d \end{aligned}$$

    Find  $u_H^n \in V_H$  such that

$$\begin{aligned} \int_\Omega \nabla u_H^n \cdot \nabla v_H = \omega \int_{\Omega \setminus \bar{\Lambda}} f v_H - \omega \int_\Gamma \lambda_h^n v_H + \omega \int_\Lambda \nabla u_H^{n-1} \cdot \nabla v_H \\ + (1 - \omega) \int_\Omega \nabla u_H^{n-1} \cdot \nabla v_H, \quad \forall v_H \in V_H \end{aligned}$$

    Set

$$u_{Hh}^{n-1/2} = \begin{cases} u_h^n, & \text{in } \Lambda_\varepsilon \\ u_H^{n-1}, & \text{outside } \Lambda \end{cases} \quad u_{Hh}^n = \begin{cases} u_h^n, & \text{in } \Lambda_\varepsilon \\ u_H^n, & \text{outside } \Lambda \end{cases}$$

**end**

**Algorithm 2.2:** Multi-model numerical zoom with discontinuous Lagrange multipliers

**Lemma 2.13.** *There exists mesh-independent constants  $\sigma_0 > 0$ ,  $C > 0$  and  $c > 0$  such that for all  $\sigma \leq \sigma_0$*

$$\inf_{(u_h, \lambda_h) \in V_h \times M_h^d} \sup_{(v_h, \mu_h) \in V_h \times M_h^d} \frac{\mathcal{B}_{\Lambda_\varepsilon}((u_h, \lambda_h), (v_h, \mu_h))}{\| \| u_h, \lambda_h \| \|_{\Lambda_\varepsilon} \| \| v_h, \mu_h \| \|_{\Lambda_\varepsilon}} \geq c, \quad (2.54)$$

$$\sup_{(u_h, \lambda_h) \in V_h^d \times M_h} \sup_{(v_h, \mu_h) \in V_h \times M_h^d} \frac{\mathcal{B}_{\Lambda_\varepsilon}((u_h, \lambda_h), (v_h, \mu_h))}{\| \| u_h, \lambda_h \| \|_{\Lambda_\varepsilon} \| \| v_h, \mu_h \| \|_{\Lambda_\varepsilon}} \leq C, \quad (2.55)$$

where the triple norm is defined by

$$\| \| u, \lambda \| \|_{\Lambda_\varepsilon} = \left( |u|_{1, \Lambda_\varepsilon}^2 + \frac{1}{h} |u|_{0, \Gamma}^2 + h \| \lambda \|_{0, \Gamma}^2 \right)^{1/2},$$

and  $c, C$  are mesh-independent constants.

The proof of this lemma is virtually the same as that of the forthcoming Lemma 2.14 and we omit it. We note only that the infsup condition (2.54) ensures indeed that the matrix of the problem for  $(u_h^n, \lambda_h^n)$  on each iteration of Algorithm 2.2 is indeed non singular and thus  $(u_h^n, \lambda_h^n)$  are well defined provided the stabilization parameter  $\sigma$  is chosen sufficiently small.

We now turn to the study of the precision of Algorithm 2.2. Assuming for the moment that this algorithm converges (this will be indeed proved in the next section), we write  $u_H^n \rightarrow u_H$ ,  $u_h^n \rightarrow u_h$  on  $\Omega$  and  $\lambda_h^n \rightarrow \lambda_h$  on  $\Gamma$  as  $n \rightarrow \infty$ . Passing to the limit in Algorithm 2, it is easy to see that the functions  $u_H \in V_H$ ,  $u_h \in V_h$  and  $\lambda_h \in M_h^d$  satisfy (2.6) and

$$\int_{\Lambda_\varepsilon} \nabla u_h \cdot \nabla v_h - \int_{\Gamma} \lambda_h v_h + \sigma h \int_{\Gamma} (\lambda_h - n \cdot \nabla u_h) n \cdot \nabla v_h = \int_{\Lambda_\varepsilon} f v_h, \quad (2.56)$$

$$\int_{\Gamma} \mu_h u_h + \sigma h \int_{\Gamma} (\lambda_h - n \cdot \nabla u_h) \mu_h = \int_{\Gamma} \mu_h u_H, \quad (2.57)$$

$\forall v_h \in V_h$  and  $\mu_h \in M_h$

Taking the difference between the two equations above, adding the result to (2.6), and combining  $u_H$  and  $u_h$  into  $u_{Hh} \in V_{Hh}^d$  where  $V_{Hh}^d$  is the space of possibly discontinuous finite element functions (2.32), we see that the problem for  $(u_{Hh}, \lambda_h) \in V_{Hh}^d \times M_h^d$  can be written in the compact form

$$\mathcal{B}((u_{Hh}, \lambda_h), (v_{Hh}, \mu_h)) = L(v_{Hh}) \quad \forall (v_{Hh}, \mu_h) \in V_{Hh}^d \times M_h^d \quad (2.58)$$

where

$$\mathcal{B}((u, \lambda), (v, \mu)) = a(u, v) + \int_{\Gamma} \lambda [v] + \int_{\Gamma} \mu [u] - \sigma h \int_{\Gamma} (\lambda - n \cdot \nabla u|_{\Lambda_\varepsilon}) (\mu - n \cdot \nabla v|_{\Lambda_\varepsilon})$$

and the brackets stand for the jump on  $\Gamma$ , i.e.  $[v] = v|_{\Omega \setminus \bar{\Lambda}} - v|_{\Lambda_\varepsilon}$ .

The following result is an adaptation of Lemma 3 from [24].

**Lemma 2.14.** *There exists mesh-independent constants  $\sigma_0 > 0$ ,  $C > 0$  and  $c > 0$  such that for all  $\sigma \leq \sigma_0$*

$$\inf_{(u_{Hh}, \lambda_h) \in V_{Hh}^d \times M_h^d} \sup_{(v_{Hh}, \mu_h) \in V_{Hh}^d \times M_h^d} \frac{\mathcal{B}((u_{Hh}, \lambda_h), (v_{Hh}, \mu_h))}{\| \| u_{Hh}, \lambda_h \| \| \| v_{Hh}, \mu_h \| \| } \geq c, \quad (2.59)$$

$$\sup_{(u_{Hh}, \lambda_h) \in V_{Hh}^d \times M_h^d} \sup_{(v_{Hh}, \mu_h) \in V_{Hh}^d \times M_h^d} \frac{\mathcal{B}((u_{Hh}, \lambda_h), (v_{Hh}, \mu_h))}{\| \| u_{Hh}, \lambda_h \| \| \| v_{Hh}, \mu_h \| \| } \leq C, \quad (2.60)$$

where the triple norm is defined by

$$\| \| u, \lambda \| \| = \left( |u|_{1, \Omega \setminus \Gamma}^2 + \frac{1}{h} \| [u] \|_{0, \Gamma}^2 + h \| \lambda \|_{0, \Gamma}^2 \right)^{1/2}, \quad |u|_{1, \Omega \setminus \Gamma}^2 := |u|_{1, \Omega \setminus \bar{\Lambda}}^2 + |u|_{1, \Lambda_\varepsilon}^2,$$

and  $c, C$  are mesh-independent constants.

*Proof.* We observe  $\forall (u_{Hh}, \lambda_h) \in V_{Hh}^d \times M_h^d$  with  $u_{Hh}|_{\Omega \setminus \bar{\Lambda}} = u_H$  and  $u_{Hh}|_{\Lambda_\varepsilon} = u_h$

$$\begin{aligned} \mathcal{B}((u_{Hh}, \lambda_h), (u_{Hh}, -\lambda_h)) &= |u_{Hh}|_{1, \Omega \setminus \Gamma}^2 - \sigma h \int_{\Gamma} |n \cdot \nabla u_h|^2 + \sigma h \int_{\Gamma} \lambda_h^2 \\ &\geq \frac{1}{2} |u_{Hh}|_{1, \Omega \setminus \Gamma}^2 + \sigma h \|\lambda_h\|_{0, \Gamma}^2. \end{aligned}$$

We have used here the inverse inequality

$$\|\nabla u_h\|_{0, \Gamma} \leq \frac{C_I}{\sqrt{h}} \|\nabla u_h\|_{0, \Lambda_\varepsilon} \quad (2.61)$$

valid for any  $u_h \in V_h$  and assumed that  $\sigma$  is small enough so that  $\sigma C_I^2 \leq \frac{1}{2}$ . Inequality (2.61) can be easily proved element by element by running over all the cells of  $\mathcal{T}_h$  adjacent to  $\Gamma$  and passing to a reference cell. This ensures in particular that  $C_I$  depends only on the regularity of  $\mathcal{T}_h$ .

Let us now take  $\bar{\mu}_h = \frac{1}{h} P_h[u_{Hh}]$  where  $P_h$  is the  $L^2(\Gamma)$ -orthogonal projector on  $M_h^d$ . Using again the inverse inequality above, we obtain

$$\begin{aligned} \mathcal{B}((u_{Hh}, \lambda_h), (0, \bar{\mu}_h)) &= \frac{1}{h} \|P_h[u_{Hh}]\|_{0, \Gamma}^2 - \sigma \int_{\Gamma} (\lambda_h - n \cdot \nabla u_h) P_h[u_{Hh}] \\ &\geq \frac{1}{h} \|P_h[u_{Hh}]\|_{0, \Gamma}^2 - \sigma \left( \sqrt{h} \|\lambda_h\|_{0, \Gamma} + \sqrt{h} \|\nabla u_h\|_{0, \Gamma} \right) \frac{1}{\sqrt{h}} \|P_h[u_{Hh}]\|_{0, \Gamma} \\ &\geq \frac{1}{2h} \|P_h[u_{Hh}]\|_{0, \Gamma}^2 - 2\sigma^2 h \|\lambda_h\|_{0, \Gamma}^2 - 2\sigma^2 C_I^2 |u_{Hh}|_{1, \Omega \setminus \Gamma}^2. \end{aligned}$$

Combining the results above and taking  $\eta > 0$  small enough yields

$$\begin{aligned} \mathcal{B}((u_{Hh}, \lambda_h), (u_{Hh}, -\lambda_h + \eta \bar{\mu}_h)) &\geq c \left( |u_{Hh}|_{1, \Omega \setminus \Gamma}^2 + h \|\lambda_h\|_{0, \Gamma}^2 + \frac{\eta}{2h} \|P_h[u_{Hh}]\|_{0, \Gamma}^2 \right) \\ &= c \left( |u_{Hh}|_{1, \Omega \setminus \Gamma}^2 + h \|\lambda_h\|_{0, \Gamma}^2 + \frac{\eta}{2h} \left( \|u_{Hh}\|_{0, \Gamma}^2 - \|P_h[u_{Hh}]\|_{0, \Gamma}^2 \right) \right) \end{aligned}$$

The equality in the last line is valid by Pythagoras theorem.

In order to eliminate the projector  $P_h$  in the last estimate, we remark first the bound

$$\|v - P_h v\|_{0, \Gamma} \leq C \sqrt{h} |v|_{1, \Lambda_\varepsilon} \quad (2.62)$$

valid for any  $v \in H^1(\Lambda_\varepsilon)$ . To prove (2.62) let us consider a boundary edge  $E$  of mesh  $\mathcal{T}_h$  attached to a mesh element (cell)  $T$ . Denoting by  $\bar{v}_E$  the average of  $v$  over  $E$ , i.e.  $\bar{v}_E = \frac{1}{|E|} \int_E v$ , we see by scaling to a reference cell

$$\|v - \bar{v}_E\|_{0, E} \leq C \sqrt{h} |v|_{1, T} \quad (2.63)$$

Since the space of piecewise constants on the boundary edges of  $\mathcal{T}_h$  on  $\Gamma$  is a subspace of  $M_h$  we see that

$$\|v - P_h v\|_{0,\Gamma} \leq \left( \sum_E \|v - \bar{v}_E\|_{0,E}^2 \right)^{1/2}$$

with the sum taken over all boundary edges of  $\mathcal{T}_h$  on  $\Gamma$ . Combining the last two bounds leads to (2.62).

We also have the bound

$$\|v - P_h v\|_{0,\Gamma} \leq C\sqrt{h}|v|_{1,\Omega \setminus \bar{\Lambda}} \quad (2.64)$$

for any  $v \in H^1(\Omega \setminus \bar{\Lambda})$ . This can be proved similar to (2.62) by associating to any boundary edge  $E$  of mesh  $\mathcal{T}_h$  a regular cell  $T$  lying inside  $\Omega \setminus \bar{\Lambda}$  and having  $E$  as a side. One can construct these cells so that they intersect each other only a finite (bounded uniformly in  $h$ ) number of times. Then summing of (2.63) with these cells over the edges  $E$  on  $\Gamma$  yields (2.64).

Applying (2.62) to  $v = u_h$  and (2.64) to  $v = u_H$  we conclude

$$\begin{aligned} \|[u_{Hh}] - P_h[u_{Hh}]\|_{0,\Gamma} &\leq \|u_H - P_h u_H\|_{0,\Gamma} + \|u_h - P_h u_h\|_{0,\Gamma} \\ &\leq C\sqrt{h} \left( |u_H|_{1,\Omega \setminus \bar{\Lambda}} + |u_h|_{1,\Lambda_\varepsilon} \right) \leq C\sqrt{h}|u_{Hh}|_{1,\Omega \setminus \Gamma} \end{aligned}$$

so that, recalling that  $\eta$  is supposed sufficiently small,

$$\mathcal{B}((u_{Hh}, \lambda_h), (u_{Hh}, -\lambda_h + \eta \bar{\mu}_h)) \geq c \left( \frac{1}{2} |u_{Hh}|_{1,\Omega \setminus \Gamma}^2 + h \|\lambda_h\|_{0,\Gamma}^2 + \frac{\eta}{2h} \|[u_{Hh}]\|_{0,\Gamma}^2 \right).$$

This proves (2.59).

In order to prove (2.60) we remark

$$\begin{aligned} \mathcal{B}((u_{Hh}, \lambda_h), (v_{Hh}, \mu_h)) &\leq \|(u_{Hh}, \lambda_h)\| \|(v_{Hh}, \mu_h)\| + \sigma h (\|\nabla u_h\|_{0,\Gamma} + \|\lambda_h\|_{0,\Gamma}) (\|\nabla v_h\|_{0,\Gamma} + \|\mu_h\|_{0,\Gamma}) \\ &\leq C \|(u_{Hh}, \lambda_h)\| \|(v_{Hh}, \mu_h)\| \end{aligned}$$

using the inverse inequality (2.61).  $\square$

**Theorem 2.15.** *Problem (2.58) admits the unique solution  $(u_{Hh}, \lambda_h) \in V_{Hh}^d \times M_h^d$  provided the stabilization parameter  $\sigma$  is sufficiently small. If  $u$ , the exact solution to (2.1), is in  $H^{k+1}(\Omega)$ , we have moreover the following a priori error estimate*

$$\|u_{Hh} - u\|_{1,\Omega \setminus \Gamma} \leq C (H^k \|u\|_{k+1,\Omega \setminus \bar{\Lambda}} + h^k \|u\|_{k+1,\Lambda_\varepsilon}) \quad (2.65)$$

with a constant  $C$  independent of  $H$ ,  $h$  and  $u$ .

*Proof.* Let

$$\begin{aligned} V^d &= \{v \in L^2(\Omega) : v|_{\Omega \setminus \bar{\Lambda}} \in H^1(\Omega \setminus \bar{\Lambda}), v|_{\Lambda_\varepsilon} \in H^1(\Lambda_\varepsilon), v|_{\partial\Omega} = 0\}, \\ M &= L^2(\Gamma). \end{aligned}$$

The exact solution  $u \in V^d$  together with  $\lambda = n \cdot \nabla u|_{\Gamma} \in M$  satisfy

$$\mathcal{B}((u, \lambda), (v, \mu)) = L(v) \quad \forall (v, \mu) \in V^d \times M$$

Subtracting (2.58) from the last equation we see that

$$\mathcal{B}((u - u_{Hh}, \lambda - \lambda_h), (v_{Hh}, \mu_h)) = L(v_{Hh}) \quad \forall (v_{Hh}, \mu_h) \in V_{Hh}^d \times M_h^d$$

so that Lemma 2.14 implies

$$\|u - u_{Hh}\|_{1, \Omega \setminus \Gamma} \leq \| |u - u_{Hh}, \lambda - \lambda_h| \| \leq C \inf_{(\tilde{u}_{Hh}, \tilde{\lambda}_h) \in V_{Hh}^d \times M_h^d} \| |u - \tilde{u}_{Hh}, \lambda - \tilde{\lambda}_h| \|. \quad (2.66)$$

It remains thus to find the interpolants  $\tilde{u}_{Hh}$  and  $\tilde{\lambda}_h$  to  $u$  and  $\lambda$  respectively that provide the optimal error estimate in the sense of inequality (2.65). We begin by constructing the appropriate  $v_{Hh}$ . Let  $\tilde{u} \in H^{k+1}(\Omega)$  be the extension of  $u$  from  $\Omega \setminus \bar{\Lambda}$  to the whole of  $\Omega$ , i.e.  $\tilde{u} = u$  on  $\Omega \setminus \bar{\Lambda}$ . By the extension theorem for Sobolev spaces [1, 38], we can construct  $\tilde{u}$  so that  $\|\tilde{u}\|_{k+1, \Omega} \leq C\|u\|_{k+1, \Omega \setminus \bar{\Lambda}}$  where  $C$  is a constant that depends only on  $\Omega$  and  $\Lambda_\varepsilon$ . Let  $I_H : H^{k+1}(\Omega) \rightarrow V_H$  and  $I_h : H^{k+1}(\Lambda_\varepsilon) \rightarrow V_h$  be the Clément type interpolation operators satisfying  $|v - I_H v|_{1, \Omega} \leq CH^k|v|_{k+1, \Omega}$  for any  $v \in H^{k+1}(\Omega)$  and  $|v - I_h v|_{1, \Omega} \leq Ch^k|v|_{k+1, \Lambda_\varepsilon}$  for any  $v \in H^{k+1}(\Lambda_\varepsilon)$  where the constant  $C$  depends only on the regularity of the meshes. Several other properties of the interpolation operators will be also used. All of them can be proven by the methods of [7, 37]. We choose now  $\tilde{u}_{Hh} \in V_{Hh}$  so that  $\tilde{u}_{Hh} = I_H \tilde{u}$  on  $\Omega \setminus \bar{\Lambda}$  and  $\tilde{u}_{Hh} = I_h(u + I_H \tilde{u} - \tilde{u})$  on  $\Lambda_\varepsilon$ . Hence

$$\begin{aligned} \|u - \tilde{u}_{Hh}\|_{1, \Omega \setminus \Gamma} &= \left( |u - I_H \tilde{u}|_{1, \Omega \setminus \bar{\Lambda}}^2 + |u - I_h u + I_h(\tilde{u} - I_H \tilde{u})|_{1, \Lambda_\varepsilon}^2 \right)^{\frac{1}{2}} \quad (2.67) \\ &\leq C \left( |\tilde{u} - I_H \tilde{u}|_{1, \Omega}^2 + |u - I_h u|_{1, \Lambda_\varepsilon}^2 \right)^{\frac{1}{2}} \\ &\leq C(H^k|\tilde{u}|_{k+1, \Omega} + h^k|u|_{k+1, \Lambda_\varepsilon}) \leq C(H^k\|u\|_{k+1, \Omega \setminus \bar{\Lambda}} + h^k|u|_{k+1, \Lambda_\varepsilon}) \end{aligned}$$

Note that we have used here, besides the above mentioned interpolation estimates, the  $H^1$ -stability of operator  $I_h$ , i.e.  $|I_h v|_{1, \Lambda_\varepsilon} \leq C|v|_{1, \Lambda_\varepsilon}$  for any  $v \in H^1(\Lambda_\varepsilon)$ .

The interpolation operator  $I_h$  also satisfies  $\|v - I_h v\|_{0, \Gamma} \leq Ch^{k+\frac{1}{2}}|v|_{k+1, \Lambda_\varepsilon}$  (resp.  $\|v - I_h v\|_{0, \Gamma} \leq C\sqrt{h}|v|_{\Lambda_\varepsilon}$ ) for any  $v \in H^{k+1}(\Lambda_\varepsilon)$  (resp.  $v \in H^1(\Lambda_\varepsilon)$ ). Operator  $I_h$  can be constructed to preserve the homogeneous boundary conditions on  $\Gamma$  so that  $I_h(u - \tilde{u}) = 0$  on  $\Gamma$ . Hence,

$$\begin{aligned} \| |u - \tilde{u}_{Hh}| \|_{0, \Gamma} &= \| |I_H \tilde{u} - I_h I_H \tilde{u}| \|_{0, \Gamma} \leq \| |I_H \tilde{u} - \tilde{u} - I_h(I_H \tilde{u} - \tilde{u})| \|_{0, \Gamma} + \| |\tilde{u} - I_h \tilde{u}| \|_{0, \Gamma} \quad (2.68) \\ &\leq C(\sqrt{h}|I_H \tilde{u} - \tilde{u}|_{1, \Lambda_\varepsilon} + h^{k+\frac{1}{2}}|\tilde{u}|_{k+1, \Lambda_\varepsilon}) \\ &\leq C\sqrt{h}(H^k|\tilde{u}|_{k+1, \Omega} + h^k|\tilde{u}|_{k+1, \Lambda_\varepsilon}) \leq C\sqrt{h}H^k\|u\|_{k+1, \Omega \setminus \bar{\Lambda}} \end{aligned}$$

Let us finally take  $\tilde{\lambda}_h = P_h \lambda$  where  $P_h$  is the  $L^2(\Gamma)$ -orthogonal projector on



$M_h^d$ . Let us recall that  $\Gamma$  consists of  $N_\Gamma$  sides  $\Gamma_1, \dots, \Gamma_{N_\Gamma}$ . The standard finite element estimates give on any side  $\Gamma_s$

$$\|v - P_h v\|_{0, \Gamma_s} \leq Ch^{k-1} \|v\|_{k-1, \Gamma_s} \text{ and } \|v - P_h v\|_{0, \Gamma_s} \leq Ch^k \|v\|_{k, \Gamma_s}$$

for any  $v \in H^{k-1}(\Gamma_s)$  (resp.  $v \in H^k(\Gamma_s)$ ) so that, by interpolation,

$$\|v - P_h v\|_{0, \Gamma_s} \leq Ch^{k-\frac{1}{2}} \|v\|_{k-\frac{1}{2}, \Gamma_s}$$

for any  $v \in H^{\frac{1}{2}}(\Gamma_s)$ . Since  $u \in H^{k+1}(\Lambda_\varepsilon)$ , the trace theorem ensures that  $\lambda|_{\Gamma_s} \in H^{k-1/2}(\Gamma_s)$  on any side  $\Gamma_s$  with the usual estimate of the norms. Hence,

$$\|\lambda - \mu_h\|_{0, \Gamma} = \left( \sum_{s=1}^{N_\Gamma} \|\lambda - P_h \lambda\|_{0, \Gamma_s}^2 \right)^{\frac{1}{2}} \leq Ch^{k-\frac{1}{2}} \sum_{s=1}^{N_\Gamma} \|\lambda\|_{k-\frac{1}{2}, \Gamma_s} \leq Ch^{k-\frac{1}{2}} \|u\|_{k+1, \Lambda_\varepsilon}. \quad (2.69)$$

Combining (2.67), (2.68) and (2.69) yields

$$\| \|u - \tilde{u}_{Hh}, \lambda - \tilde{\lambda}_h \| \| \leq C (H^k \|u\|_{k+1, \Omega \setminus \bar{\Lambda}} + h^k \|u\|_{k+1, \Lambda_\varepsilon}).$$

which leads to (2.65) in view of (2.66).  $\square$

## 2.4.2 Convergence of the iterative algorithm 2.2

The proof of the convergence of Algorithm 2.2 will be based on a study of operator  $A_{Hh}^d : V_H \rightarrow V_H$  defined for fixed  $\mathcal{T}_H$  and  $\mathcal{T}_h$  as follows: for any  $z_H \in V_H$  the function  $A_{Hh}^d z_H \in V_H$  solves

$$c(A_{Hh}^d z_H, v_H) = \int_{\Omega \setminus \bar{\Lambda}} \nabla z_H \cdot \nabla v_H + \int_{\Gamma} \nu_h v_H, \quad \forall v_H \in V_H \quad (2.70)$$

where  $(\cdot, \cdot)$  is the scalar product (2.15) and  $\nu_h \in M_h^d$  together with  $z_h \in V_h$  come as the solution to

$$\int_{\Lambda_\varepsilon} \nabla z_h \cdot \nabla v_h - \int_{\Gamma} \nu_h v_h + \sigma h \int_{\Gamma} (\nu_h - n \cdot \nabla z_h) n \cdot \nabla v_h = 0, \quad \forall v_h \in V_h \quad (2.71)$$

$$\int_{\Gamma} z_h \mu_h + \sigma h \int_{\Gamma} (\nu_h - n \cdot \nabla z_h) \mu_h = \int_{\Gamma} z_H \mu_h, \quad \forall \mu_h \in M_h^d. \quad (2.72)$$

Repeating the calculation from the beginning of Section 2.2.2, we easily see that  $u_H^n$  evolves from one iteration to another as

$$u_H^n = (I - \omega A_{Hh}^d) u_H^{n-1} + \omega F_H \quad (2.73)$$

with  $F_H \in V_H$  defined by (2.19).

Taking the linear combination of equations (2.70), (2.71), (2.72) with coefficients 1, -1, 1 we observe

$$c(A_{Hh}^d z_H, v_H) = \mathcal{B}((z_{Hh}, \nu_h), (v_{Hh}, \mu_h)) \quad (2.74)$$

where  $z_{Hh} \in V_{Hh}^d$  is the combination of  $z_H$  and  $z_h$  given by (2.71)–(2.72),  $\nu_h$  is also given by (2.71)–(2.72), while  $v_{Hh} \in V_{Hh}^d$  and  $\mu_h \in M_{Hh}^d$  are arbitrary.

We will now prove that operator  $A_{Hh}^d$  is self-adjoint and coercive with respect to the scalar product (2.15) on  $V_H^1 \subset V_H$ , i.e. the orthogonal complement of  $V_H^0$  as defined by (2.24).

**Lemma 2.16.** *Operator  $A_{Hh}^d$  is self-adjoint with respect to the scalar product (2.15)*

$$c(A_{Hh}^d z_H, z_H^*) = c(z_H, A_{Hh}^d z_H^*), \quad \forall z_H, z_H^* \in V_H \quad (2.75)$$

*Proof.* Take any  $z_H, z_H^* \in V_H$  and let  $(z_h, \nu_h) \in V_h \times M_h^d$ , resp.  $(z_h^*, \nu_h^*) \in V_h \times M_h^d$  be the solutions to (2.71)–(2.72) with  $z_H$ , resp.  $z_H^*$ , on the right hand side of (2.72). The relation (2.74) then gives

$$c(A_{Hh}^d z_H, z_H^*) = \mathcal{B}((z_{Hh}, \nu_h), (z_{Hh}^*, \nu_h^*))$$

where  $z_{Hh}^* \in V_{Hh}^d$  is the combination of  $z_H^*$  and  $z_h^*$ . This entails (2.75) since the bilinear form  $\mathcal{B}$  is symmetric.  $\square$

In what follows we shall work with the ensemble  $\Lambda_H$  of the cells from the coarse mesh that lie inside  $\Lambda$  and we shall need to introduce some assumptions about this set, cf. Definitions 2.3, 2.4 and 2.5.

**Lemma 2.17.** *The kernel of operator  $A_{Hh}^d$  coincides with  $V_H^0$ , cf. (2.24), and  $A_{Hh}^d$  is coercive on its orthogonal complement  $V_H^1$ . More precisely, assuming that  $\Lambda$  is regular with respect to  $\mathcal{T}_H$ , there exists  $m > 0$  depending only on the regularity parameters of  $\Lambda$  with respect to  $\mathcal{T}_H$ , on  $\kappa_H \in (0, 1]$ , and on the regularity parameters of  $\mathcal{T}_H$  itself, such that*

$$c(A_{Hh}^d v_H, v_H) \geq m |v_H|_{1,\Omega}^2 \quad \forall v_H \in V_H^1. \quad (2.76)$$

*The norm of  $A_{Hh}^d$  as an operator in the Hilbert space  $H_0^1(\Omega)$  equipped with the scalar product (2.15) is bounded by a mesh-independent constant.*

*Proof.* Let us first prove that  $\ker A_{Hh}^d \subset V_H^0$ . If  $z_H \in \ker A_{Hh}^d$ , then  $z_H = 0$  on  $\Omega \setminus \bar{\Lambda}$  as follows from the expression for  $c(A_{Hh}^d z_H, z_H)$  in (2.22). This means that  $z_H = 0$  on every cell  $T \in \mathcal{T}_H$  which is not entirely inside  $\Lambda$ , since  $z_H$  is a polynomial. We have thus  $z_H = 0$  on  $\Omega \setminus \bar{\Lambda}_H$ . On the other hand, if  $z_H \in V_H^0$  then  $z_h = 0$  on  $\Lambda_\varepsilon$  and  $\nu_h = 0$  on  $\Gamma$  so that  $A_{Hh}^d z_H = 0$ . This entails  $\ker A_{Hh}^d = V_H^0$ .

In order to prove the coercivity estimate we invoke again (2.74) with  $v_H = z_H \in V_H^1$ , which implies for  $\sigma$  sufficiently small thanks to the inverse

inequality (2.61)

$$\begin{aligned} c(A_{Hh}^d z_H, z_H) &= \mathcal{B}((z_{Hh}, \nu_h), (z_{Hh}, -\nu_h)) = \|z_{Hh}\|_{1, \Omega \setminus \Gamma}^2 + \sigma h \|\nu_h\|_{0, \Gamma}^2 - \sigma h \|n \cdot \nabla u_h\|_{0, \Gamma}^2 \\ &\geq \int_{\Omega \setminus \bar{\Lambda}} \nabla z_H \cdot \nabla z_H \geq \sum_{T \in \mathcal{T}_H} \int_{T \setminus \bar{\Lambda}} |\nabla z_H|^2 \geq \delta \int_{\Omega \setminus \bar{\Lambda}_H} |\nabla z_H|^2 \end{aligned} \quad (2.77)$$

From this point on, we can repeat the proof of the similar Lemma 2.11, leading to

$$c(A_{Hh}^d z_H, z_H) \geq \frac{\delta}{(\|R_H\|^2 \|E\|^2 + 1) C_P} |z_H|_{1, \Omega}^2,$$

which is equivalent to (2.76).

The last statement of the Lemma concerns the norm of operator  $A_{Hh}^d$ . In order to prove it, we first observe that problem (2.71)–(2.72) for  $(z_h, \nu_h) \in V_h \times M_h$  can be written as

$$\mathcal{B}_{\Lambda_\varepsilon}((z_h, \nu_h), (v_h, \mu_h)) = - \int z_H \mu_h, \quad \forall (v_h, \mu_h) \in V_h \times M_h^d$$

Let  $\tilde{z}_h = I_h z_H$  with  $I_h$  being an appropriate Clément-like interpolation operator on  $V_h$ . Let  $r_h = \tilde{z}_h - z_h$  and observe

$$\begin{aligned} \mathcal{B}_{\Lambda_\varepsilon}((r_h, \nu_h), (v_h, \mu_h)) &= -a(\tilde{z}_h, v_h) - \int_{\Gamma} (z_H - \tilde{z}_h) \mu_h - \sigma h \int_{\Gamma} n \cdot \nabla \tilde{z}_h (\mu_h - n \cdot \nabla v_h) \\ &\leq |\tilde{z}_h|_{1, \Lambda_\varepsilon} |v_h|_{1, \Lambda_\varepsilon} + \|z_H - \tilde{z}_h\|_{0, \Gamma} \|\mu_h\|_{0, \Gamma} + |\tilde{z}_h|_{1, \Lambda_\varepsilon} (\sqrt{h} \|\mu_h\|_{0, \Gamma} + |v_h|_{1, \Lambda_\varepsilon}) \\ &\leq (|\tilde{z}_h|_{1, \Lambda_\varepsilon} + \frac{1}{\sqrt{h}} \|z_H - \tilde{z}_h\|_{0, \Gamma}) \| |v_h, \mu_h| \|_{\Lambda_\varepsilon} \end{aligned}$$

Lemma 2.13 together with the properties of the interpolation  $I_h$  imply

$$\| |z_h - \tilde{z}_h, \nu_h| \|_{\Lambda_\varepsilon} = \| |r_h, \nu_h| \|_{\Lambda_\varepsilon} \leq C (|I_h z_H|_{1, \Lambda_\varepsilon} + \frac{1}{\sqrt{h}} \|z_H - I_h z_H\|_{0, \Gamma}) \leq C \|z_H\|_{1, \Omega}$$

with a constant that depends only on  $\Lambda_\varepsilon$ . Using (2.71) we obtain for any  $v \in H^1(\Omega)$

$$\begin{aligned} \int_{\Gamma} \nu_h v &= \int_{\Gamma} \nu_h (v - I_h v) + \int_{\Gamma} \nu_h I_h v \quad (2.78) \\ &= \int_{\Gamma} \nu_h (v - I_h v) + \int_{\Lambda_\varepsilon} \nabla z_h \cdot \nabla I_h v + \sigma h \int_{\Gamma} (\nu_h - n \cdot \nabla z_h) n \cdot \nabla I_h v \\ &\leq \|\nu_h\|_{0, \Gamma} \|v - I_h v\|_{0, \Gamma} + C \|z_h\|_{1, \Lambda_\varepsilon} \|I_h v\|_{1, \Lambda_\varepsilon} + Ch (\|\nu_h\|_{0, \Gamma} + \|\nabla z_h\|_{0, \Gamma}) \|\nabla I_h v\|_{0, \Gamma} \\ &\leq C (\sqrt{h} \|\nu_h\|_{0, \Gamma} + \|z_h\|_{1, \Lambda_\varepsilon}) \|v\|_{1, \Omega} \\ &\leq C (\| |z_h - \tilde{z}_h, \nu_h| \|_{\Lambda_\varepsilon} + \|\tilde{z}_h\|_{1, \Lambda_\varepsilon}) \|v\|_{1, \Omega} \leq C \|z_H\|_{1, \Omega} \|v\|_{1, \Omega} \end{aligned}$$

The definition of operator  $A_{Hh}^d$  now gives  $\forall z_H, v_H \in V_H$

$$\begin{aligned} c(A_{Hh}^d z_H, v_H) &\leq C(|z_H|_{1,\Omega \setminus \bar{\Lambda}} |v_H|_{1,\Omega \setminus \bar{\Lambda}} + \|z_H\|_{1,\Omega} \|v_H\|_{1,\Omega}) \\ &\leq C \|z_H\|_{1,\Omega} \|v_H\|_{1,\Omega} \end{aligned}$$

where we have used (2.78) with  $v = v_H$ . This proves  $\|A_{Hh}^d\| \leq C$  with a mesh-independent constants  $C$ . □

**Theorem 2.18.** *Algorithm 2.2 converges to the solution to (2.58) provided  $0 < \omega < \omega^*$  where  $\omega^*$  is a mesh-independent constant. This means that  $u_{Hh}^n \rightarrow u_{Hh}$  and  $\lambda_h^n \rightarrow \lambda_h$  as  $n \rightarrow \infty$  where  $(u_{Hh}, \lambda_h) \in V_{Hh}^d \times M_h^d$  is solution to (2.9). The convergence rate depends on the regularity of  $\mathcal{T}_H$ , on  $\Lambda_\varepsilon$  and on its regularity with respect to  $\mathcal{T}_H$  and also on the parameter  $\kappa_H$  introduced in Lemma 2.3.*

The proof of this Theorem is completely the same as that of Theorem 2.4 and we omit it.

## 2.5 A modification of the algorithm for the case of a strongly non conforming interface

Algorithm 2.2 presented in the last section improves (at least in theory) the accuracy of the original Algorithm 2.1 in the case of general non  $\Gamma$ -nested meshes. However, it does not resolve the issue of slow convergence on meshes without conformal interface, which can be of practical importance, as outlined in Remark 2.3. In this section, we present a slight modification of Algorithm 2.2, namely Algorithm 2.3. Choosing the patch  $\Lambda$  conveniently (possibly slightly larger than what was required in Algorithm 2.2), we can always ensure that the multi-scale geometrical perturbation  $\omega_\varepsilon$  is inside  $\Lambda_H$ , cf. Definition 2.3. This is implicitly assumed from now on. We shall show that the rate of convergence of the new Algorithm 2.3 is essentially independent of the manner in which the patch  $\Lambda$  cuts the coarse mesh  $\mathcal{T}_H$ .

Note that the reconstruction of the global solution  $u_{Hh}$  is now intentionally ambiguous: we can take both  $u_H$  and  $u_h$  as good approximations to  $u$  on the sub-domain  $\Lambda \setminus \Lambda_H$ , cf. the error estimate below. In fact, the whole idea behind Algorithm 3 is to impose on  $u_H$  to be approximately equal to  $u_h$  on  $\Lambda \setminus \Lambda_H$  in order to control better the behaviour of  $u_H$  there. Intuitively, one can say that the term with  $\lambda_h$  is not sufficient alone, as in Algorithm 2.2, to impose the correct normal derivative on  $u_H$  near  $\Gamma$ . We emphasize that this remark holds only in the case of a non conforming interface. If the interface is conforming, i.e.  $\Lambda_\varepsilon = \Lambda_H$ , the two Algorithms 2.2 and 2.3 are exactly the same.

Choose an initial guess  $u_H^0 \in V_H$  and the parameters  $\omega \in (0, 1]$ ,  $\sigma > 0$   
**for**  $n = 1, 2, 3, \dots$  **do**  
  Find  $u_h^n \in V_h$  and  $\lambda_h^n \in M_h^d$  such that

$$\begin{aligned} \int_{\Lambda_\varepsilon} \nabla u_h^n \cdot \nabla v_h - \int_{\Gamma} \lambda_h^n v_h + \sigma h \int_{\Gamma} (\lambda_h^n - n \cdot \nabla u_h^n) n \cdot \nabla v_h \\ = \int_{\Lambda_\varepsilon} f v_h, \quad \forall v_h \in V_h \\ - \int_{\Gamma} u_h^n \mu_h + \sigma h \int_{\Gamma} (\lambda_h^n - n \cdot \nabla u_h^n) \mu_h \\ = - \int_{\Gamma} u_H^{n-1} \mu_h, \quad \forall \mu_h \in M_h^d \end{aligned}$$

  Find  $u_H^n \in V_H$

$$\begin{aligned} \int_{\Omega} \nabla u_H^n \cdot \nabla v_H = \omega \int_{\Omega \setminus \bar{\Lambda}} f v_H - \omega \int_{\Gamma} \lambda_h^n v_H + \omega \int_{\Lambda_H} \nabla u_H^{n-1} \cdot \nabla v_H \\ + \omega \int_{\Lambda \setminus \bar{\Lambda}_H} \nabla u_h^n \cdot \nabla v_H \\ + (1 - \omega) \int_{\Omega} \nabla u_H^{n-1} \cdot \nabla v_H, \quad \forall v_H \in V_H \end{aligned}$$

  Set

$$u_{Hh}^{n-1/2} = \begin{cases} u_h^n, & \text{in } \Lambda_\varepsilon \\ u_H^{n-1}, & \text{outside } \Lambda \end{cases} \quad u_{Hh}^n = \begin{cases} u_h^n, & \text{in } \Lambda_\varepsilon \\ u_H^n, & \text{outside } \Lambda \end{cases}$$

**end**

**Algorithm 2.3:** Numerical zoom for non conforming interfaces

### 2.5.1 An a priori error estimate for Algorithm 2.3

Our first goal is to characterize the limit of the iterative process in Algorithm 2.3 (provided it converges) and to study the precision of this limit with respect to the exact solution of problem (2.1). We suppose thus that  $u_H^n \rightarrow u_H$ ,  $u_h^n \rightarrow u_h$  on  $\Omega$  and  $\lambda_h^n \rightarrow \lambda_h$  on  $\Gamma$  as  $n \rightarrow \infty$ . Then, the limit  $(u_H, u_h, \lambda_h) \in V_H \times V_h \times M_h^d$  satisfies

$$\int_{\Omega \setminus \bar{\Lambda}_H} \nabla u_H \cdot \nabla v_H - \int_{\Lambda \setminus \bar{\Lambda}_H} \nabla u_h \cdot \nabla v_H + \int_{\Gamma} \lambda_h v_H = \int_{\Omega \setminus \bar{\Lambda}} f v_H, \quad (2.79)$$

$\forall v_H \in V_H$

together with (2.56)–(2.57). If we compare this with the previous versions of our algorithm leading to the discrete problem (2.6), we observe again that there is now an overlap between the limit solutions  $u_H$  and  $u_h$  on  $\Lambda \setminus \bar{\Lambda}_H$  while

these solutions lived on non overlapping subdomains  $\Omega \setminus \bar{\Lambda}$  and  $\Lambda_\varepsilon$  in the original version. We need to adjust accordingly the functional setting to analyse the new formulation. We introduce the space of functions represented by two contributions that are defined on overlapping domains:

$$\begin{aligned} \hat{V} &= \{v \in H^1(\Omega \setminus \bar{\Lambda}_H) : v|_{\partial\Omega} = 0\} \times H^1(\Lambda_\varepsilon) \\ &= \{v = (v_1, v_2) \text{ such that } v_1 \in H^1(\Omega \setminus \bar{\Lambda}_H), v_2 \in H^1(\Lambda_\varepsilon) \text{ and } v_1|_{\partial\Omega} = 0\} \end{aligned}$$

equipped with the norm

$$\|v\|_{\hat{V}} = \|(v_1, v_2)\|_{\hat{V}} = \left( \|v_1\|_{1, \Omega \setminus \bar{\Lambda}_H}^2 + \|v_2\|_{1, \Lambda_\varepsilon}^2 \right)^{1/2}.$$

We introduce also a bilinear form  $\hat{a}$  on  $\hat{V} \times \hat{V}$  defined on any  $u = (u_1, u_2)$  and  $v = (v_1, v_2)$  as

$$\hat{a}(u, v) = \int_{\Omega \setminus \bar{\Lambda}_H} \nabla u_1 \cdot \nabla v_1 + \int_{\Lambda_\varepsilon} \nabla u_2 \cdot \nabla v_2 - \int_{\Lambda \setminus \bar{\Lambda}_H} \nabla u_2 \cdot \nabla v_1.$$

and the bilinear form  $\hat{B}$  on  $(\hat{V} \times M)^2$

$$\hat{B}((u, \lambda), (v, \mu)) = \hat{a}(u, v) + \int_{\Gamma} \lambda[v] + \int_{\Gamma} \mu[u] - \sigma h \int_{\Gamma} (\lambda - n \cdot \nabla u_2)(\mu - n \cdot \nabla v_2)$$

where  $[u]$  stands for the jump on  $\Gamma$ , i.e.  $[u] = (u_1 - u_2)|_{\Gamma}$  for any  $u = (u_1, u_2) \in \hat{V}$ . We can now rewrite problem (2.79)–(2.56)–(2.57) as: find  $(u_{Hh}, \lambda_h) \in V_{Hh}^d \times M_h^d$  such that

$$\hat{B}((u_{Hh}, \lambda_h), (v_{Hh}, \mu_h)) = \int_{\Omega} f v_{Hh} \quad \forall (v_{Hh}, \mu_h) \in V_{Hh}^d \times M_h^d \quad (2.80)$$

We have interpreted here the combined finite element space  $V_{Hh}^d$  as  $V_H \times V_h$  so that any  $v_{Hh} \in V_{Hh}^d$  is simply a combination of  $v_H \in V_H$  and  $v_h \in V_h$ . Note that the exact solution  $u$  to (2.1) can be viewed as an element of  $\hat{V}$  if we redefine  $u = (u_1, u_2)$  with  $u_1 = u|_{\Omega \setminus \bar{\Lambda}_H}$  and  $u_2 = u|_{\Lambda_\varepsilon}$ . We see thus that  $u \in \hat{V}$  and  $\lambda = \nabla u \cdot n|_{\Gamma} \in M$  satisfy

$$\hat{B}((u, \lambda), (v, \mu)) = \int_{\Omega} f v \quad \forall (v, \mu) \in \hat{V} \times M \quad (2.81)$$

We see thus that the finite element problem (2.80) is consistent with (2.81) and an a priori error estimate for (2.80) can be proved in the same way as that for problem (2.6)–(2.56)–(2.57) once one properly modifies Lemma 2.14.

**Lemma 2.19.** *There exists mesh-independent constants  $\sigma_0 > 0$ ,  $C > 0$  and  $c > 0$  such that for all  $\sigma \leq \sigma_0$*

$$\inf_{(u_{Hh}, \lambda_h) \in V_{Hh}^d \times M_h^d} \sup_{(v_{Hh}, \mu_h) \in V_{Hh}^d \times M_h^d} \frac{\hat{\mathcal{B}}((u_{Hh}, \lambda_h), (v_{Hh}, \mu_h))}{\| \|u_{Hh}, \lambda_h\| \| \|v_{Hh}, \mu_h\| \|} \geq c, \quad (2.82)$$

$$\sup_{(u_{Hh}, \lambda_h) \in V_{Hh}^d \times M_h^d} \sup_{(v_{Hh}, \mu_h) \in V_{Hh}^d \times M_h^d} \frac{\hat{\mathcal{B}}((u_{Hh}, \lambda_h), (v_{Hh}, \mu_h))}{\| \|u_{Hh}, \lambda_h\| \|_{\hat{V}} \| \|v_{Hh}, \mu_h\| \|_{\hat{V}}} \leq C, \quad (2.83)$$

where the triple norm is defined by

$$\| \|u, \lambda\| \|_{\hat{V}} = \left( \|u\|_{\hat{V}}^2 + \frac{1}{h} \|[u]\|_{0,\Gamma}^2 + h \|\lambda\|_{0,\Gamma}^2 \right)^{1/2},$$

and  $c, C$  are mesh-independent constants.

*Proof.* We observe first that for any  $u = (u_1, u_2) \in \hat{V}$

$$\begin{aligned} \hat{a}(u, u) &= \int_{\Omega \setminus \bar{\Lambda}_H} K |\nabla u_1|^2 + \int_{\Lambda_\varepsilon} K |\nabla u_2|^2 - \int_{\Lambda \setminus \Lambda_H} \nabla u_2 \cdot \nabla u_1 \quad (2.84) \\ &\geq \frac{1}{2} \int_{\Omega \setminus \bar{\Lambda}_H} K |\nabla u_1|^2 + \frac{1}{2} \int_{\Lambda_\varepsilon} K |\nabla u_2|^2 \geq \frac{\alpha}{2} \|u\|_{\hat{V}}^2 \end{aligned}$$

by Young's inequality. It is now easy to modify the proof of Lemma 2.14 to the present context. For example, we have for any  $(u_{Hh}, \lambda_h) \in V_{Hh}^d \times M_h^d$

$$\begin{aligned} \hat{\mathcal{B}}((u_{Hh}, \lambda_h), (u_{Hh}, -\lambda_h)) &= \hat{a}(u_{Hh}, u_{Hh}) - \sigma h \int_{\Gamma} |n \cdot \nabla u_h|^2 + \sigma h \int_{\Gamma} \lambda_h^2 \\ &\geq \frac{\alpha}{4} \|u_{Hh}\|_{\hat{V}}^2 + \sigma h \|\lambda_h\|_{0,\Gamma}^2. \end{aligned}$$

by the inverse inequality (2.61). The rest of the proof of (2.82) goes as that of (2.59) without major changes. Similarly, to prove (2.83) it suffices to repeat that of (2.60) and remark that

$$\hat{a}(u, v) \leq \|u\|_{\hat{V}} \|v\|_{\hat{V}}, \quad \forall u, v \in \hat{V} \quad (2.85)$$

□

**Theorem 2.20.** *Problem (2.80) admits a unique solution  $(u_{Hh}, \lambda_h) \in V_{Hh}^d \times M_h^d$ . Provided  $u \in H^{k+1}(\Omega)$ , we have moreover the following a priori error estimate*

$$\|u_{Hh} - u\|_{\hat{V}} = \left( \|u_H - u\|_{1,\Omega \setminus \bar{\Lambda}_H}^2 + \|u_h - u\|_{1,\Lambda_\varepsilon}^2 \right)^{1/2} \leq C(H^k \|u\|_{k+1,\Omega \setminus \bar{\Lambda}_H} + h^k \|u\|_{k+1,\Lambda_\varepsilon})$$

with a constant  $C$  independent of  $H$ ,  $h$  and  $u$ .

*Proof.* We can repeat the proof of Theorem 2.15 using the lemma above and the fact that the exact solution  $u$  to (2.1), viewed as an element of  $\hat{V}$ , satisfies (2.81).  $\square$

### 2.5.2 Convergence on iterations in Algorithm 2.3

In order to study the convergence of the iterative procedure in Algorithm 2.3, we introduce the operator  $\hat{A}_{Hh}^d : V_H \rightarrow V_H$

$$\int_{\Omega} \nabla(\hat{A}_{Hh}^d z_H) \cdot \nabla v_H = \int_{\Omega \setminus \bar{\Lambda}_H} \nabla u_H \cdot \nabla v_H + \int_{\Gamma} \nu_h v_H - \int_{\Lambda \setminus \bar{\Lambda}_H} \nabla z_h \cdot \nabla v_H, \quad \forall v_H \in V_H \quad (2.86)$$

where  $(z_h, \nu_h) \in V_h \times M_h^d$  come as the solution to (2.71)–(2.72). Unlike operator  $A_{Hh}^d$ , operator  $\hat{A}_{Hh}^d$  is not symmetric, but it still coercive and bounded.

**Lemma 2.21.** *The kernel of  $\hat{A}_{Hh}^d$  coincides with  $V_H^0$  and the image of  $\hat{A}_{Hh}^d$  coincides with  $V_H^1$ . Operator  $\hat{A}_{Hh}^d$  is coercive and bounded on  $V_H^1$ , i.e.  $\forall z_H, v_H \in V_H$*

$$\begin{aligned} (\hat{A}_{Hh}^d z_H, z_H) &\geq m |z_H|_{1,\Omega}^2 \\ (\hat{A}_{Hh}^d z_H, v_H) &\leq M |z_H|_{1,\Omega} |v_H|_{1,\Omega} \end{aligned}$$

with positive constants  $m$  and  $M$  that depend only on the regularity of  $\mathcal{T}_H$  and  $\mathcal{T}_h$ .

*Proof.* The statements about the kernel and the image of  $\hat{A}_{Hh}^d$  are immediately seen from the definition of this operator. Taking the linear combination of equations (2.86), (2.71), (2.72) with coefficients 1, -1, 1 we observe

$$(\hat{A}_{Hh}^d z_H, v_H) = \hat{\mathcal{B}}((z_{Hh}, \nu_h), (v_{Hh}, \mu_h)) \quad (2.87)$$

where  $z_{Hh} \in V_{Hh}^d$  is the combination of  $z_H$  and  $z_h$  given by (2.71)–(2.72),  $\nu_h$  is also given by (2.71)–(2.72), while  $v_{Hh} \in V_{Hh}^d$  and  $\mu_h \in M_{Hh}^d$  are arbitrary. In order to prove the coercivity estimate we invoke again (2.87) with  $v_H = z_H \in V_H^1$ , which implies for  $\sigma$  sufficiently small thanks to the inverse inequality (2.61)

$$\begin{aligned} (\hat{A}_{Hh}^d z_H, z_H) &= \hat{\mathcal{B}}((z_{Hh}, \nu_h), (z_{Hh}, -\nu_h)) \\ &= \hat{a}(z_{Hh}, z_{Hh}) + \sigma h \|\nu_h\|_{0,\Gamma}^2 - \sigma h \|n \cdot \nabla z_h\|_{0,\Gamma}^2 \\ &\geq \int_{\Omega \setminus \bar{\Lambda}_H} \nabla z_H \cdot \nabla z_H + \frac{1}{2} \int_{\Lambda_\varepsilon} \nabla z_h \cdot \nabla z_h - \int_{\Lambda \setminus \bar{\Lambda}_H} \nabla z_H \cdot \nabla z_h \\ &\geq \frac{1}{2} \int_{\Omega \setminus \bar{\Lambda}} \nabla z_H \cdot \nabla z_H \geq n |z_H|_{1,\Omega}^2 \end{aligned}$$

with a mesh independent constant  $m > 0$ . The last inequality here is borrowed from the proof of Lemma 2.17. The boundness of the operator  $\hat{A}_{Hh}^d$



with a mesh independent constant is also proved exactly as in the proof of Lemma 2.17, using now the boundedness of form  $\hat{a}$ , cf. (2.85).  $\square$

**Theorem 2.22.** *Algorithm 2.3 converges to the solution of (2.80) provided one takes the relaxation parameter  $\omega > 0$  small enough. This means that  $u_{Hh}^n \rightarrow u_{Hh}$  and  $\lambda_h^n \rightarrow \lambda_h$  as  $n \rightarrow \infty$ . Moreover, the convergence rate depends only on the regularity of  $\mathcal{T}_H$  and  $\mathcal{T}_h$ .*

*Proof.* As in the proof of Theorem 2.4, we decompose each iterate of Algorithm 2.3 as  $u_H^n = u_H^{n,0} + u_H^{n,1}$  with  $u_H^{n,0} \in V_H^0$  and  $u_H^{n,1} \in V_H^1$  which evolve as

$$\begin{aligned} u_H^{n,0} &= u_H^{n-1,0} \\ u_H^{n,1} &= (I - \omega \hat{A}_{Hh}^d) u_H^{n-1,1} + \omega F_H \end{aligned}$$

with some fixed  $F_H$ . Again, as in the proof of Theorem 2.4, it is sufficient to study the convergence of  $u_H^{n,1}$ . It is sufficient to this end to prove that the norm of operator  $(I - \omega \hat{A}_{Hh}^d)$  is  $< 1$ . This follows from Lemma 2.21. Indeed,  $\forall u_H \in V_H$

$$\begin{aligned} & \left( (I - \omega \hat{A}_{Hh}^d) u_H, (I - \omega \hat{A}_{Hh}^d) u_H \right) \\ &= (u_H, u_H) - 2\omega \left( \hat{A}_{Hh}^d u_H, u_H \right) + \omega^2 \left( \hat{A}_{Hh}^d u_H, \hat{A}_{Hh}^d u_H \right) \\ & \leq (1 - 2c\omega + C\omega^2)(u_H, u_H). \end{aligned}$$

and  $1 - 2c\omega + C\omega^2 < 1$  for sufficiently small  $\omega$ .  $\square$

## 2.6 Numerical tests

We shall test our methods on a slightly more general version of Problem (2.1):

$$\begin{aligned} -\Delta u &= f \quad \text{in } \Omega_\varepsilon, \\ u &= g \quad \text{on } \partial\Omega, \\ \nabla u \cdot n &= 0 \quad \text{on } \partial\omega_\varepsilon, \end{aligned} \tag{2.88}$$

We add namely the possibility for a non-homogeneous Dirichlet boundary condition on the external border  $\partial\Omega$ . The only modification that it induces into the Algorithms 2.1–2.3 is that the contributions on the coarse mesh should be adapted on the boundary  $\partial\Omega$  by setting  $u_H^n = g_H$  where  $g_H$  is the nodal interpolation of  $g$  on  $\partial\Omega$ .

For our numerical experiments, we have chosen the domain as in Fig. 2.1. The boundary of  $\omega_\varepsilon$  is the curve given in the parameterized form as

$$x = \varepsilon \cos(t), \quad y = \varepsilon \frac{\sin(t) + \cos^2(t)}{2}, \quad t \in [0, 2\pi]$$

This curve can be also be represented by the level-set function

$$\varphi(x, y) = \left(\frac{x}{\varepsilon}\right)^2 + \left(\frac{2y}{\varepsilon} - \frac{x^2}{\varepsilon^2}\right)^2 - 1 \quad (2.89)$$

We mean by this that  $\partial\omega_\varepsilon$  is given by the equation  $\varphi(x, y) = 0$ . Here,  $\varepsilon > 0$  is a parameter which serves also as the characteristic size of the perforation  $\omega_\varepsilon$  (in fact,  $\text{diam}(\omega_\varepsilon) = 2\varepsilon$ ). In Fig. 2.1 we have set  $\varepsilon = 0.1$  while the whole domain  $\Omega$  is set as the square  $(-1, 1)^2$ .

The exact solution  $u$  to (2.88) is taken as

$$u = \exp\left(-\frac{\varphi^2}{2\delta}\right) \quad (2.90)$$

where  $\varphi$  is the level set (2.89) and  $\delta$  is a positive parameter. In this way, the Neumann boundary condition on  $\partial\omega_\varepsilon$  is automatically satisfied. Indeed, the normal  $n$  is colinear with  $\nabla\varphi$  on  $\partial\omega_\varepsilon = \{\varphi = 0\}$  and

$$\nabla\varphi \cdot \nabla u = -\frac{\varphi}{\delta} u |\nabla\varphi|^2 = 0 \quad \text{on } \partial\omega_\varepsilon.$$

The data  $f$  and  $g$  in (2.88) are calculated from  $u$  as  $f = -\Delta u$  and  $g = u$  on  $\Gamma$ .

We have implemented Algorithms 2.1–2.3 in the general purpose finite element software FreeFEM [26]. The implementation is particularly straightforward in the case of Algorithm 2.1 on  $\Gamma$ -nested meshes. The only non standard feature from the implementation viewpoint is the presence of integrals on the boundary of the patch mixing the contributions from the two meshes of the type  $\int_\Gamma \lambda_h^n v_H$ . These integrals are computed exactly by FreeFEM if we take care to define them on the boundary of the fine mesh  $\mathcal{T}_h$  by writing `int1d(Th) (...)` with `Th` being the FreeFEM's name for the fine mesh. This is achieved by the interpolation from  $V_H$  to  $V_h$  which is (implicitly) performed by FreeFEM. Another slightly non-trivial feature of our algorithms, the integrals of the type  $\int_\Lambda \nabla u_H \cdot \nabla v_H$ , is implemented by the standard integration on the whole mesh  $\mathcal{T}_H$  by multiplying the integrand by a piecewise constant indicator function (1 on  $\Lambda$ , 0 elsewhere). The things become more complicated when we implement the methods on general meshes, not necessarily  $\Gamma$ -nested meshes. We return to this issue in the corresponding paragraph below.

### 2.6.1 Algorithm 2.1 on $\Gamma$ -nested meshes

The behavior of our simplest Algorithm 2.1 without relaxation (i.e.  $\omega = 1$ ) in the simplest case of  $\Gamma$ -nested meshes  $\mathcal{T}_H$  and  $\mathcal{T}_h$  is illustrated at Fig. 2.2. We use the meshes depicted at Fig. 2.1, cf. a more detailed description of the parameters in the caption of Fig. 2.2. We observe that the initial approximation (on the coarse mesh without the patch) is (not surprisingly) very bad and it gets corrected essentially on first 4 iterations.

These observations are made more precise and complete by more numerical experiments reported at Fig. 2.3. We consider there the same test case as before and refine both meshes  $\mathcal{T}_H$  and  $\mathcal{T}_h$  twofold several times. The relative errors are reported in  $H^1$  and  $L^2$  norms for both reconstruction  $u_{Hh}^n$  and  $u_{Hh}^{n-1/2}$ . We observe that the method stabilizes indeed at  $n = 4$  on the original meshes with  $H = 0.2$ ,  $h = 0.01$  and the convergence occurs even faster on finer meshes (after 2 or 3 iterations). The numerical results also confirm the optimal convergence with respect to the mesh size in both  $H^1$  and  $L^2$  norms.

## 2.6.2 A numerical comparison of Algorithms 2.1–2.3 on general meshes

Before presenting the result on general meshes, we return to some implementation issues in this case. The implementation of our methods in FreeFEM remains rather simple, but it now involves several extra approximations with respect to what is written on paper. These additional approximations are difficult to analyze theoretically and we do not attempt to do it here. We note the following details:

- The integrals of the type  $\int_{\Gamma} \lambda_h^n v_H$  are still evaluated by FreeFEM command `int1d(Th) ( . . . )` on the boundary of the fine mesh  $\mathcal{T}_h$ . This still involves the interpolation from  $V_H$  to  $V_h$  (more strictly speaking, the interpolation to some Gauss points on the boundary of  $\mathcal{T}_h$ ). The resulting evaluation is not exact.
- The integrals of the type  $\int_{\Lambda} \nabla u_H \cdot \nabla v_H$  are now also difficult to implement exactly. The difficulty is not interpolating from mesh to another (both integrands are defined on the coarse mesh  $\mathcal{T}_H$ ) but rather in the fact that the integration domain  $\Lambda$  is no longer a union of triangles of  $\mathcal{T}_H$ : the boundary  $\Gamma$  cuts the mesh cells in an arbitrary manner. We have chosen to implement this integral by the command `int2d(TH, levelset=phiP)` where `TH` denotes the coarse mesh, and `phiP` is a level-set for the patch  $\Lambda$ , i.e. a continuous function that is negative inside  $\Lambda$  and positive outside it. The keyword `levelset` makes FreeFEM to perform the integration only on the cut portion of mesh triangles. However, this cut is performed approximately by interpolating the level-set `phiP` by a piecewise linear function on  $\mathcal{T}_H$ . The resulting integration is thus not exact.
- Algorithm 2.3 avoids the integration on  $\Lambda$  of quantities defined on the coarse mesh  $\mathcal{T}_H$ , and introduces instead the integrals on  $\Lambda_H$  which are computed exactly in our code by multiplying the integrand by a piecewise constant indicator function on  $\mathcal{T}_H$ . However, there is now another difficult integral  $\int_{\Lambda \setminus \bar{\Lambda}_H} \nabla u_h^n \cdot \nabla v_H$ . We have chosen to approximate those

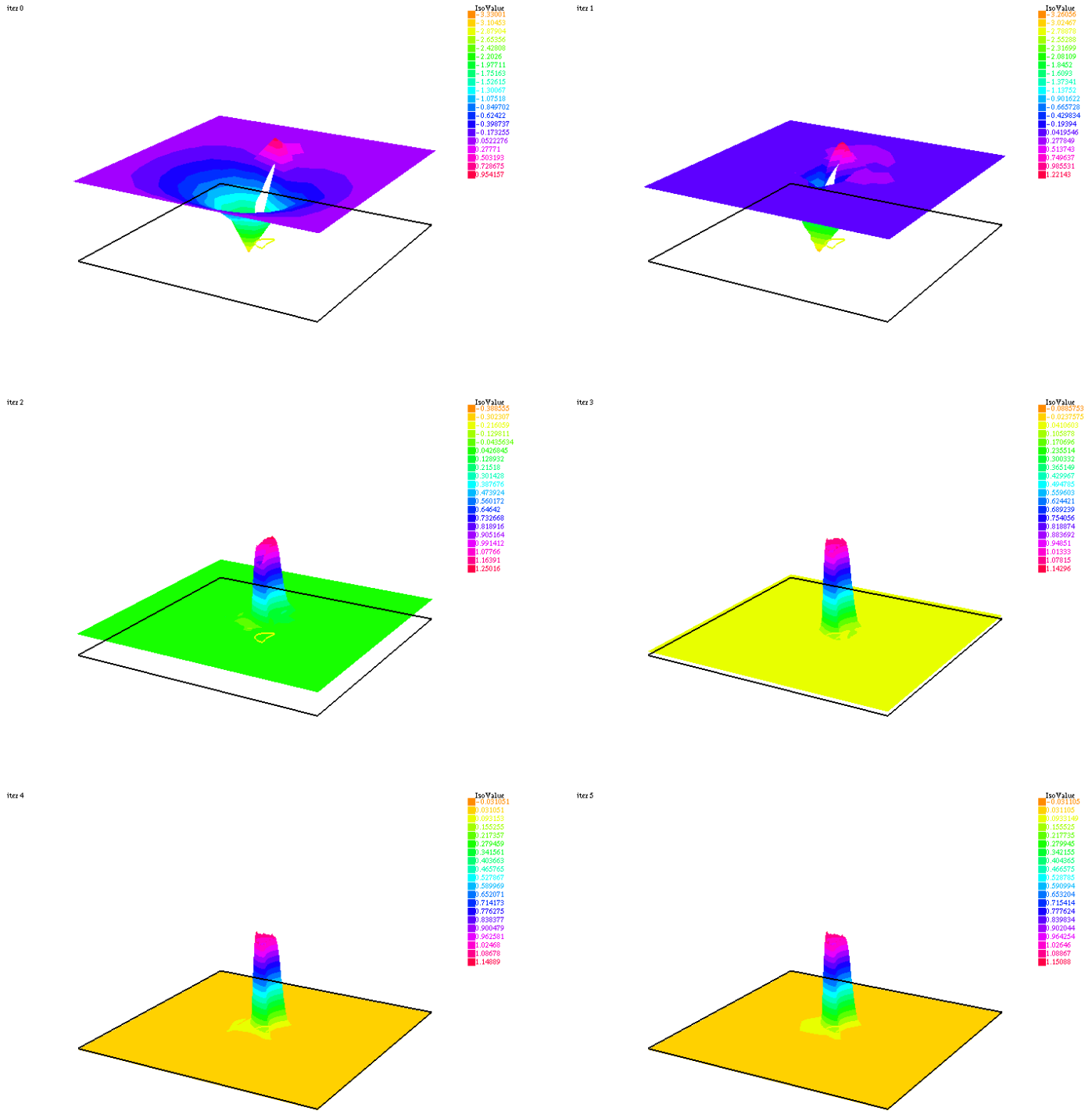


FIGURE 2.2: Evolution on iterations of Algorithm 2.1 in the  $\Gamma$ -nested case. The test case (2.89)–(2.90) with  $\varepsilon = 0.1$ ,  $\delta = 0.5$ , the mesh sizes  $H = 0.2$ ,  $h = 0.01$  on the patch  $\Lambda = (-0.2, 0.2)^2$ . The initial coarse approximation (Iter 0,  $u_H^0$ ) and the first 5 iterations ( $u_{Hh}^n$ ,  $n = 1, \dots, 5$ ) of Algorithm 2.1 are presented from top to bottom, left to right.

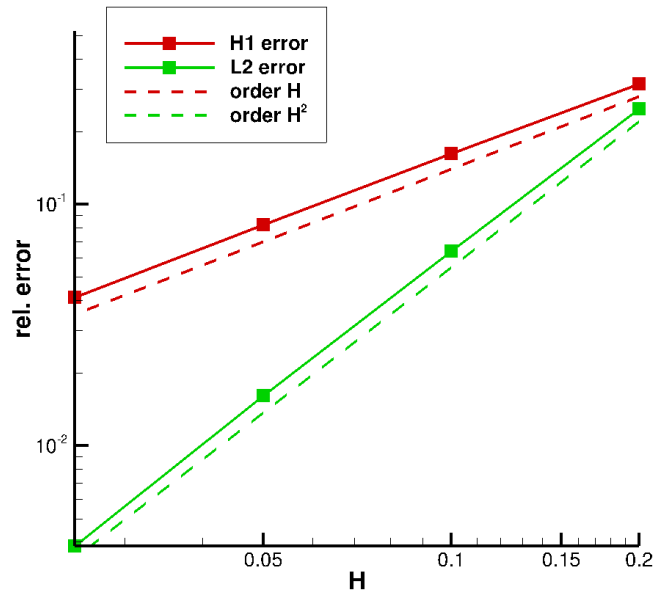
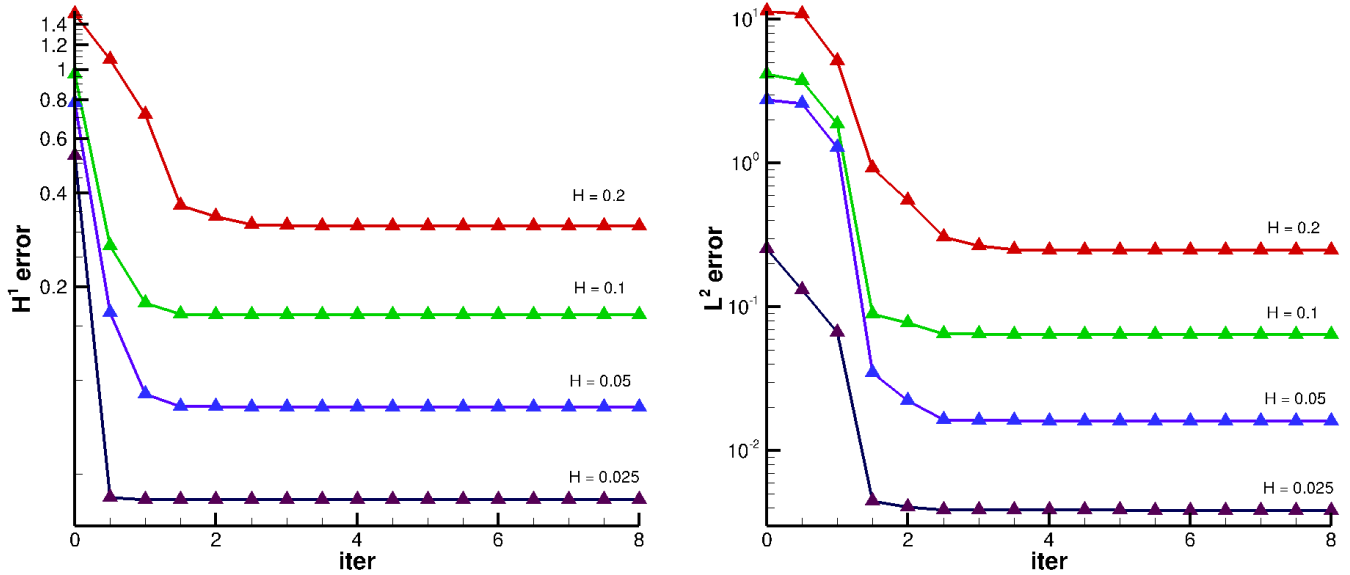


FIGURE 2.3: Convergence of Algorithm 2.1 under the mesh refinement in the  $\Gamma$ -nested case. The test case (2.89)–(2.90) with  $\varepsilon = 0.1$ ,  $\delta = 0.5$ , the varying mesh size  $H$ , and the fine mesh size  $h = H/20$  on the patch  $\Lambda = (-0.2, 0.2)^2$ .

Top left: the relative  $H^1$ -error on iterations; Top right: the relative  $L^2$ -error on iterations; Bottom: the relative errors as functions on the mesh size  $H$

by a numerical quadrature on the fine mesh involving the multiplication by a piecewise constant indicator function on  $\mathcal{T}_H$  taking into account  $\Lambda_H$ . It involves thus an interpolation of discontinuous functions from one mesh to another and the resulting computation is not exact.

In order to investigate the behavior of our methods on general, not necessary  $\Gamma$ -nested meshes, we take the benchmark as above ( $\Omega = (-1, 1)^2$ , the perforation  $\omega_\varepsilon$  given by (2.89), the exact solution (2.90) with  $\varepsilon = 0.1$ ,  $\delta = 0.5$ ) and slightly vary one of the mesh configurations considered above, cf. Fig. 2.4:

**Situation 1**  $\Gamma$ -nested meshes as in Fig. 3.1, refined 4 times. Recalling Definition 2.4, this corresponds to  $\kappa_H = 1$ .

**Situation 2** We slightly enlarge the patch  $\Lambda$  (with respect to Situation 1) so that some of the coarse mesh triangles are only slightly covered by  $\Lambda$  (the majority of coarse triangles being either completely inside the patch or completely outside it). This corresponds to  $\kappa_H$  close to 1, in fact  $\kappa_H \approx 0.8$ .

**Situation 3** We slightly shrink the patch  $\Lambda$  (with respect to Situation 1) so that some of the coarse mesh triangles are almost covered by  $\Lambda$  with only a small portion of the triangle being outside the patch. This corresponds to  $\kappa_H$  close to 0, in fact  $\kappa_H \approx 0.2$ .

**Situation 4** A less artificial configuration where some of coarse triangles are "badly" cut by  $\Lambda$  (as in Situation 3), the others "well" cut by  $\Lambda$  (as in Situation 2). This is achieved by going to a non-uniform coarse mesh  $\mathcal{T}_H$ .

We present the convergence of our 3 algorithms in the 4 situations above at Figs. 2.5–2.7. We note that the possible "bad" intersections of the coarse mesh cells with  $\Lambda$  do not seem to influence significantly the speed of convergence towards the exact solution on iterations. On the other hand, the precision of the methods (especially when measured in the  $L^2$  norm) can be largely deteriorated on the "dangerous" meshes (Situations 3 and 4) if one measures the error in the  $L^2$  norm.

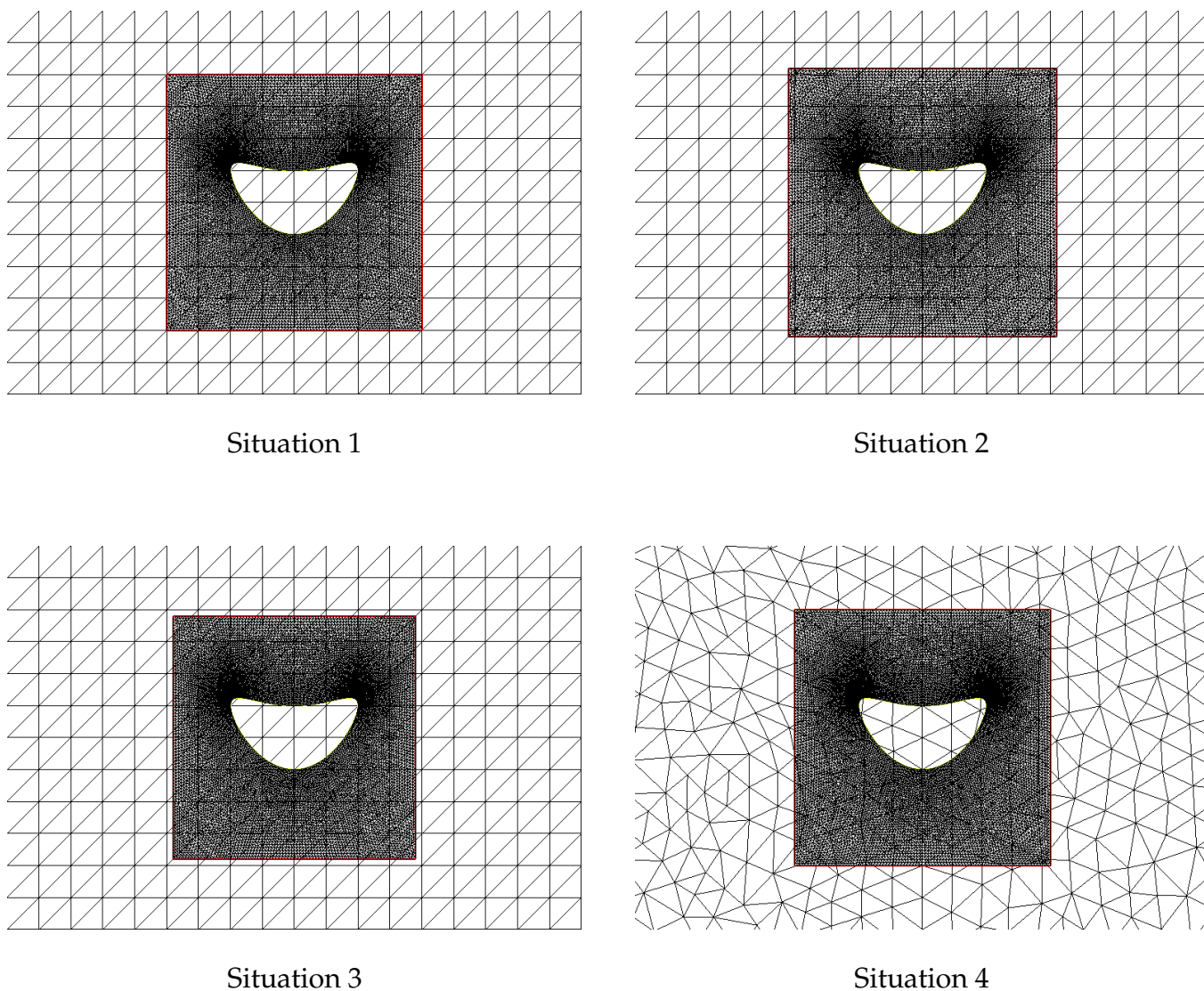


FIGURE 2.4: The meshes (partial view around  $\Lambda$ ) in 4 situations. The coarse mesh with  $H \approx 0.05$  on  $\Omega = (-1, 1)^2$ . The fine mesh with  $h \approx 0.025$  on the patch  $\Lambda = (-L, L)^2$ . Situation 1:  $L = 0.2$ ; Situation 2:  $L = 0.21$ ; Situation 3:  $L = 0.19$ ; Situation 4:  $L = 0.2$  and a non-uniform coarse mesh  $\mathcal{T}_H$ .

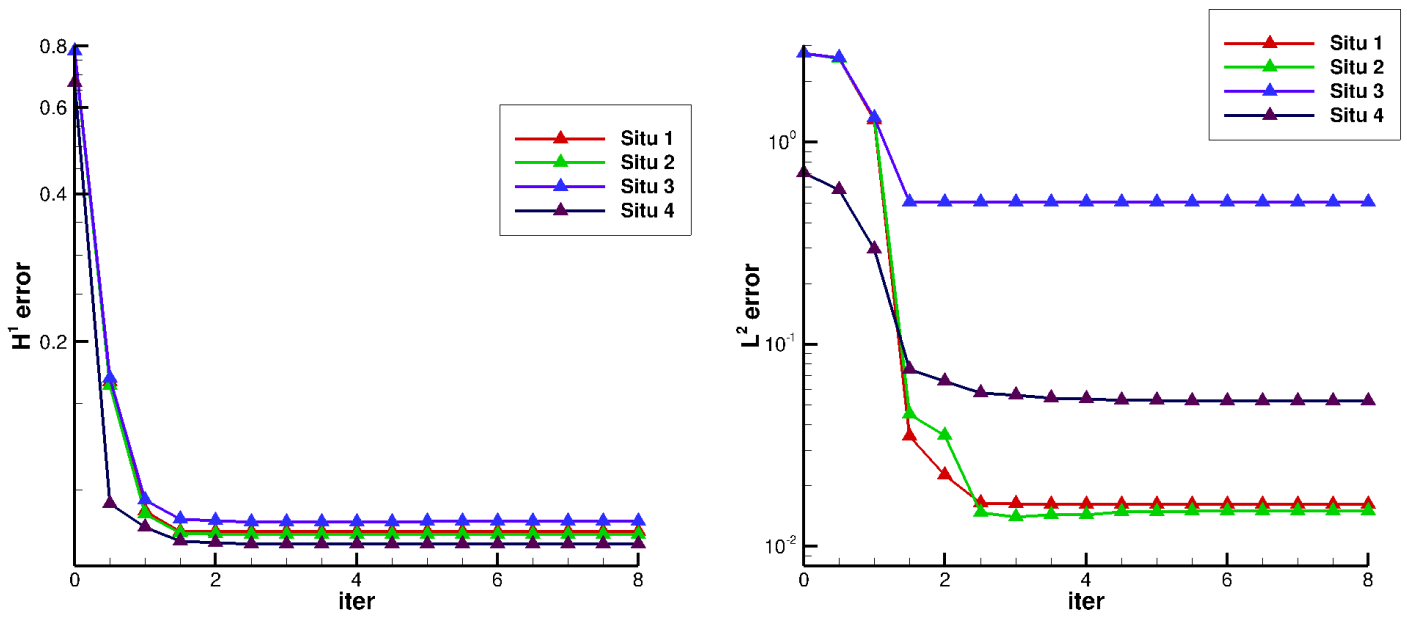


FIGURE 2.5: Evolution of Algorithm 2.1 in 4 situations, as in Fig. 2.4.

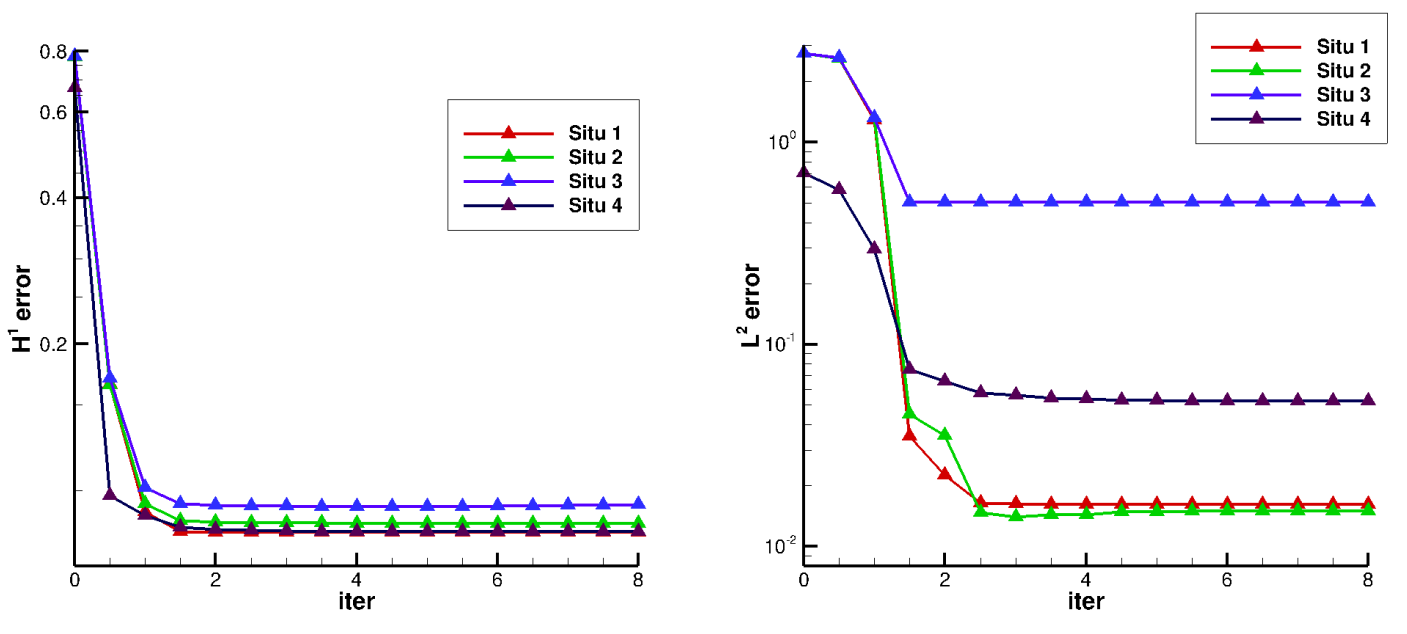


FIGURE 2.6: Evolution of Algorithm 2.2 in 4 situations, as in Fig. 2.4.



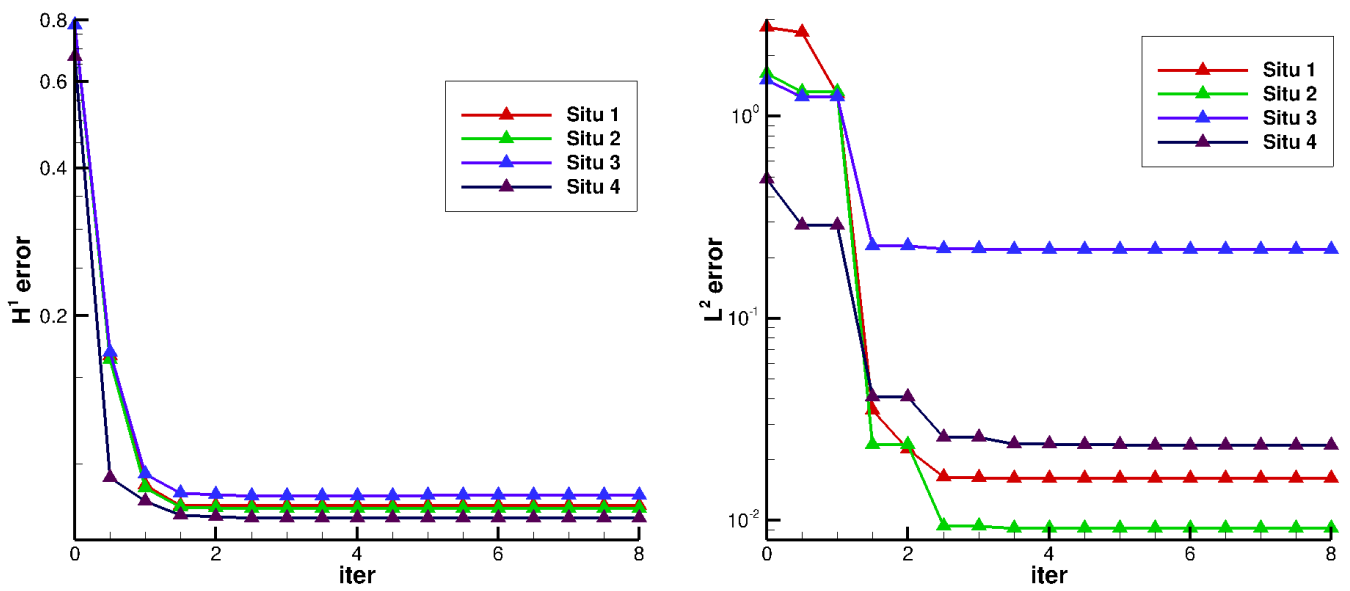


FIGURE 2.7: Evolution of Algorithm 2.3 in 4 situations, as in Fig. 2.4.

## Chapter 3

# The approach of matched asymptotic expansions and comparisons with the numerical zoom

---

In this chapter, we study an alternative approach to the numerical solution of Problem (2.1) in domain  $\Omega$  with a small hole  $\omega_\varepsilon$ . We shall consider the solution to this problem as a perturbation to that of a simpler problem posed in the whole domain  $\Omega$  and employ the approach of the matched asymptotic expansions treating the size of the hole  $\varepsilon$  as the small perturbation parameter. Our work will be inspired by that of V. Bonnaillie-Noël, G. Vial et al [9–11, 42] although we only consider here the simplest case of a single inclusion. The basic mathematical principles of the approach of the matched asymptotic expansions are well known and can be found, for example, in monographs [28, 33]. In the following section, we recall some basic results of this theory and give formally the construction of the expansion.

### 3.1 The method of matched asymptotic expansions

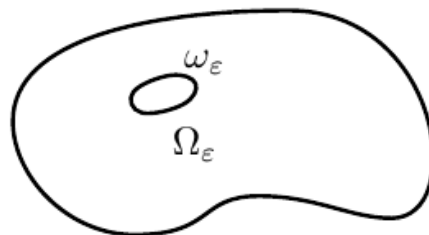


FIGURE 3.1: A domain  $\Omega_\varepsilon$  with a small perforation  $\omega_\varepsilon$ .

The assumptions on the geometry of the computational domain remain essentially the same as in the preceding chapter. We consider a fixed domain  $\Omega \subset \mathbb{R}^2$  with a hole  $\omega_\varepsilon$ . However, we should now be more precise about the geometry of the hole: we assume that  $\omega_\varepsilon$  is obtained from a fixed domain  $\omega$ , centered at the origin, shrinking it by the factor  $\varepsilon$ . In order to be sure that  $\omega_\varepsilon$  is inside  $\Omega$  we assume that both  $\Omega$  and  $\omega$  contain the origin and that  $\varepsilon$  is sufficiently small. We define now the perturbed domain  $\Omega_\varepsilon$ , see Fig. 3.1, as

$$\Omega_\varepsilon = \Omega \setminus \omega_\varepsilon, \quad \text{with } \omega_\varepsilon = \varepsilon\omega$$

The problem we are interested in reads

$$\begin{cases} -\Delta u_\varepsilon = f & \text{in } \Omega_\varepsilon \\ u_\varepsilon = 0 & \text{on } \partial\Omega \\ \partial_n u_\varepsilon = 0 & \text{on } \partial\omega_\varepsilon, \end{cases} \quad (3.1)$$

for some  $f \in L^2(\Omega)$ . As  $\varepsilon \rightarrow 0$ , we should recover, at least formally, the solution  $u_0$  of the Dirichlet-Laplacian on the unperturbed domain  $\Omega$ :

$$\begin{cases} -\Delta u_0 = f & \text{in } \Omega \\ u_0 = 0 & \text{on } \partial\Omega \end{cases} \quad (3.2)$$

Now, for small  $\varepsilon > 0$ , we can represent the solution  $u_\varepsilon$  as the asymptotic series

$$u_\varepsilon = u_0 + \varepsilon u_1 + \varepsilon^2 u_2 + \dots$$

with  $u_0$  being the solution to the non-perturbed problem (3.2). The following terms  $u_1, u_2, \dots$  should decay away from the origin at the lengthscale  $\sim \varepsilon$ . We can take this into account by postulating that these terms are functions of the "fast variable"  $x/\varepsilon$ . We shall thus search for the asymptotic development of the form

$$u_\varepsilon(x) = u_0(x) + \varepsilon u_1\left(\frac{x}{\varepsilon}\right) + \varepsilon^2 u_2\left(\frac{x}{\varepsilon}\right) + \dots$$

One can estimate  $r_\varepsilon^0 := u_\varepsilon - u_0$  and thus prove that  $u_0$  is the zeroth order term of the expansion of  $u_\varepsilon$ , cf. the literature cited above.

Let us explain formally how we determine the following term in the asymptotic expansion. To determine the first order term, we notice that  $r_\varepsilon^0$  satisfies:

$$\begin{cases} -\Delta r_\varepsilon^0 = 0 & \text{in } \Omega_\varepsilon \\ r_\varepsilon^0 = 0 & \text{on } \partial\Omega \\ \partial_n r_\varepsilon^0 = -\partial_n u_0 & \text{on } \partial\omega_\varepsilon \end{cases}$$

where  $\mathbf{n}$  denotes the unit normal outward looking from  $\Omega_\varepsilon$ , thus pointing into  $\omega_\varepsilon$ . At the leading order, we can approximate  $\partial_n u_0$  on  $\partial\omega_\varepsilon$  by its value at 0:

$$\partial_n r_\varepsilon^0 = -\nabla u_0(0) \cdot \mathbf{n} + O(\varepsilon) \quad \text{on } \partial\omega_\varepsilon.$$

Let us now rescale the small domain  $\omega_\varepsilon$  of size  $\sim \varepsilon$  to the "reference" domain  $\omega$  of size  $\sim 1$  and represent  $r_\varepsilon^0$  in the rescaled variables as  $r_\varepsilon^0(\cdot) = \varepsilon V\left(\frac{\cdot}{\varepsilon}\right)$ . Note,

by the chain rule,  $\partial_i r_\varepsilon^0(\cdot) = (\partial_i V) \left( \frac{\cdot}{\varepsilon} \right)$  where  $\partial_i$  denotes the partial derivative in the  $i$ -th direction. Neglecting the higher order terms in the boundary conditions on  $\partial\omega_\varepsilon$  and assuming that the outer boundary  $\partial\Omega$  is sufficiently far for  $\omega_\varepsilon$  to treat it essentially as the infinity, we obtain the following problem for  $V$ :

$$\begin{cases} -\Delta V & = & 0 & \text{in } \mathbb{R}^2 \setminus \bar{\omega} \\ \partial_n V & = & -\nabla u_0(0) \cdot n & \text{on } \partial\omega \\ V & \longrightarrow & 0 & \text{at infinity} \end{cases} \quad (3.3)$$

By linearity we get then at the leading order

$$r_\varepsilon^0(\cdot) \approx \varepsilon \sum_{i=1}^2 (\partial_i u_0)(0) V_i \left( \frac{\cdot}{\varepsilon} \right) \quad (3.4)$$

where  $V_1, V_2$  are so called profiles:

$$\begin{cases} -\Delta V_i & = & 0 & \text{in } \mathbb{R}^2 \setminus \bar{\omega} \\ \partial_n V_i & = & -n_i & \text{on } \partial\omega \\ V_i & \longrightarrow & 0 & \text{at infinity} \end{cases} \quad (3.5)$$

The validity of the asymptotic expansion (3.4) is established thanks to the decay of the profiles at the infinity. We recall in particular a result from [3]:

**Proposition 3.1.** *Let  $\omega$  be a smooth bounded domain of  $\mathbb{R}^2$  with  $0 \in \omega$ . We assume that  $g \in H^{-1/2}(\partial\omega)$  satisfies  $\langle g, 1 \rangle_{H^{-1/2} * H^{1/2}} = 0$ . Then the boundary value problem*

$$\begin{cases} -\Delta v & = & 0 & \text{in } \mathbb{R}^2 \setminus \bar{\omega} \\ \partial_n v & = & g & \text{on } \partial\omega \\ v & \longrightarrow & 0 & \text{at infinity} \end{cases} \quad (3.6)$$

*admits a unique weak solution  $v_0$  in the variational space*

$$\left\{ v : \nabla v \in L^2(\mathbb{R}^2 \setminus \bar{\omega}) \text{ and } \frac{v}{(1 + |X|) \log(2 + |X|)} \in L^2(\mathbb{R}^2 \setminus \bar{\omega}) \right\}$$

Starting from this result one can indeed show that the error in the approximation (3.4) is of order  $\varepsilon^2$ . Finally, the first order expansion of  $u_\varepsilon$  takes the form

$$u_{\varepsilon,1}(\cdot) = u_0(\cdot) + \varepsilon \sum_{i=1}^2 (\partial_i u_0)(0) V_i \left( \frac{\cdot}{\varepsilon} \right) \quad (3.7)$$

and one can prove

$$u_\varepsilon = u_{\varepsilon,1} + r_\varepsilon^1 \quad \text{with} \quad \|r_\varepsilon^1\|_{H^1(\Omega_\varepsilon)} \leq C\varepsilon^2. \quad (3.8)$$

## 3.2 Finite element methods based on asymptotic expansions

### 3.2.1 Superposition method

The numerical computation of the solution  $u_\varepsilon$  to problem (3.1) can be difficult since a very fine mesh is required if  $\varepsilon$  is small. For such values of  $\varepsilon$ , it is natural to use the asymptotic expansion (3.7). We thus introduce a coarse global mesh  $\mathcal{T}_H$  of meshsize  $H$  on  $\Omega$ , with  $H$  typically bigger than  $\varepsilon$ . Introducing the  $P_k$  finite element space  $V_H$  on  $\mathcal{T}_H$  (with functions vanishing on  $\partial\Omega$ ) we approximate the zeroth order term  $u_0$  in (3.7) by  $u_{0,H} \in V_H$  such that

$$\int_{\Omega} \nabla u_{0,H} \cdot \nabla v = \int_{\Omega} f v, \quad \forall v \in V_H \quad (3.9)$$

We also need to approximate the profiles  $V_i$  that are solutions to (3.5). The difficulty lies in the fact that these problems are posed on an unbounded domain with zero Dirichlet boundary conditions at infinity. The simplest approach to discretize such a problem is to truncate the whole space  $\mathbb{R}^2$  to a sufficiently large ball and to impose homogeneous Dirichlet boundary conditions on the boundary of this ball. For our numerical purposes it is more convenient to transform the problems (3.5) back to the original scale  $\varepsilon$ . We thus introduce the “patch”  $\Lambda = B_R(0)$  with  $R \gg \varepsilon$  but still  $R$  not too big so that  $\Lambda \subset \Omega$ . We denote  $\Gamma = \partial\Lambda$  and  $\Lambda_\varepsilon = \Lambda \setminus \omega_\varepsilon$  and are looking to  $V_i^\varepsilon(\cdot) \approx \varepsilon V_i(\frac{\cdot}{\varepsilon})$  on  $\Lambda_\varepsilon$ . The problems (3.5) are now truncated and rewritten as

$$\begin{cases} -\Delta V_i^\varepsilon = 0 & \text{in } \Lambda_\varepsilon \\ \partial_n V_i^\varepsilon = -n_i & \text{on } \partial\omega_\varepsilon \\ V_i^\varepsilon = 0 & \text{on } \Gamma \end{cases} \quad (3.10)$$

We now introduce the fine local mesh  $\mathcal{T}_h$  on  $\Lambda_\varepsilon$  (typically, the meshsize  $h$  is thus much smaller than  $\varepsilon$ ). Introducing the  $P_k$  finite element space  $V_h^0$  on  $\mathcal{T}_h$  (with functions vanishing on  $\Gamma$ ) we approximate the profiles  $V_i^\varepsilon$  by  $V_{i,h}^\varepsilon \in V_h^0$  such that

$$\int_{\Lambda_\varepsilon} \nabla V_{i,h}^\varepsilon \cdot \nabla v = - \int_{\partial\omega_\varepsilon} n_i v, \quad \forall v \in V_h^0 \quad (3.11)$$

Finally, we propose the following approximation to the exact solution  $u_\varepsilon$  of Problem (3.1) inspiring ourselves from the asymptotic expansion (3.7):

$$u_{\varepsilon,1,Hh} = u_{0,H} + \sum_{i=1}^2 (\partial_i u_{0,H})(0) V_{i,h}^\varepsilon \quad (3.12)$$

We call this approach “the superposition method” since the global approximation is corrected by superimposing the local corrections  $V_{i,h}^\varepsilon$  on it, multiplying them with easily computable coefficients borrowed from the asymptotic expansions theory on the continuous level. Note that the resulting approximation  $u_{\varepsilon,1,Hh}$  is conforming, i.e. continuous on  $\Omega_\varepsilon$ , since  $V_{i,h}^\varepsilon$  vanish on  $\Gamma = \partial\Lambda$ .

### 3.2.2 A variational method with profiles vanishing on $\partial\Lambda$

One can argue that taking  $(\partial_i u_{0,H})(0)$  as coefficients in the linear combination of profiles in (3.12) is not necessarily the best choice because the finite element approximation of the derivatives  $\partial_i u_0$  may be rather poor pointwise. One can try then to automatically adjust these coefficients by putting the profiles  $V_{i,h}^\varepsilon$  directly into an approximate (Galerkin) variational formulation. We thus introduce a “locally corrected” finite element space

$$V_H^{c,Dir} = V_H \oplus \text{span} \{V_{1,h}^\varepsilon, V_{2,h}^\varepsilon\}$$

We put the abbreviation “c” and “Dir” to emphasize the fact that homogeneous Dirichlet boundary conditions on  $\Gamma$  were used for  $V_{1,h}^\varepsilon, V_{2,h}^\varepsilon$  here and the resulting augmented finite element space is thus conforming (it contains only continuous functions).

The method that we call Variational Superposition goes now as: find  $u_H^{c,Dir} \in V_H^{c,Dir}$  such that

$$\int_{\Omega_\varepsilon} \nabla u_H^{c,Dir} \cdot \nabla v = \int_{\Omega_\varepsilon} f v, \quad \forall v \in V_H^{c,Dir} \quad (3.13)$$

This method is of course much more expensive than the superposition method which consists in solving the standard finite element problem (3.9) and then putting things together as in (3.12). To implement (3.13) one should calculate the integrals involving both the profiles  $V_{2,h}^\varepsilon$  and the basis functions of  $V_H$ . Moreover, even the part of the problem on  $V_H$  is not standard since the integrals are performed on the perforated domain  $\Omega_\varepsilon$  while the basis functions of  $V_H$  live on the triangles of the mesh  $\mathcal{T}_H$  which is cut by the hole  $\omega_\varepsilon$ .

### 3.2.3 Variational methods with more accurate profiles

The accuracy and computational cost of the methods above can be greatly affected by the truncation parameter  $R$ . The choice of  $R$  may be not easy to do in practice: on one hand, we want  $R$  to be sufficiently large so that the truncated problem (3.10) approximates well the original problem for the profiles (3.5), which is set in an unbounded domain. On the other hand,  $R$  should be not too large to keep the method computationally attractive (the problem on the perforated patch  $\Lambda_\varepsilon$  is discretized on the fine mesh  $\mathcal{T}_h$  with  $h \ll \varepsilon$ ) and to keep  $\Lambda$  inside  $\Omega$ .

We know from [10] that one can choose artificial boundary conditions on  $\Gamma$ , more intricate than the homogeneous Dirichlet ones used above, allowing us to obtain more accurate approximation of the profiles at a given truncation radius  $R$  or, more interestingly for us, to obtain sufficient accuracy at reduced  $R$ . The derivation of these conditions is based on the representation of the profile by the sum of harmonics that behave at infinity as  $|x|^{-p-1}$ ,  $p = 0, 1, \dots$ . One seeks then for a linear combination of  $V_i$  with its derivatives on  $\Gamma$  that vanishes on a certain number of leading terms in this sum. If one stops at orders  $p = 0, 1, 2$ , one obtains respectively Dirichlet, Robin, and Ventcel conditions. In particular, the last two boundary conditions are written as

**Robin boundary conditions** to truncate (3.5):

$$V_i + R\partial_n V_i = 0, \quad (3.14)$$

**Ventcel boundary conditions** to truncate (3.5)

$$V_i + \frac{3R}{2}\partial_n V_i - \frac{R^2}{2}\Delta_\Gamma V_i = 0 \quad (3.15)$$

where  $\Delta_\Gamma$  is the Laplace-Beltrami operator on  $\Gamma$ .

In order to discretize the truncated problems (3.10) with Robin or Ventcel boundary conditions on  $\Gamma$  instead of the Dirichlet ones, we introduce again the fine mesh  $\mathcal{T}_h$  on  $\Lambda_\varepsilon$ , and the  $P_k$  finite element space  $V_h$  on  $\mathcal{T}_h$  (note that the functions in  $V_h$  are free on  $\Gamma$ ). The approximated profiles  $V_{i,h}^{\varepsilon,R}$  with Robin boundary conditions are then defined by:  $V_{i,h}^{\varepsilon,R} \in V_h$  such that

$$\int_{\Lambda_\varepsilon} \nabla V_{i,h}^{\varepsilon,R} \cdot \nabla v + \frac{1}{R} \int_\Gamma V_{i,h}^{\varepsilon,R} v = - \int_{\partial\omega_\varepsilon} n_i v, \quad \forall v \in V_h \quad (3.16)$$

The approximated profiles  $V_{i,h}^{\varepsilon,V}$  with Ventcel boundary conditions are then defined by:  $V_{i,h}^{\varepsilon,V} \in V_h$  such that

$$\int_{\Lambda_\varepsilon} \nabla V_{i,h}^{\varepsilon,V} \cdot \nabla v + \frac{2}{3R} \int_\Gamma V_{i,h}^{\varepsilon,V} v + \frac{R}{3} \int_\Gamma \nabla_\Gamma V_{i,h}^{\varepsilon,V} \cdot \nabla_\Gamma v = - \int_{\partial\omega_\varepsilon} n_i v, \quad \forall v \in V_h \quad (3.17)$$

where  $\nabla_\Gamma$  is the tangential part of the gradient on  $\Gamma$ :  $\nabla_\Gamma v = \nabla v - (\nabla v \cdot n)n$ .

The technical problem with the approximate profiles above is that they do not vanish on  $\Gamma$ , unlike the Dirichlet case. They are not even supposed to be very small on  $\Gamma$ . Indeed, the whole point of introducing the approximation with Robin or Ventcel boundary conditions is to be able to reduce the size of the “patch”  $\Lambda$  so that its boundary  $\Gamma$  is not too far from the perforation  $\omega_\varepsilon$ . We thus cannot simply add these approximate profiles to the coarse space  $V_H$ , as we did in the Dirichlet case. Our solution to this problem is to work with

discontinuous approximations, and to impose an approximate continuity by Lagrange multipliers.

We introduce the coarse mesh approximation of the patch  $\Lambda$

$$\Lambda_H = \left( \cup_{T \in \mathcal{T}_H, T \subset \bar{\Lambda}} T \right)^\circ$$

and denote its boundary by  $\Gamma_H = \partial\Lambda_H$ , as in Definition 2.3. The corrections  $V_{i,h}^{\varepsilon,R}$  or  $V_{i,h}^{\varepsilon,V}$  will be used on  $\Lambda_H$  only and will introduce a discontinuity across  $\Gamma_H$ . In order to treat this discontinuity and to impose a weak continuity in a finite element fashion, we introduce the space of Lagrange multipliers on  $\Gamma_H$

$$M_H = \{ \mu_H : \Gamma_H \rightarrow \mathbb{R} \quad \text{such that } \exists v_H \in V_H \text{ with } \mu_H = v_H|_{\Gamma_H} \}$$

We are now set to propose a finite element approximation augmented by the asymptotic profiles truncated with the Robin boundary condition. We thus introduce the discontinuous counterpart of  $V_H$  (with discontinuity possible on  $\Gamma_H$  only) and augment it by approximate profiles  $V_{i,h}^{\varepsilon,R}$  (inside  $\Lambda_H$  only):

$$V_H^{d,Rob} = \left\{ v_H : \Omega_\varepsilon \rightarrow \mathbb{R} \text{ such that } \exists v_H^{(out)} \in V_H, v_H^{(in)} \in V_H \text{ and} \right. \\ \left. v_H = v_H^{(out)} \text{ on } \Omega \setminus \bar{\Lambda}_H, \right. \\ \left. v_H = v_H^{(in)} + \sum_{i=1}^2 \alpha_i V_{i,h}^{\varepsilon,R} \text{ with some } \alpha_1, \alpha_2 \in \mathbb{R} \text{ on } \Lambda_H \setminus \omega_\varepsilon \right\}$$

The method, referred to as the Robin Zoom, finds an approximation in this discontinuous space  $V_H^{d,Rob}$  and imposes continuity weakly on  $\Gamma_H$  using the Lagrange multipliers from  $M_H$ . It reads thus: find  $u_H^{d,Rob} \in V_H^{d,Rob}$ ,  $\lambda_H \in M_H$  such that

$$\int_{\Omega_\varepsilon} \nabla u_H^{d,Rob} \cdot \nabla v + \int_{\Gamma_H} \lambda_H[v] = \int_{\Omega_\varepsilon} f v, \quad \forall v \in V_H^{d,Rob} \quad (3.18) \\ \int_{\Gamma_H} \mu[u_H^{d,Rob}] = 0, \quad \forall \mu \in M_H$$

Here  $[\cdot]$  stand for the jump over  $\Gamma_H$ .

Similarly, for Ventcel based approximate profiles, we introduce the discontinuous counterpart of  $V_H$  augmented by approximate profiles  $V_{i,h}^{\varepsilon,V}$  (inside  $\Lambda_H$  only):

$$V_H^{d,Ven} = \left\{ v_H : \Omega_\varepsilon \rightarrow \mathbb{R} \text{ such that } \exists v_H^{(out)} \in V_H, v_H^{(in)} \in V_H \text{ and} \right. \\ \left. v_H = v_H^{(out)} \text{ on } \Omega \setminus \bar{\Lambda}_H, \right. \\ \left. v_H = v_H^{(in)} + \sum_{i=1}^2 \alpha_i V_{i,h}^{\varepsilon,V} \text{ with some } \alpha_1, \alpha_2 \in \mathbb{R} \text{ on } \Lambda_H \setminus \omega_\varepsilon \right\}$$



The Ventcel Zoom method reads then: find  $u_H^{d,Ven} \in V_H^{d,Ven}$ ,  $\lambda_H \in M_H$  such that

$$\begin{aligned} \int_{\Omega_\varepsilon} \nabla u_H^{d,Ven} \cdot \nabla v + \int_{\Gamma_H} \lambda_H[v] &= \int_{\Omega_\varepsilon} f v, & \forall v \in V_H^{d,Ven} \\ \int_{\Gamma_H} \mu[u_H^{d,Ven}] &= 0, & \forall \mu \in M_H \end{aligned} \quad (3.19)$$

To complete our palette of methods, we introduce a discontinuous treatment for Dirichlet based approximate profiles (as an alternative to the continuous treatment (3.13) although the latter was already well suited to the Dirichlet case). We introduce the discontinuous counterpart of  $V_H$  augmented by approximate profiles  $V_{i,h}^\varepsilon$ , as defined by (3.11), inside  $\Lambda_H$  only:

$$\begin{aligned} V_H^{d,Dir} = \left\{ v_H : \Omega_\varepsilon \rightarrow \mathbb{R} \text{ such that } \exists v_H^{(out)} \in V_H, v_H^{(in)} \in V_H \text{ and} \right. \\ \left. v_H = v_H^{(out)} \text{ on } \Omega \setminus \bar{\Lambda}_H, \right. \\ \left. v_H = v_H^{(in)} + \sum_{i=1}^2 \alpha_i V_{i,h}^\varepsilon \text{ with some } \alpha_1, \alpha_2 \in \mathbb{R} \text{ on } \Lambda_H \setminus \omega_\varepsilon \right\} \end{aligned}$$

The Dirichlet Zoom method reads then: find  $u_H^{d,Dir} \in V_H^{d,Dir}$ ,  $\lambda_H \in M_H$  such that

$$\begin{aligned} \int_{\Omega_\varepsilon} \nabla u_H^{d,Dir} \cdot \nabla v + \int_{\Gamma_H} \lambda_H[v] &= \int_{\Omega_\varepsilon} f v, & \forall v \in V_H^{d,Dir} \\ \int_{\Gamma_H} \mu[u_H^{d,Dir}] &= 0, & \forall \mu \in M_H \end{aligned} \quad (3.20)$$

### 3.3 Numerical results

We illustrate all the methods presented above on the example of Problem (3.1) in the domain  $\Omega_\varepsilon$  as in Fig. 2.1. We set namely  $\Omega = (-1, 1)^2$ ,  $\omega_\varepsilon$  given by the level-set (2.89) with  $\varepsilon = 0.1$ , and  $\Omega_\varepsilon = \Omega \setminus \omega_\varepsilon$ . Unlike the numerical experiments of the previous chapter, we choose here a simpler expression for the right-hand side<sup>1</sup>

$$f = x + y. \quad (3.21)$$

In all our numerical tests, we use piecewise linear finite elements on a coarse mesh  $\mathcal{T}_H$  on  $\Omega$ . We set the patch  $\Lambda$  as the circle of radius 0.2 centered at the origin, and use piecewise linear finite elements on a fine mesh  $\mathcal{T}_h$  on  $\Lambda$ . Typical meshes are given at Fig. 3.2. As our problem does not have an analytic solution, we should also employ a fine global mesh  $\mathcal{T}_h^{glob}$  to compute

---

<sup>1</sup>We have also tried the test case with the exact solution (2.90) but found the asymptotic expansion methods inappropriate. Indeed, these methods are designed work only if  $u_\varepsilon$  is a small perturbation of  $u_0$  which is not the case of (2.90).

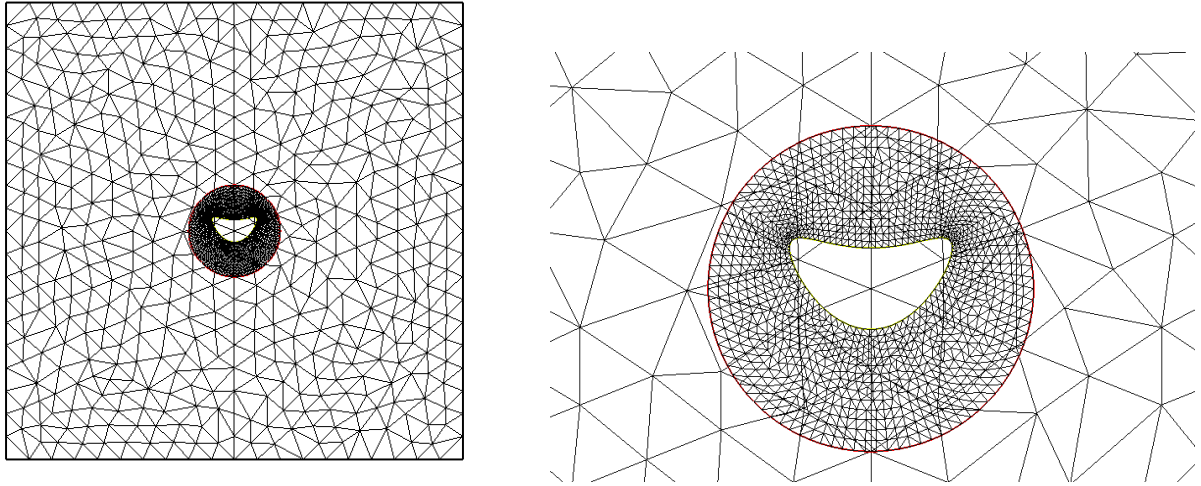


FIGURE 3.2: The coarse mesh  $\mathcal{T}_H$  on  $\Omega$  and the fine mesh  $\mathcal{T}_h$  on  $\Lambda_\varepsilon$ ,  $H = 0.15$ ,  $h = 0.02$ . Left: the whole picture; Right: a zoom around  $\Lambda$ .

a reference solution on  $\Omega_\varepsilon$ . We always construct  $\mathcal{T}_h^{glob}$  with approximately the same mesh size as that of  $\mathcal{T}_h$ .

We start by summarizing the methods to be tested, giving them "nick-names" for future reference.

**Zoom** The Numerical Zoom Algorithm 2.1. We shall also use the abbreviation "Zoom  $n$ " to designate the result obtained after  $n$  iteration of the method, i.e.  $u_{Hh}^n$ .

**Superpos** The simplest implementatino of the approach of matched asymptotic expansions where we solve first the unperturbed problem on the coarse mesh and then superimpose the corrections by (3.12).

**SupVar** Variational superposition approach where the corrections (Dirichlet profiles (3.11), the same as in the previous method) are incorporated in the variational formulation, cf. (3.13).

**DirZoom** Dirichlet Zoom method, using the same profiles as abobe, but on  $\Lambda_H$  only, coupling everything together by (3.20).

**RobZoom** Robin Zoom method, using profiles (3.16) on  $\Lambda_H$  only, coupling everything together by (3.18).

**VenZoom** Ventcel Zoom method, using profiles (3.17) on  $\Lambda_H$  only, coupling everything together by (3.19).

We present first the convergence of the Zoom method, Fig. 3.3. We observe that the method has essentially converged in 4 iterations. The same is true on finer meshes, cf. Fig. 3.9. We recall now that the asymptotic expansion methods arrive to correct the coarse solution at "one shot" by precalculating the profiles as presented at Figs. 3.4, 3.5, and 3.6 for, respectively,

Dirichlet, Robin, and Ventcel boundary conditions on  $\Gamma$ . The results obtained using these profiles are presented at Fig. 3.7. Visually, all of them resemble much the results obtained by 4 iterations of Zoom method. This is confirmed by a mesh convergence study at Fig. 3.8. All the methods arrive at very similar precision with the exception of the simplest (and cheapest) superposition method, which degrades significantly, especially on the finer meshes.

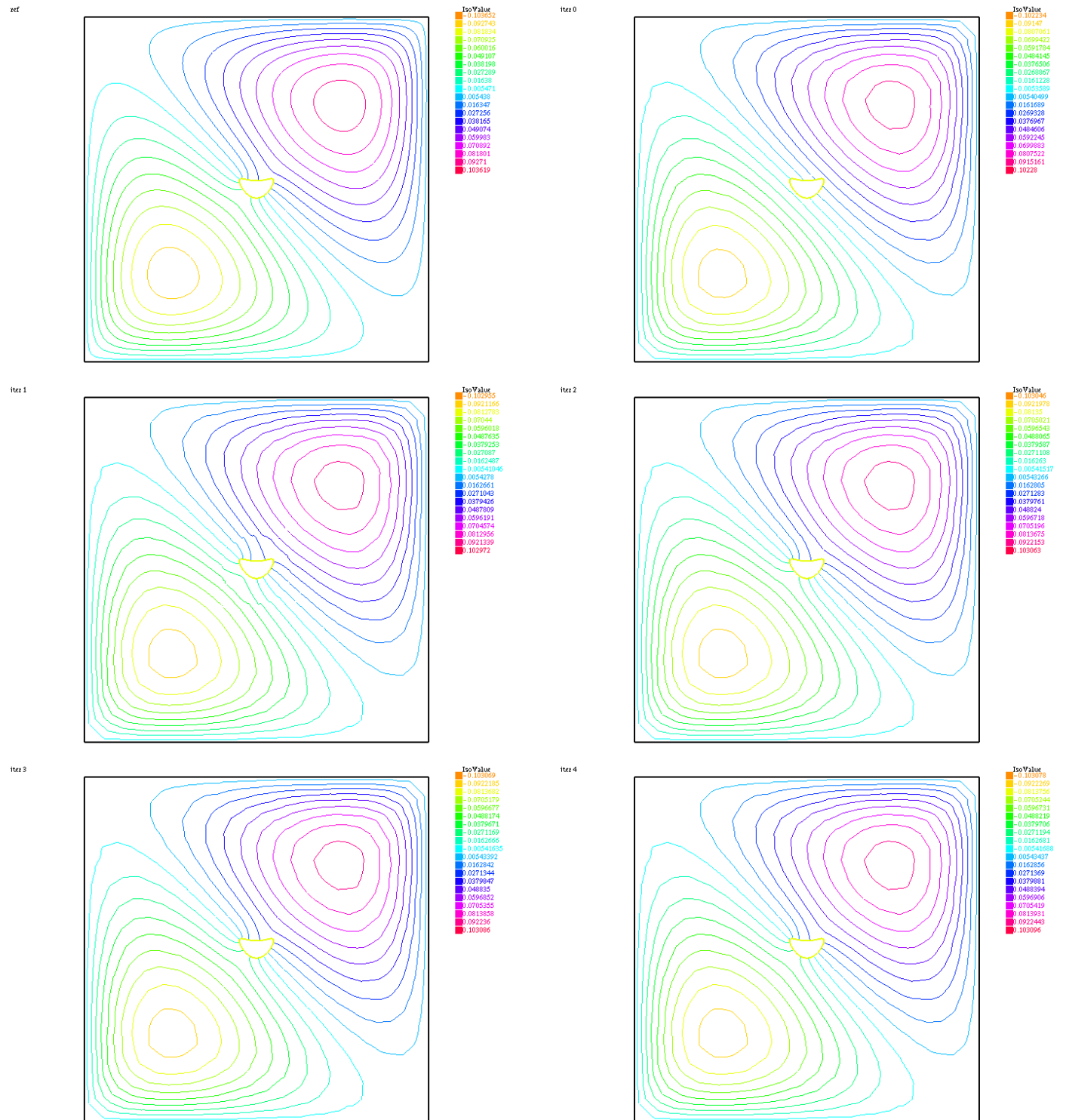


FIGURE 3.3: Evolution on iterations of Algorithm 2.1 in the test case (2.89)–(3.21) with  $\varepsilon = 0.1$ , the meshes as in Fig. 3.2. The reference solution, the initial coarse approximation (Iter 0,  $u_H^0$ ) and the first 4 iterations ( $u_{Hh}^n$ ,  $n = 1, \dots, 5$ ) of Algorithm 2.1 are presented from top to bottom, left to right.

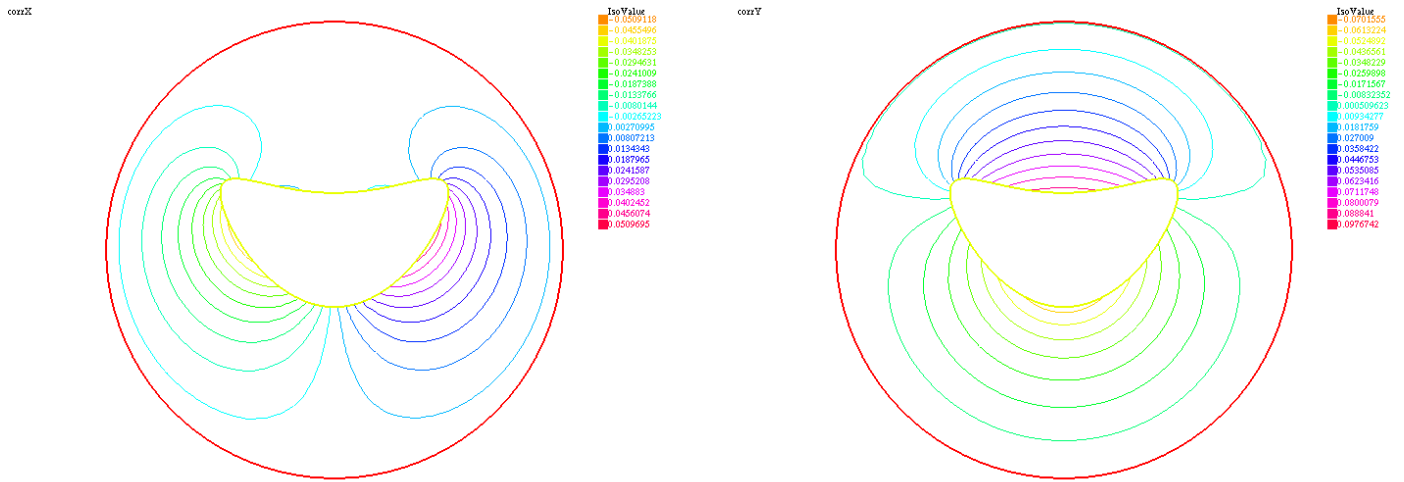


FIGURE 3.4: Dirichlet correctors.

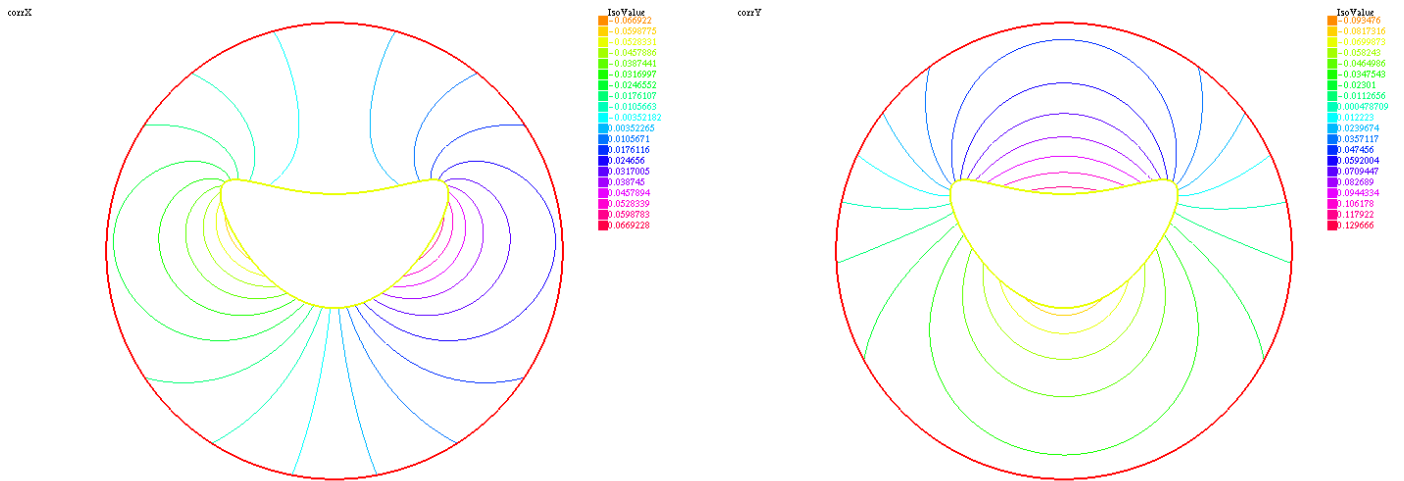


FIGURE 3.5: Robin correctors.

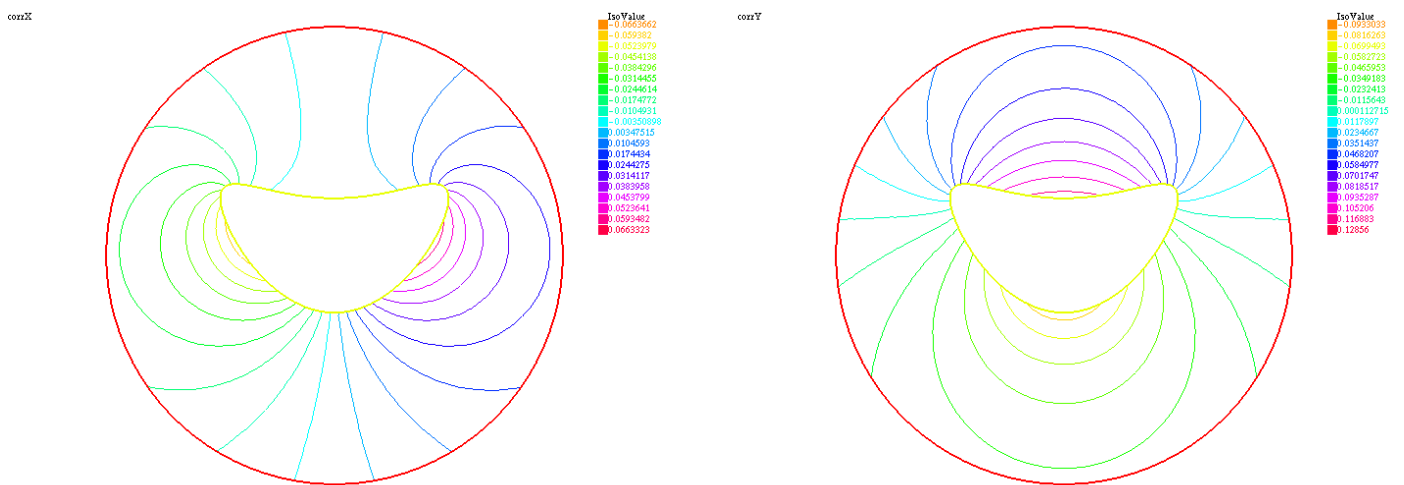
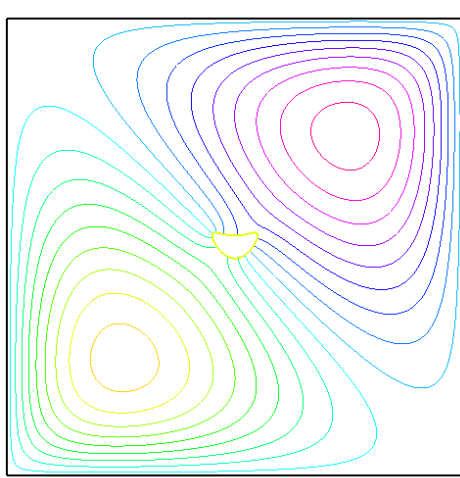
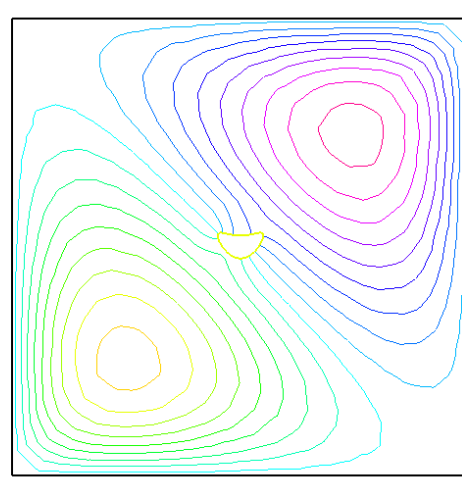


FIGURE 3.6: Vencel correctors.

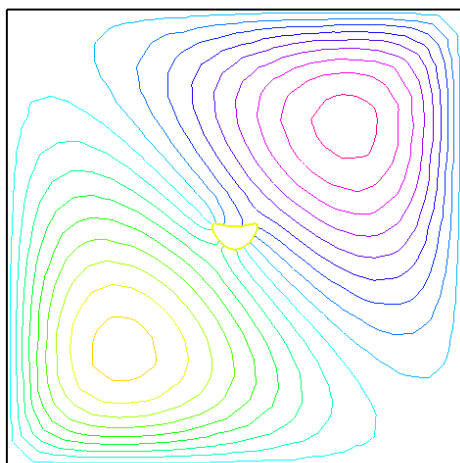
ref



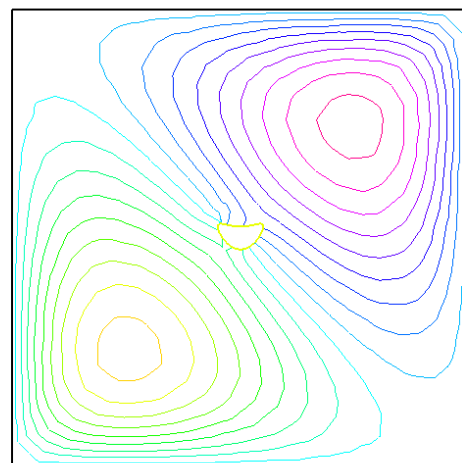
Reference solution



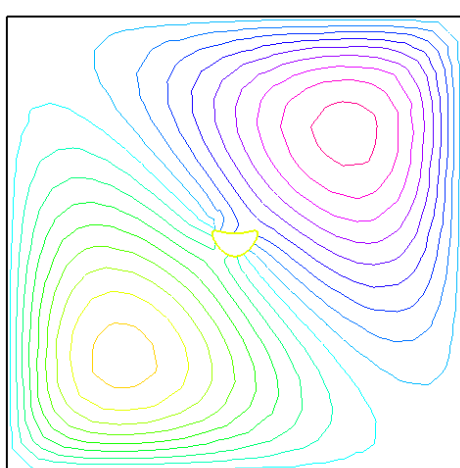
Superpos



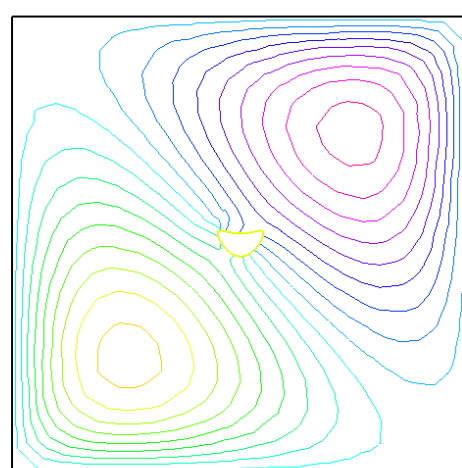
SupVar



DirZoom



RobZoom



VenZoom

FIGURE 3.7: All methods.

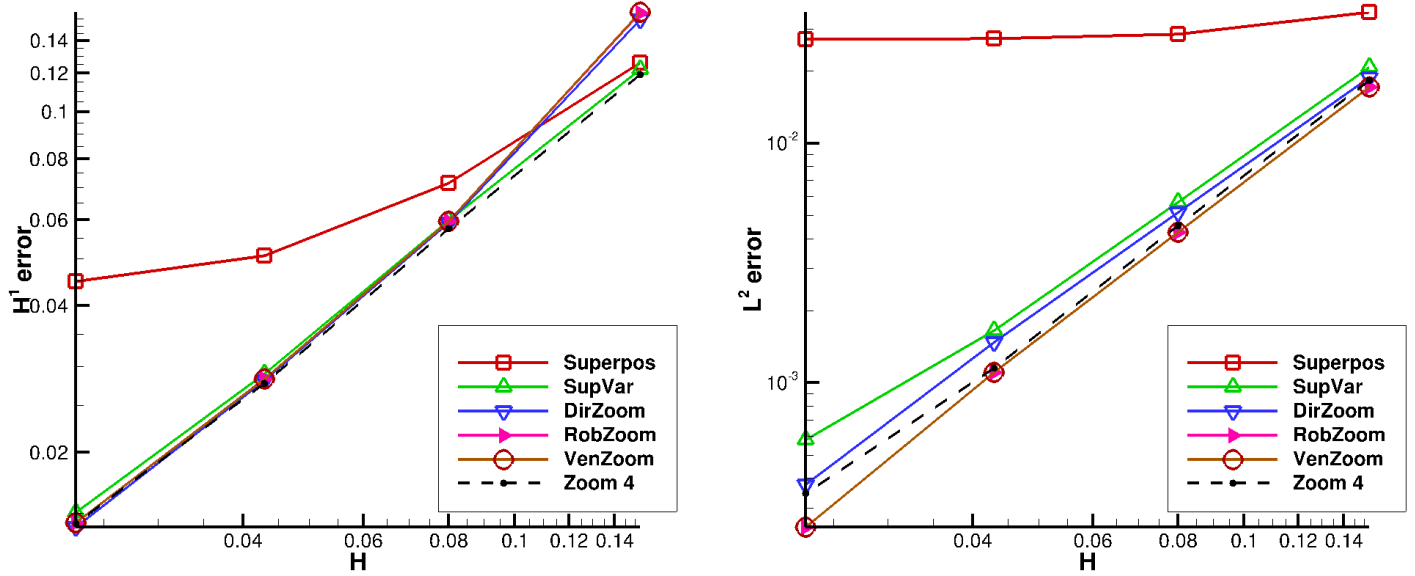


FIGURE 3.8: The relative errors in  $H^1$  and  $L^2$  norms as functions of the mesh size  $H$ .

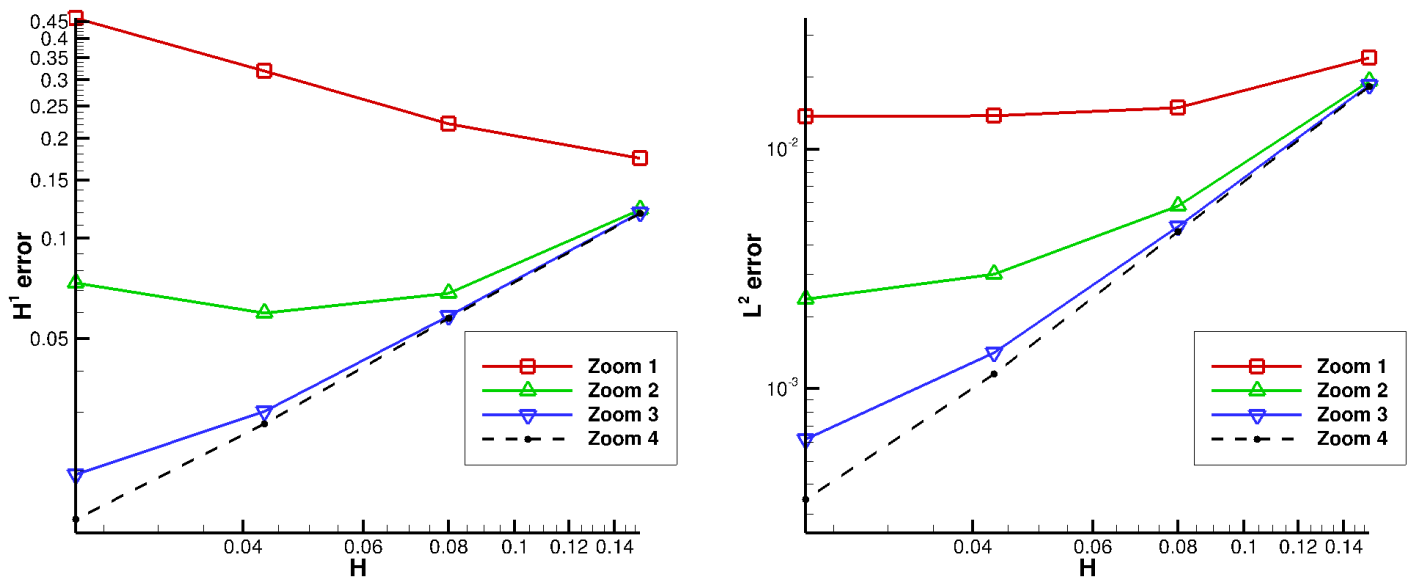


FIGURE 3.9: The relative errors in  $H^1$  and  $L^2$  norms as functions of the mesh size  $H$ .

## Chapter 4

# Numerical zoom for monotone non linear problems

---

In this chapter, we shall consider non-linear monotone problems with localized non-linearity. We shall adapt the multi-model numerical zoom (Algorithm 2.1) to this situation, by introducing a non-linear local problem on the fine mesh in this algorithm. Such an algorithm has been already proposed and theoretically investigated on the continuous level in [34]. Here, we shall prove the *a priori* error estimate and the convergence of the algorithm on the discrete level, restricting our attention to the case of  $\Gamma$ -nested meshes.

### 4.1 General properties of monotone operators and applications to PDEs

Let us start by some generalities on non-linear monotone problems, following [35]. We shall assume  $V$  a real Hilbert space (the general theory can be also set in reflexive Banach spaces). We consider mappings  $\mathcal{A} : V \rightarrow V^*$  with  $V^*$  being the dual space, i.e. the space of continuous linear functions on  $V$ . For element  $g \in V^*$  and  $v \in V$ , we write  $(g, v)$  for  $g(v)$ .

**Definition 4.1.** We say that a mapping  $\mathcal{A} : V \rightarrow V^*$  is bounded if it maps bounded sets in  $V$  to bounded sets in  $V^*$ . The mapping is continuous if for every  $u \in V$  and any sequence  $\{u_n\} \subset V$  such that  $u_n \rightarrow u$  we have

$$\|\mathcal{A}(u) - \mathcal{A}(u_n)\|_{V^*} \rightarrow 0.$$

**Definition 4.2.** We say that a mapping  $\mathcal{A} : V \rightarrow V^*$  is monotone if

$$(\mathcal{A}(u) - \mathcal{A}(v), u - v) \geq 0 \text{ for all } u, v \in V,$$

and strictly monotone if this inequality is strict whenever  $u \neq v$ .



**Definition 4.3.** We say that a mapping  $\mathcal{A} : V \rightarrow V^*$  is coercive if

$$\frac{(\mathcal{A}(u), u)}{\|u\|_V} \rightarrow \infty \text{ as } \|u\|_V \rightarrow \infty$$

The properties above can be seen as a non-linear generalization of the assumption of the Lax-Milgram lemma. In particular, they ensure the existence and uniqueness of solutions to equation with non-linear monotone operators, as specified by the following theorem due to Browder and Minty. We shall further reformulate this theorem in a form closer to the Lax-Milgram lemma, cf. Corollary 4.2 below.

**Theorem 4.1.** Let  $V$  be a real Hilbert space and let  $\mathcal{A} : V \rightarrow V^*$  be bounded, continuous, coercive and monotone. Then  $\mathcal{A}(V) = V^*$ , i.e. for any  $g \in V^*$  there exists a solution  $u \in V$  of the equation

$$\mathcal{A}(u) = g.$$

**Remark 4.1.** The solution given by Browder-Minty theorem is unique if the mapping  $\mathcal{A}$  is strictly monotone. Indeed, supposing that there are two different solutions  $u \neq \tilde{u}$  of  $\mathcal{A}(u) = \mathcal{A}(\tilde{u}) = g$  leads to

$$(\mathcal{A}(u) - \mathcal{A}(\tilde{u}), u - \tilde{u}) = 0$$

in contradiction with the property of the strictly monotone mapping.

In practice, the mapping  $\mathcal{A}$  is usually introduced by a variational formulation of a partial differential equation. We thus associate with  $\mathcal{A} : V \rightarrow V^*$  a semi-linear form (a real-valued functional of two variables, which is linear with respect to the second parameter, but generally non-linear with respect to the first one)  $a : V \times V \rightarrow \mathbb{R}$  defined by

$$a(u, v) = (\mathcal{A}(u), v) \text{ for all } u, v \in V. \quad (4.1)$$

We shall always assume that the form  $a$  satisfies the following 3 assumptions which are more stringent than the properties required by Browder-Minty theorem:

**Assumption 4.1.** There exists  $\alpha > 0$  such that for all  $u, v \in V$

$$a(u, u - v) - a(v, u - v) \geq \alpha \|u - v\|_V^2 \quad (4.2)$$

**Assumption 4.2.** There exists a non decreasing function  $\phi : \mathbb{R}^+ \rightarrow \mathbb{R}^+$  such that for all  $u, v, w \in V$

$$|a(u, w) - a(v, w)| \leq \phi(\|u\|_V + \|v\|_V) \|u - v\|_V \|w\|_V \quad (4.3)$$

**Assumption 4.3.** It holds for all  $v \in V$

$$a(0, v) = 0.$$

**Remark 4.2.** Assumption 4.1 is known as strong monotonicity. Assumption 4.2 means that the mapping  $\mathcal{A}$  is locally Lipschitz continuous, i.e. Lipschitz continuous on any ball. Note that we do not necessarily suppose that  $\mathcal{A}$  is Lipschitz continuous on  $V$ . The last Assumption 4.3 says simply  $\mathcal{A}(0) = 0$  and is not essential. Indeed if  $\mathcal{A}(0) \neq 0$  one can introduce a corrected mapping  $\mathcal{A}'(u) = \mathcal{A}(u) - \mathcal{A}(0)$  so that  $\mathcal{A}'(0) = 0$  and the Assumptions 4.1 and 4.2 hold for  $\mathcal{A}'$  if they hold for  $\mathcal{A}$ , when one associates with them the semi-linear forms  $a'$  and  $a$  via (4.1). We prefer however to announce Assumption 4.3 since it is natural for applications in PDEs and it simplifies some calculations below.

Under Assumptions 4.1–4.3, the mapping  $\mathcal{A}$  is

- bounded; indeed  $\|u\|_V \leq C$  implies  $\|\mathcal{A}(u)\|_{V^*} \leq \phi(C)$  by (4.3) with  $v = 0$ .
- continuous; indeed if  $u_n \rightarrow u$  then  $\|\mathcal{A}(u_n) - \mathcal{A}(u)\|_{V^*} \leq \phi(\|u_n\|_V + \|u\|_V)\|u_n - u\|_V \rightarrow 0$  so that  $\mathcal{A}(u_n) \rightarrow \mathcal{A}(u)$  since the sequence  $\{u_n\}$  is bounded in  $V$ .
- strictly monotone; indeed for all  $u, v \in V$  we have  $(\mathcal{A}(u) - \mathcal{A}(v), u - v) \geq \alpha\|u - v\|_V^2$  by (4.2).
- coercive; indeed for all  $u \in V$  we have  $(\mathcal{A}(u), u) \geq \alpha\|u\|_V^2$  by (4.2) with  $v = 0$ .

We have thus the following simple corollary of Browder-Minty Theorem:

**Corollary 4.2.** Let  $V$  be a real Hilbert space and suppose that the semi-linear form  $a : V \times V \rightarrow \mathbb{R}$  satisfies Assumptions 4.1–4.3. Then, for any  $g \in V^*$  there exists the unique solution  $u \in V$  of the equation

$$a(u, v) = (g, v) \text{ for all } v \in V. \quad (4.4)$$

Under Assumptions 4.1–4.3, we can also easily prove the analogue of Céa lemma for the Galerkin approximation.

**Lemma 4.3.** Let  $V$  be a real Hilbert space and suppose that the semi-linear form  $a : V \times V \rightarrow \mathbb{R}$  satisfies Assumptions 4.1–4.3. Let  $g \in V^*$  and  $u \in V$  the unique solution of equation (4.4). Take a subspace  $V_h \subset V$  and consider the unique solution  $u_h \in V_h$  of equation

$$a(u_h, v_h) = (g, v_h) \text{ for all } v_h \in V_h. \quad (4.5)$$

Then,

$$\|u - u_h\|_V \leq C \inf_{\tilde{u}_h \in V_h} \|u - \tilde{u}_h\|_V$$

with a constant that depends on  $a$  and  $g$  but does not depend on the choice of the subspace  $V_h$ .

*Proof.* Put  $v = u$  in (4.4) and apply Assumptions 4.1, 4.3

$$\alpha \|u\|_V^2 \leq a(u, u) - a(0, u) = (g, u) \leq \|g\|_{V^*} \|u\|_V$$

so that  $\|u\|_V \leq \|g\|_{V^*}/\alpha$ . Similarly,  $\|u_h\|_V \leq \|g\|_{V^*}/\alpha$ .

Put  $v = v_h$  for any  $v_h \in V_h$  in (4.4) and subtract (4.5) from it. This gives the Galerkin orthogonality relation

$$a(u, v_h) - a(u_h, v_h) = 0, \quad \forall v_h \in V_h.$$

Take any  $\tilde{u}_h \in V_h$ . By Assumption 4.1, the linearity of  $a$  with respect to the second argument, and the relation above for  $v_h = u_h - \tilde{u}_h$ ,

$$\alpha \|u - u_h\|_V^2 \leq a(u, u - u_h) - a(u_h, u - u_h) = a(u, u - \tilde{u}_h) - a(u_h, u - \tilde{u}_h)$$

We continue using Assumption 4.2

$$\alpha \|u - u_h\|_V^2 \leq \phi(\|u\|_V + \|u_h\|_V) \|u - u_h\|_V \|u - \tilde{u}_h\|_V$$

By the estimates above

$$\|u - u_h\|_V \leq \frac{1}{\alpha} \phi(2\|g\|_{V^*}/\alpha) \|u - \tilde{u}_h\|_V$$

□

**Example 4.1.** Consider the non-linear PDE with Dirichlet boundary conditions in a bounded domain  $\Omega \subset \mathbb{R}^2$  or  $\mathbb{R}^3$

$$-\Delta u + u^3 = f \text{ in } \Omega$$

$$u = 0 \text{ on } \partial\Omega$$

Supposing  $f \in L^2(\Omega)$ , the weak formulation is posed in the Hilbert space  $V = H_0^1(\Omega)$  and reads: find  $u \in V$  such that

$$a(u, v) = \int_{\Omega} f v \text{ for all } v \in V$$

where

$$a(u, v) = \int_{\Omega} \nabla u \cdot \nabla v + \int_{\Omega} u^3 v$$

We equip the space  $V$  with the  $H^1$  semi-norm  $\|\cdot\|_V = |\cdot|_{1,\Omega}$  and prove that Assumptions 4.1 and 4.2 are satisfied (Assumption 4.3 is obvious). Indeed, for all  $u, v \in V$

$$a(u, u - v) - a(v, u - v) = |u - v|_{1,\Omega}^2 + \int_{\Omega} (u^3 - v^3)(u - v) \geq |u - v|_{1,\Omega}^2$$

since

$$(u^3 - v^3)(u - v) = (u - v)^2(u^2 + uv + v^2) \geq \frac{1}{2}(u - v)^2(u^2 + v^2) \geq 0.$$

This proves Assumption 4.1.

Now, for all  $u, v, w \in V$

$$|a(u, w) - a(v, w)| \leq |u - v|_{1,\Omega} |w|_{1,\Omega} + \left| \int_{\Omega} (u^3 - v^3)w \right|$$

Note that

$$|u^3 - v^3| = |u - v|(u^2 + uv + v^2) \leq \frac{3}{2}|u - v|(u^2 + v^2)$$

so that by Hölder inequality

$$\begin{aligned} \left| \int_{\Omega} (u^3 - v^3)w \right| &\leq \frac{3}{2} \|u - v\|_{L^3(\Omega)} \|u^2 + v^2\|_{L^3(\Omega)} \|w\|_{L^3(\Omega)} \\ &\leq \frac{3}{2} \|u - v\|_{L^3(\Omega)} (\|u\|_{L^6(\Omega)}^2 + \|v\|_{L^6(\Omega)}^2) \|w\|_{L^3(\Omega)} \end{aligned}$$

By Sobolev embedding  $H^1(\Omega) \subset L^6(\Omega) \subset L^3(\Omega)$  and the fact the  $H^1$  semi-norm is equivalent to the full  $H^1$  norm on  $H_0^1(\Omega)$ , we conclude

$$\left| \int_{\Omega} (u^3 - v^3)w \right| \leq C |u - v|_{1,\Omega} (|u|_{1,\Omega} + |v|_{1,\Omega})^2 |w|_{1,\Omega}$$

This proves Assumption 2 with  $\phi(t) = 1 + Ct^2$ .

**Example 4.2.** A more practical example is provided by the stationary (Kirchhoff transformed) Richards equation that describes the groundwater flow in unsaturated soils (c.f. [2, 8]). The equation reads

$$\nabla \cdot (K \nabla u) - \nabla \cdot (K kr(M(u)) \vec{g}) = f,$$

where  $u$  is the so-called generalized pressure,  $K$  is the hydraulic conductivity in the soil,  $kr$  the relative permeability depending on the saturation,  $M$  is some nonlinearity arising from the Kirchhoff transformation and  $\vec{g}$  denotes the gravity vector. Various explicit formulas for  $kr \circ M$  are available and, usually, this is a Lipschitz continuous function on  $\mathbb{R}$  (after a possible regularization).

Introducing the semi-linear form of the weak formulation of the problem on  $V = H_0^1(\Omega)$

$$a(u, v) = \int_{\Omega} K \nabla u \cdot \nabla v + \int_{\Omega} K kr(M(u)) \vec{g} \cdot \nabla v$$

we see that it is globally Lipschitz continuous, i.e. Assumption 4.2 is satisfied with  $\phi = \text{const}$ . Moreover, if the Lipschitz constant  $L$  of  $kr \circ M$  is sufficiently small, then

$a$  is strongly monotone, i.e. Assumption 4.1 is satisfied. Indeed, assuming

$$\alpha|\xi|^2 \leq K\xi \cdot \xi \leq \beta|\xi|^2, \quad \forall \xi \in \mathbb{R}^d$$

we have for all  $u, v \in V$

$$\begin{aligned} a(u, u-v) - a(v, u-v) &\geq \int_{\Omega} K \nabla(u-v) \cdot \nabla(u-v) - \int_{\Omega} KL|u-v|\vec{g} \cdot \nabla(u-v) \\ &\geq \alpha|u-v|_{1,\Omega}^2 - \beta L|\vec{g}|\|u-v\|_{0,\Omega}|u-v|_{1,\Omega} \geq (\alpha - \beta L|\vec{g}|C_P)|u-v|_{1,\Omega}^2 \end{aligned}$$

where  $C_P$  is the constant in Poincaré inequality on  $\Omega$ . Hence, Assumption 4.1 is satisfied if  $\alpha - \beta L|\vec{g}|C_P > 0$ .

## 4.2 A class of monotone PDEs with localized non-linearity and a Numerical Zoom for it

We are here interested in monotone PDEs, as in Examples 4.1–4.2, assuming that the non-linearity is present only in a small sub-region of the whole computational domain. Let  $\Omega \in \mathbb{R}^d$  be a bounded domain,  $\omega \subset \Omega$  its small sub-domain, and  $V = H_0^1(\Omega)$ . We consider the problem: find  $u \in V$  such that

$$a_{\Omega}(u, v) = (f, v)_{\Omega}, \quad \forall v \in V \quad (4.6)$$

where  $a_{\Omega}$  is a semi-linear form satisfying Assumptions 4.1–4.3 on space  $V$  equipped with the norm  $\|\cdot\|_V = |\cdot|_{1,\Omega}$  and  $(\cdot, \cdot)_{\Omega}$  stands for the scalar product in  $L^2(\Omega)$ . More precisely

$$a_{\Omega}(u, v) = c_{\Omega}(u, v) + a_{\omega}^{nl}(u, v) \quad (4.7)$$

where  $c_{\Omega}$  is a coercive continuous symmetric bi-linear form on  $V$  and  $a_{\omega}^{nl}$  is a semi-linear form on  $H^1(\omega)$  satisfying properly modified Assumptions 4.1–4.3, namely:

**Monotonicity:** There exists  $\alpha > 0$  such that for all  $u, v \in H^1(\omega)$

$$a_{\omega}^{nl}(u, u-v) - a_{\omega}^{nl}(v, u-v) \geq 0 \quad (4.8)$$

**Lipschitz:** There exists a non decreasing function  $\phi : \mathbb{R}^+ \rightarrow \mathbb{R}^+$  such that for all  $u, v, w \in H^1(\omega)$

$$|a_{\omega}^{nl}(u, w) - a_{\omega}^{nl}(v, w)| \leq \phi(\|u\|_{1,\omega} + \|v\|_{1,\omega})\|u-v\|_{1,\omega}\|w\|_{1,\omega} \quad (4.9)$$

**Vanishing at 0:** It holds for all  $v \in H^1(\omega)$

$$a_{\omega}^{nl}(0, v) = 0. \quad (4.10)$$

In all the assumptions above and in (4.7), we implicitly assume that  $a_\omega^{nl}$  works on the restrictions to  $\omega$  of functions in  $H_0^1(\Omega)$ . Note that monotonicity of  $a_\omega^{nl}$  in (4.8) implies the strong monotonicity of  $a_\Omega$ , as in (4.1), thanks to the coerciity of  $c_\Omega$ .

In order to have concrete examples in mind, we may consider localized version of problems in Examples 4.1–4.2.

**Example 4.3.** Consider the non-linear PDE with Dirichlet boundary conditions in a bounded domain  $\Omega \subset \mathbb{R}^2$  or  $\mathbb{R}^3$

$$\begin{aligned} -\Delta u + \chi u^3 &= f \text{ in } \Omega \\ u &= 0 \text{ on } \partial\Omega \end{aligned} \tag{4.11}$$

where  $\chi : \Omega \rightarrow \mathbb{R}$  is localized in a small subdomain  $\omega \subset \Omega$ , i.e.  $\text{supp}(\chi) \subset \omega$ . Supposing  $f \in L^2(\Omega)$ ,  $\chi \geq 0$ , and  $\chi \in L^\infty(\Omega)$ , the weak formulation in  $V = H_0^1(\Omega)$  reads: find  $u \in V$  such that

$$a(u, v) = \int_{\Omega} f v \text{ for all } v \in V$$

where

$$a(u, v) = \int_{\Omega} \nabla u \cdot \nabla v + \int_{\Omega} \chi u^3 v$$

Assumptions (4.8)–(4.10) are satisfied setting

$$c_\Omega(u, v) = \int_{\Omega} \nabla u \cdot \nabla v \quad \text{and} \quad a_\Omega^{nl}(u, v) = \int_{\omega} \chi u^3 v$$

This is proved in the same manner as in Example 4.1. Thus, Assumptions 4.1–4.3 are also satisfied and the problem admits the unique solution.

**Example 4.4.** We reconsider Richards equation modeling the groundwater flow in unsaturated soils, as in Example 4.2, but assume in addition that one can simplify the equation to the linear Darcy equation everywhere on  $\Omega$  except a small subdomain  $\omega$ . The governing equation then reads

$$\nabla \cdot (K \nabla u) - \nabla \cdot (K \chi_\omega k r(M(u)) \vec{g}) = f,$$

where  $\chi_\omega$  is the characteristic function of the subdomain  $\omega$ . The semi-linear form of the weak formulation of the problem on  $V = H_0^1(\Omega)$  is now

$$a(u, v) = \int_{\Omega} K \nabla u \cdot \nabla v + \int_{\omega} K k r(M(u)) \vec{g} \cdot \nabla v$$

Assumptions (4.8)–(4.10) are satisfied setting

$$c_\Omega(u, v) = \int_{\Omega} K \nabla u \cdot \nabla v \quad \text{and} \quad a_\Omega^{nl}(u, v) = \int_{\omega} K k r(M(u)) \vec{g} \cdot \nabla v$$

Thus, Assumptions 4.1–4.3 are also satisfied and the problem admits a unique solution. In particular, Assumptions 4.9 and 4.2 are satisfied with  $\phi = \text{const}$ .

We want to devise a finite element method that works on a relatively coarse mesh  $\mathcal{T}_H$  on  $\Omega$  and solves on this mesh only the linear part of the problem, with the bilinear form  $c_\Omega$ . The mesh  $\mathcal{T}_H$  will be typically too coarse to take properly into account the small inclusion  $\omega$ , and the possibly sharp behavior of the solution on it. Any way, the global coarse solver on  $\mathcal{T}_H$  will not see the nonlinearity inside  $\omega$ . This coarse approximation will be then corrected iteratively using another sufficiently fine mesh around  $\omega$ . We introduce thus the patch  $\Lambda$ ,  $\omega \subset \Lambda \subset \Omega$ , and the fine local mesh  $\mathcal{T}_h$  on  $\Lambda$ . For the sake of simplicity, both domains  $\Omega$  and  $\Lambda$  are supposed polygonal and  $\Lambda$  is supposed to lie inside  $\Omega$ , i.e. the boundaries of  $\Lambda$  and  $\Omega$  do not intersect each other. Both meshes  $\mathcal{T}_h$  and  $\mathcal{T}_H$  are supposed regular simplicial triangulations of  $\Omega$  and  $\Lambda$  respectively, i.e. the maximal aspect ratio of the triangles/tetrahedrons in both these meshes is fixed once for all.

Introduce the finite element spaces

$$V_H = \{v_H \in C^0(\Omega) : v_H|_T \in P_k \forall T \in \mathcal{T}_H, v_H|_{\partial\Omega} = 0\}$$

and

$$V_h = \{v_h \in C^0(\Lambda) : v_h|_T \in P_k \forall T \in \mathcal{T}_h\}.$$

where  $P_k$  is the set of polynomials in  $d$  real variables of a given degree  $k \geq 1$ . Let  $\Gamma = \partial\Lambda$ . We shall need a finite element space on  $\Gamma$  to be used for Lagrange multipliers and defined as the space of traces of functions in  $V_h$ :

$$M_h = \{\mu_h \in C^0(\Gamma) : \mu_h|_E \in P_k \text{ on every boundary facet } E \text{ of mesh } \mathcal{T}_h\}$$

The approach outlined above is formalized as Algorithm 4.1, which is a natural extension of our basic Algorithm 2.1 to the present nonlinear setting. In writing this algorithm, we adopt the following assumptions and notations:

- $(\cdot, \cdot)_\Omega$  and  $(\cdot, \cdot)_\Lambda$  stand for the scalar product in  $L^2(\Omega)$  and  $L^2(\Lambda)$  respectively.
- $\langle \cdot, \cdot \rangle$  the scalar product in  $L^2(\Gamma)$
- We suppose that the bilinear form  $c_\Omega$  can be decomposed as

$$c_\Omega(u, v) = c_\Lambda(u, v) + c_{\Omega \setminus \bar{\Lambda}}(u, v) \quad (4.12)$$

with bilinear forms  $c_\Lambda$  which is semicoercive and continuous on  $H^1(\Lambda)$  in the sense

$$c_\Lambda(u, u) \geq \alpha |u|_{1,\Lambda}^2, \quad c_\Lambda(u, v) \leq M |u|_{1,\Lambda} |v|_{1,\Lambda}, \quad \forall u, v \in H^1(\Lambda), \quad (4.13)$$

and  $c_{\Omega \setminus \bar{\Lambda}}$  which is coercive and continuous on the restriction of  $V$  on  $\Omega \setminus \bar{\Lambda}$ .

Compute the initial guess  $u_H^0 \in V_H$  such that

$$c_\Omega(u_H^0, v_H) = (f, v_H)_\Omega, \quad \forall v_H \in V_H$$

and choose the relaxation parameter  $\omega \in (0, 1]$ .

**for**  $n = 1, 2, 3, \dots$  **do**

Find  $u_h^n \in V_h$  and  $\lambda_h^n \in M_h$  such that

$$\begin{aligned} a_\Lambda(u_h^n, v_h) - \langle \lambda_h^n, v_h \rangle &= (f, v_h)_\Lambda, \quad \forall v_h \in V_h \\ \langle u_h^n, \mu_h \rangle &= \langle u_H^{n-1}, \mu_h \rangle, \quad \forall \mu_h \in M_h \end{aligned}$$

Find  $u_H^n \in V_H$  such that

$$\begin{aligned} c_\Omega(u_H^n, v_H) &= \omega(f, v_H)_{\Omega \setminus \bar{\Lambda}} - \omega \langle \lambda_h^n, v_H \rangle + \omega c_\Lambda(u_H^{n-1}, v_H) \\ &\quad + (1 - \omega)c_\Omega(u_H^{n-1}, v_H), \quad \forall v_H \in V_H \end{aligned}$$

Set

$$u_{Hh}^{n-1/2} = \begin{cases} u_h^n, & \text{in } \Lambda \\ u_H^{n-1}, & \text{outside } \Lambda \end{cases} \quad u_{Hh}^n = \begin{cases} u_h^n, & \text{in } \Lambda \\ u_H^n, & \text{outside } \Lambda \end{cases}$$

**end**

**Algorithm 4.1:** Numerical zoom for monotone nonlinear problems

Similarly, the semi-linear form  $a_\Omega$  is decomposed as

$$a_\Omega(u, v) = a_\Lambda(u, v) + a_{\Omega \setminus \bar{\Lambda}}(u, v) \quad (4.14)$$

where

$$a_\Lambda(u, v) = c_\Lambda(u, v) + a_\omega^{nl}(u, v)$$

and  $a_{\Omega \setminus \bar{\Lambda}} = c_{\Omega \setminus \bar{\Lambda}}$ .

### 4.3 Analysis of Algorithm 4.1 on $\Gamma$ -nested meshes

We shall analyze the accuracy and convergence of Algorithm 4.1 only in the case of  $\Gamma$ -nested meshes in the sense of Definition 2.1. We assume throughout the Section that the localized linearity satisfies (4.8)–(4.10) so that Assumptions 4.1–4.3 hold true. We shall prove the convergence of iterations, under 2 additional alternative assumptions:

**Non-linearity localized well away from  $\Gamma$**  as in [34]: the nonlinearity region  $\omega$  is well inside  $\Lambda$ , i.e. there is a big enough gap between  $\partial\omega$  and  $\Gamma = \partial\Lambda$ . The (theoretical) convergence rate depends on the width of the gap so that the iterative algorithm can converge very slowly is the gap is very narrow. The proofs are in Subsection 4.3.2.



**Globally Lipschitz non-linearity:** Assumption 4.9 is satisfied with  $\phi = \text{const}$ . The proofs are in Subsection 4.3.3.

### 4.3.1 The finite element problem: an a priori error estimate

Assume for the moment that Algorithm 4.1 converges (as proved in the next subsections under some additional assumptions). Here, we are going to characterize the limit of the iterative process in Algorithm 4.1 and examine the precision of this limit with respect to the exact solution of problem (4.6). Let us suppose thus that  $u_H^n \rightarrow u_H$  on  $\Omega$ ,  $u_h^n \rightarrow u_h$  on  $\Lambda$ , and  $\lambda_h^n \rightarrow \lambda_h$  on  $\Gamma$  as  $n \rightarrow \infty$ . Passing to the limit in Algorithm 1, it is easy to see that the functions  $u_H \in V_H$ ,  $u_h \in V_h$  and  $\lambda_h \in M_h$  satisfy

$$c_{\Omega \setminus \bar{\Lambda}}(u_H, v_H) + \langle \lambda_h, v_H \rangle = (f, v_H)_{\Omega \setminus \bar{\Lambda}}, \quad \forall v_H \in V_H \quad (4.15)$$

$$a_{\Lambda}(u_h, v_h) - \langle \lambda_h, v_h \rangle = (f, v_h)_{\Lambda}, \quad \forall v_h \in V_h \quad (4.16)$$

$$\langle \mu_h, u_H - u_h \rangle = 0, \quad \forall \mu_h \in M_h. \quad (4.17)$$

We emphasize that  $u_H$  survives at the limit  $n \rightarrow \infty$  only outside  $\Lambda$ .

Assuming that the meshes are  $\Gamma$ -nested, cf. Definition 2.1, let us denote the combined approximation space

$$V_{Hh} = \{v \in C(\bar{\Omega}) \text{ such that } v = v_H \text{ on } \Omega \setminus \bar{\Lambda}, v = v_h \text{ on } \Lambda \\ \text{with some } v_H \in V_H, v_h \in V_h\}$$

and gather  $u_H$  and  $u_h$  into  $u_{Hh} \in V_{Hh}$  such that  $u_{Hh} = u_H$  on  $\Omega \setminus \bar{\Lambda}$  and  $u_{Hh} = u_h$  on  $\Lambda$ . Note that  $u_{Hh}$  is indeed continuous on  $\Gamma$  thanks to (4.17) which is equivalent to say  $u_H = u_h$  on  $\Gamma$  in the case of  $\Gamma$ -nested meshes. Taking the sum of (4.15) and (4.16) we can easily eliminate  $\lambda_h$  and rewrite this problem in terms of  $u_{Hh}$  alone: find  $u_{Hh} \in V_{Hh}$  such that

$$a_{\Omega}(u_{Hh}, v_{Hh}) = (f, v_{Hh})_{\Omega}, \quad \forall v_{Hh} \in V_{Hh}. \quad (4.18)$$

**Theorem 4.4.** *Problem (4.18) admits a unique solution  $u_{Hh} \in V_{Hh}$ . If  $u$ , the exact solution to (4.6), is in  $H^{k+1}(\Omega)$ , we have moreover the following a priori error estimate*

$$\|u_{Hh} - u\|_{1,\Omega} \leq C (H^k |u|_{k+1,\Omega \setminus \bar{\Lambda}} + h^k |u|_{k+1,\Lambda}) \quad (4.19)$$

with a constant  $C$  independent of  $H$ ,  $h$  and  $u$ .

*Proof.* The semi-linear form  $a_{\Omega}$  satisfies Assumptions 4.1–4.3 so that Problem (4.18) admits the unique solution thanks to Browder-Minty theorem. Recall the interpolation estimate from the proof of Theorem 2.1: there exists  $\tilde{u}_{Hh} \in V_{Hh}$  such that

$$\|u - \tilde{u}_{Hh}\|_{1,\Omega_{\varepsilon}} \leq C (H^k |u|_{k+1,\Omega \setminus \bar{\Lambda}} + h^k |u|_{k+1,\Lambda}) \quad (4.20)$$

In view of (4.18), (4.6) and the fact that  $V_{Hh} \subset V$ , the nonlinear adaptation of Céa lemma 4.3 ensures that  $\|u_{Hh} - u\|_{1,\Omega} \leq C \|\tilde{u}_{Hh} - u\|_{1,\Omega}$  so that (4.20) leads to (4.19).  $\square$

### 4.3.2 Convergence of the iterative algorithm for well localized non-linearities

The proof of the convergence of Algorithm 4.1 will be here done under the additional geometrical assumption, also introduced in [34]:

**Assumption 4.4.** *There is a gap between  $\partial\omega$  and  $\Gamma$ , i.e.  $\delta := \text{dist}(\partial\omega, \Gamma) > 0$ . Moreover, the meshsize of  $\mathcal{T}_h$  is small enough so that the mesh cells of  $\mathcal{T}_h$  adjacent to  $\Gamma$  do not intersect  $\omega$ .*

Let us recall the decomposition of the finite element space  $V_H = V_H^0 \oplus V_H^1$  where  $V_H^0$  is defined by (2.24) and  $V_H^1$  is the orthogonal complement of  $V_H^0$  with respect to the scalar product  $c_\Omega$ . The proof of the convergence of Algorithm 4.1 will be based on a study of the mapping  $A_{Hh} : V_H^1 \rightarrow V_H^1$  defined for fixed  $\mathcal{T}_H$  and  $\mathcal{T}_h$  as follows: for any  $z_H \in V_H^1$  the function  $A_{Hh}z_H \in V_H^1$  solves

$$c_\Omega(A_{Hh}z_H, v_H) = c_{\Omega \setminus \bar{\Lambda}}(z_H, v_H) + \langle \nu_h, v_H \rangle - (f, v_H)_{\Omega \setminus \bar{\Lambda}}, \forall v_H \in V_H^1 \quad (4.21)$$

where  $\nu_h \in M_h$  together with  $z_h \in V_h$  come as the solution to

$$a_\Lambda(z_h, v_h) - \langle \nu_h, v_h \rangle = (f, v_h)_\Lambda, \quad \forall v_h \in V_h \quad (4.22)$$

$$\langle z_h, \mu_h \rangle = \langle z_H, \mu_h \rangle, \quad \forall \mu_h \in M_h. \quad (4.23)$$

Comparing with Algorithm 4.1 we observe that the iterates  $u_H^n$  evolve in this Algorithm from one iteration to another as

$$u_H^n = (I - \omega A_{Hh})u_H^{n-1}. \quad (4.24)$$

It is thus a fixed point algorithm to solve the equation

$$A_{Hh}u_H = 0 \quad (4.25)$$

Combining (4.21) and (4.22), we observe  $\forall z_H, v_H \in V_H$

$$c_\Omega(A_{Hh}z_H, v_H) = c_{\Omega \setminus \bar{\Lambda}}(z_H, v_H) + a_\Lambda(z_h, v_h) - (f, v_H)_{\Omega \setminus \bar{\Lambda}} - (f, v_h)_\Lambda \quad (4.26)$$

where  $z_h \in V_h$  is the solution to (4.22)–(4.23) and  $v_h \in V_h$  is such that  $v_h = v_H$  on  $\Gamma$ .

We will now prove that the mapping  $A_{Hh}$  is a contraction in the norm  $\|\cdot\|_c$  associated to the scalar product  $c_\Omega$ , provided  $\omega > 0$  is chosen sufficiently small.

**Lemma 4.5.** *Assuming properties (4.8)–(4.10) together with the properties of  $c_\Lambda$  and  $c_{\Omega \setminus \bar{\Lambda}}$  listed on page 82, the mapping  $A_{Hh}$  is strictly monotone on  $V_H^1$  with respect to the scalar product  $c_\Omega$ : there exists  $\gamma > 0$  such that for all  $z_H, \tilde{z}_H \in V_H^1$*

$$c_\Omega(A_{Hh}z_H, z_H - \tilde{z}_H) - c_\Omega(A_{Hh}\tilde{z}_H, z_H - \tilde{z}_H) \geq \gamma \|z_H - \tilde{z}_H\|_c^2 \quad (4.27)$$

*Proof.* Take any  $z_H, \tilde{z}_H \in V_H^1$  and let  $(z_h, \nu_h) \in V_h \times M_h$ , resp.  $(\tilde{z}_h, \tilde{\nu}_h) \in V_h \times M_h$  be the solutions to (4.22)–(4.23) with  $z_H$ , resp.  $\tilde{z}_H$ , in the right hand side of (4.23). Set  $v_H = z_H - \tilde{z}_H$ ,  $v_h = z_h - \tilde{z}_h$ . By (4.26), the linearity of the form  $c_\Omega$ , and (4.8),

$$\begin{aligned} c_\Omega(A_{Hh}z_H, v_H) - c_\Omega(A_{Hh}\tilde{z}_H, v_H) &= c_{\Omega \setminus \bar{\Lambda}}(z_H - \tilde{z}_H, v_H) + a_\Lambda(z_h, v_h) - a_\Lambda(\tilde{z}_h, v_h) \\ &\geq c_{\Omega \setminus \bar{\Lambda}}(v_H, v_H) \geq C|v_H|_{1, \Omega \setminus \bar{\Lambda}}^2. \end{aligned}$$

The last inequality is valid since  $c_{\Omega \setminus \bar{\Lambda}}$  is coercive. We now recall from the proof of Lemma 2.3

$$|v_H|_{1, \Omega \setminus \bar{\Lambda}} \geq C|v_H|_{1, \Omega}$$

since  $v_H \in V_H^1$ . This entails (4.27).  $\square$

**Lemma 4.6.** *Assuming properties (4.8)–(4.10) and Assumption 4.4, the mapping  $A_{Hh}$  is Lipschitz continuous on  $V_H^1$  with respect to the scalar product  $c_\Omega$ : there exists  $M > 0$  such that for all  $z_H, \tilde{z}_H \in V_H^1$*

$$\|A_{Hh}z_H - A_{Hh}\tilde{z}_H\|_c \leq M\|z_H - \tilde{z}_H\|_c \quad (4.28)$$

with  $M \sim 1/\delta$ .

*Proof.* Take any  $z_H, \tilde{z}_H \in V_H^1$  and let  $(z_h, \nu_h) \in V_h \times M_h$ , resp.  $(\tilde{z}_h, \tilde{\nu}_h) \in V_h \times M_h$  be the solutions to (4.22)–(4.23) with  $z_H$ , resp.  $\tilde{z}_H$ , in the right hand side of (4.23).

Introduce a lifting operator  $R_h^\Gamma : M_h \rightarrow V_h$  that takes a function on  $\Gamma$  in the trace space of  $V_h$  and reconstructs a function in  $V_h$  having the prescribed trace on  $\Gamma$ . Thanks to Assumption 4.4, we can safely assume that for any  $\mu_h \in M_h$

$$R_h^\Gamma \mu_h = 0 \text{ on } \omega, \text{ and } |R_h^\Gamma \mu_h|_{1, \Lambda} \leq C_\Gamma |\mu_h|_{\frac{1}{2}, \Gamma} \quad (4.29)$$

with a constant  $C_\Gamma$  of order  $1/\delta$ .

We decompose  $z_h = z_h^0 + R_h^\Gamma z_H$  with  $z_h^0 \in V_h$ ,  $z_h^0|_\Gamma = 0$  and similarly for  $\tilde{z}_h$ . Problems (4.22)–(4.23) can be then rewritten as

$$a_\Lambda(z_h^0 + R_h^\Gamma z_H, v_h^0) = (f, v_h^0)_\Lambda$$

$$a_\Lambda(\tilde{z}_h^0 + R_h^\Gamma \tilde{z}_H, v_h^0) = (f, v_h^0)_\Lambda$$

for any  $v_h^0 \in V_h$  such that  $v_h^0|_\Gamma = 0$ . Since the non-linearity in  $a_\Lambda$  acts only inside  $\omega$ , it does not affect the contributions with  $R_h^\Gamma$  which are non-zero only

on  $\Lambda \setminus \omega$ . The problems above can be thus recast as

$$a_\Lambda(z_h^0, v_h^0) + c_\Lambda(R_h^\Gamma z_H, v_h^0) = (f, v_h^0)_\Lambda$$

$$a_\Lambda(\tilde{z}_h^0, v_h^0) + c_\Lambda(R_h^\Gamma \tilde{z}_H, v_h^0) = (f, v_h^0)_\Lambda$$

Taking the difference between these two equations, setting  $v_h^0 = z_h^0 - \tilde{z}_h^0$  and applying the monotonicity property (4.8) gives

$$\alpha |z_h^0 - \tilde{z}_h^0|_{1,\Lambda}^2 \leq a_\Lambda(z_h^0, v_h^0) - a_\Lambda(\tilde{z}_h^0, v_h^0) = -c_\Lambda(R_h^\Gamma z_H - R_h^\Gamma \tilde{z}_H, v_h^0)$$

so that, by (4.13),

$$|z_h^0 - \tilde{z}_h^0|_\Lambda \leq C |R_h^\Gamma z_H - R_h^\Gamma \tilde{z}_H|_{1,\Lambda} \quad (4.30)$$

We now note that the calculation of  $\nu_h$  in (4.22) is only affected by the test functions  $v_h$  attached to  $\Gamma$ , i.e. (having already computed  $z_h$ ) we can assume that  $v_h$  in (4.22) vanishes on  $\omega$  thanks to Assumption 4.4. But  $a_\Lambda$  coincides on  $\Lambda$  with the bilinear form  $c_\Lambda$  so that (4.22) can be rewritten for such test functions as

$$c_\Lambda(z_h, v_h) - \langle \nu_h, v_h \rangle = (f, v_h)_\Lambda$$

Writing the same for  $\tilde{z}_h, \tilde{\nu}_h$  and taking  $v_h = R_h^\Gamma v_H$  for  $v_H = z_H - \tilde{z}_H$ , we see that

$$\begin{aligned} \langle \nu_h - \tilde{\nu}_h, v_H \rangle &= c_\Lambda(z_h - \tilde{z}_h, R_h^\Gamma v_H) \leq C |z_h - \tilde{z}_h|_{1,\Lambda} |R_h^\Gamma v_H|_{1,\Lambda} \\ &\leq C (|z_h^0 - \tilde{z}_h^0|_{1,\Lambda} + |R_h^\Gamma z_H - R_h^\Gamma \tilde{z}_H|_{1,\Lambda}) |v_H|_{1,\Omega \setminus \bar{\Lambda}} \\ &\leq C C_\Gamma |z_H - \tilde{z}_H|_{1,\Omega \setminus \bar{\Lambda}} |v_H|_{1,\Omega \setminus \bar{\Lambda}} \end{aligned}$$

We have used here (4.30) and (4.29) together with a trace inequality on  $\Omega \setminus \bar{\Lambda}$ . Substituting this into (4.21) gives

$$\begin{aligned} c_\Omega(A_{Hh} z_H - A_{Hh} \tilde{z}_H, v_H) &= c_{\Omega \setminus \bar{\Lambda}}(z_H - \tilde{z}_H, v_H) + \langle \nu_h - \tilde{\nu}_h, v_H \rangle \\ &\leq C C_\Gamma |z_H - \tilde{z}_H|_{1,\Omega \setminus \bar{\Lambda}} |v_H|_{1,\Omega \setminus \bar{\Lambda}} \end{aligned}$$

which implies (4.28) with a constant of order  $1/\delta$ .  $\square$

**Corollary 4.7.** *Assuming properties (4.8)–(4.10) and Assumption 4.4, the mapping  $I - \omega A_{Hh}$  is a contraction on  $V_H^1$  for  $0 < \omega < \omega_0$  with some sufficiently small  $\omega_0 > 0$ .*

*Proof.* For any  $u_H, v_H \in V_H^1$ , using (4.27) and (4.28),

$$\begin{aligned} &\|(I - \omega A_{Hh})u_H - (I - \omega A_{Hh})v_H\|_c^2 \\ &= \|u_H - v_H\|_c^2 - 2\omega c_\Omega(A_{Hh}u_H - A_{Hh}v_H, u_H - v_H) + \|A_{Hh}u_H - A_{Hh}v_H\|_c^2 \\ &\leq \|u_H - v_H\|_c^2 (1 - 2\omega\gamma + \omega^2 M^2) \end{aligned}$$

We note that  $1 - 2\omega\gamma + \omega^2 M^2 < 1$  for all  $\omega \in (0, \omega_0)$  with  $\omega_0 = \frac{2\gamma}{M^2}$ . Hence,  $(I - \omega A_{Hh})$  is a contraction for these  $\omega$ .  $\square$

**Theorem 4.8.** *Assuming properties (4.8)–(4.10) and Assumption 4.4, Algorithm 4.1 converges to the solution of (4.18) provided  $0 < \omega < \omega^*$  where  $\omega^*$  is a mesh-independent constant, i.e.  $u_{Hh}^n \rightarrow u_{Hh}$  as  $n \rightarrow \infty$  where  $u_{Hh} \in V_{Hh}$  is the unique solution of (4.18). The convergence rate is independent from  $h$  and  $H$ , but may depend on  $\delta$  from Assumption 4.4.*

*Proof.* We decompose each iterate of Algorithm 4.1 as  $u_H^n = u_H^{n,0} + u_H^{n,1}$  with  $u_H^{n,0} \in V_H^0$  and  $u_H^{n,1} \in V_H^1$ . Taking the test functions  $v_H \in V_H^0$  in the equation for  $u_H^n$  of Algorithm 4.1 we see immediately

$$u_H^{n,0} = u_H^{n-1,0}$$

Similarly, taking the test functions  $v_H \in V_H^1$ , we rediscover

$$u_H^{n,1} = (I - \omega A_{Hh})u_H^{n-1,1}$$

As proved in the preceding corollary,  $(I - \omega A_{Hh})$  is a contraction on  $V_H^1$ . This shows the convergence of the sequence  $\{u_H^{n,1}\}$ . The iterates  $u_h^n$  are uniquely determined by the traces of  $\{u_H^n\}$  on  $\Gamma$  which coincide with those of  $u_{Hh}^{n,1}$ . We see thus that the sequence  $\{u_h^n\}$  is also convergent, as is the sequence  $\{u_{Hh}^n\}$  since  $u_{Hh}^n = u_H^{n,1}$  on  $\Omega \setminus \bar{\Lambda}$  and  $u_{Hh}^n = u_H^n$  on  $\Lambda$ .  $\square$

An unfortunate feature of Algorithm 4.1 is that its convergence rate strongly depends on the distance  $\delta$  between  $\partial\omega$  and  $\Gamma$  in Assumption 4.4 so that, at least according to our proofs, the patch  $\Lambda$  should be taken much larger than the nonlinearity zone  $\omega$ . The (theoretical) reason for this lies in the Dirichlet boundary conditions for  $u_h^n$ . Technically, this obliges us to introduce the lifting operator  $R_h^\Gamma$  in the analysis of Lemma 4.6 that should live in the gap between  $\partial\omega$  and  $\Gamma$  and thus prevents us from shrinking this gap. In the next Subsection, we present a convergence analysis avoiding the annoying geometrical Assumption 4.4.

### 4.3.3 Convergence of the iterative algorithm for globally Lipschitz non-linearities

The proof of the convergence of Algorithm 4.1 will be done here under the additional assumption about the form  $a_\Lambda$ , which is stronger than property (4.9):

**Assumption 4.5.** *There exists  $L > 0$  such that for all  $u, v, w \in H^1(\Lambda)$*

$$|a_\Lambda(u, w) - a_\Lambda(v, w)| \leq L \|u - v\|_{1,\Lambda} |w|_{1,\Lambda}$$

**Remark 4.3.** *The assumption of the global Lipschitz continuity is of course rather restrictive. We argue however that we can often adopt it in practice. For instance, Richards equation (Examples 4.2 or 4.4) leads naturally to global Lipschitz problems. On the other hand, the cubic linearity in Examples 4.1 or 4.3 is only locally Lipschitz.*

However, if the solution to (4.11) is bounded, i.e.  $|u(x)| \leq \theta$  for all  $x \in \Omega$  for some  $\theta > 0$ , we can replace the governing equation with

$$-\Delta u + \chi N_\theta(u) = f \quad (4.31)$$

where

$$N_\theta(u) = \begin{cases} u^3, & \text{for } |u| \leq \theta \\ \theta^2 u, & \text{for } |u| > \theta \end{cases} \quad (4.32)$$

This does not change the solution and the associated semi-linear form is globally Lipschitz.

**Lemma 4.9.** Under Assumption 4.5 and properties (4.8), (4.10), the mapping  $A_{Hh}$  is Lipschitz continuous on  $V_H^1$  with respect to the scalar product  $c_\Omega$ : there exists  $M > 0$  such that for all  $z_H, \tilde{z}_H \in V_H^1$

$$\|A_{Hh}z_H - A_{Hh}\tilde{z}_H\|_c \leq M\|z_H - \tilde{z}_H\|_c \quad (4.33)$$

*Proof.* Take any  $z_H, \tilde{z}_H \in V_H^1$  and let  $(z_h, v_h) \in V_h \times M_h$ , resp.  $(\tilde{z}_h, \tilde{v}_h) \in V_h \times M_h$  be the solutions to (4.22)–(4.23) with  $z_H$ , resp.  $\tilde{z}_H$ , in the right hand side of (4.23).

Introduce  $w \in H^1(\Lambda)$  as the solution to

$$-\Delta w = 0 \text{ in } \Lambda, \quad w = z_H - \tilde{z}_H \text{ on } \Gamma$$

and construct  $w_h \in V_h$  as a Scott-Zhang interpolation of  $w$  being a projection on the finite element trace space on  $\Gamma$  so that we have  $w_h = z_H - \tilde{z}_H$  on  $\Gamma$ . By the properties of Scott-Zhang interpolation

$$\|w_h\|_{1,\Lambda} \leq C\|w\|_{1,\Lambda} \leq C\|z_H - \tilde{z}_H\|_{0,\Gamma} \quad (4.34)$$

Take  $v_h = z_h - \tilde{z}_h - w_h$  in problems (4.22)–(4.23). Noting that  $v_h = 0$  on  $\Gamma$ , these problems can be then rewritten as

$$a_\Lambda(z_h, v_h) = (f, v_h)_\Lambda$$

$$a_\Lambda(\tilde{z}_h, v_h) = (f, v_h)_\Lambda$$

Taking the difference between these two equations gives

$$a_\Lambda(z_h, v_h) - a_\Lambda(\tilde{z}_h, v_h) = 0$$

which we can rewrite, thanks to the linearity of  $a_\Lambda$  with respect to the second argument, as

$$a_\Lambda(z_h, z_h - \tilde{z}_h) - a_\Lambda(\tilde{z}_h, z_h - \tilde{z}_h) = a_\Lambda(z_h, w_h) - a_\Lambda(\tilde{z}_h, w_h)$$

This gives, since  $a_\Lambda$  is monotone and globally Lipschitz,

$$\alpha|z_h - \tilde{z}_h|_{1,\Lambda}^2 \leq L\|z_h - \tilde{z}_h\|_{1,\Lambda}\|w_h\|_{1,\Lambda} \leq \frac{L\varepsilon}{2}\|z_h - \tilde{z}_h\|_{1,\Lambda}^2 + \frac{L}{2\varepsilon}\|w_h\|_{1,\Lambda}^2$$

for any  $\varepsilon > 0$ . Using Poincaré and trace inequalities, one can prove

$$\|z_h - \tilde{z}_h\|_{1,\Lambda}^2 = |z_h - \tilde{z}_h|_{1,\Lambda}^2 + \|z_h - \tilde{z}_h\|_{0,\Lambda}^2 \leq C(|z_h - \tilde{z}_h|_{1,\Lambda}^2 + \|z_h - \tilde{z}_h\|_{0,\Gamma}^2).$$

Hence, taking  $\varepsilon$  small enough

$$|z_h - \tilde{z}_h|_{1,\Lambda}^2 \leq C(\|z_H - \tilde{z}_H\|_{0,\Gamma}^2 + \|w_h\|_{1,\Lambda}^2) \leq C\|z_H - \tilde{z}_H\|_{0,\Gamma}^2$$

thanks to (4.34). We now use a trace inequality on  $\Omega \setminus \bar{\Lambda}$  to conclude

$$\|z_h - \tilde{z}_h\|_{1,\Lambda} \leq C|z_H - \tilde{z}_H|_{1,\Omega \setminus \bar{\Lambda}}$$

Substituting this into (4.26) gives

$$\begin{aligned} c_\Omega(A_{Hh}z_H - A_{Hh}\tilde{z}_H, v_H) &= c_{\Omega \setminus \bar{\Lambda}}(z_H - \tilde{z}_H, v_H) + a_\Lambda(z_h, v_h) - a_\Lambda(\tilde{z}_h, v_h) \\ &\leq C|z_H - \tilde{z}_H|_{1,\Omega \setminus \bar{\Lambda}}|v_H|_{1,\Omega \setminus \bar{\Lambda}} \end{aligned}$$

which implies (4.33).  $\square$

We note that the monotonicity of the mapping  $A_{Hh}$  without additional Assumptions 4.4 and 4.5, cf. Lemma 4.5. Thus, combining Lemmas 4.5 and 4.9, we arrive at

**Theorem 4.10.** *Under Assumptions 4.1–4.3 and 4.5 and properties (4.8), (4.10), Algorithm 4.1 converges to the solution of (4.18) provided  $0 < \omega < \omega^*$  where  $\omega^*$  is a mesh-independent constant, i.e.  $u_{Hh}^n \rightarrow u_{Hh}$  as  $n \rightarrow \infty$  where  $u_{Hh} \in V_{Hh}$  is the unique solution of (4.18). The convergence rate is independent of  $h$  and  $H$ .*

## 4.4 Numerical tests

We shall test the numerical zoom Algorithm 4.1 on a problem with localized cubic non-linearity (4.11). We choose the domain  $\Omega$  as the square  $(-1, 1)^2$  and the subdomain  $\omega$  where the non-linearity is active in the disk of radius  $r$ :  $\omega = \{(x, y) : x^2 + y^2 < r^2\}$ . We set  $\chi$  accordingly and choose the right-hand side as

$$\chi(x, y) = \begin{cases} \eta, & \text{if } x^2 + y^2 < r^2 \\ 0, & \text{otherwise} \end{cases} \quad \text{and } f = \text{const} \quad (4.35)$$

We have thus three numerical parameters  $r$ ,  $\eta$ , and  $f$  to fix in each numerical experiment.

We use the uniform Cartesian mesh of size  $h$  in  $x$  and  $y$  directions on  $\Lambda = (-L, L)^2$  with  $L, H, h$  set so that  $L/H$  and  $H/h$  are integers. The non-linear problems on the fine mesh in Algorithm 4.1 are solved by Newton's method with the stopping criterion  $\|u_h^{n(k)} - u_h^{n(k-1)}\|_{0,\Lambda} \leq 10^{-8}$ . Problem (4.11) with the settings above does not have an analytical solution. We have thus compared the approximation with the reference solution computed on a global uniform Cartesian mesh of size  $h$ .

**First test case (well localized non linearity).** We consider Problem (4.11) with coefficients (4.35) and  $r = \sqrt{0.02}$ ,  $\eta = f = 10$ . We take the patch  $\Lambda = (-0.2, 0.2)^2$  so that the non-linearity zone  $\omega$  (the disc or radius  $\sqrt{0.02}$ ) is separated from  $\Gamma = \partial\Lambda$  by a comfortable gap. We present the convergence of Algorithm 4.1 without relaxation (i.e.  $\omega = 1$ ) at Fig. 4.1. Visually, we observe that the algorithm converges, but its first iterations are very far from the final solution, and the convergence is rather slow. This is confirmed by convergence curve at Fig. 4.2. We report there the relative errors in  $H^1$  and  $L^2$  norms on iteration using several, more and more refined grids. The convergence becomes slower on more refined meshes, and one needs 40 iterations in order to observe the converged solution on all the meshes if one looks at the  $H^1$  norm. One observes the optimal  $O(H)$  behavior of the error in this norm for the converged approximate solutions. On the contrary, these 40 iterations seem not enough when we look at the  $L^2$  norm, which can explain the lack of the optimal  $O(H^2)$  behavior of the error.

**Second test case (non linearity touching  $\Gamma$ ).** We consider again Problem (4.11) with coefficients (4.35) and put  $r = 0.02$ , while keeping  $\eta = f = 10$  and the patch  $\Lambda = (-0.2, 0.2)^2$  so that the non-linearity zone  $\omega$  (the disc or radius 0.02) touches  $\Gamma$ . Algorithm 4.1 without relaxation (i.e.  $\omega = 1$ ) does not converge in this case, as reported at Fig. 4.3 (red curves). We have tried to make the cubic non linearity by a globally Lipschitz one (4.31)–(4.32) with  $\theta = 6$ . This, however, does not make the method convergent, only slowing the divergence, as seen at Fig. 4.3 (green curves). The only trick to retrieve convergence is to introduce some relaxation in the method, i.e. take  $\omega < 1$ . For example, taking  $\omega = 0.2$ , the method converges at essentially 5 iteration, see Fig. 4.3 (blue curves). Note that we do not introduce the cut-off in these last experiments. The convergence is thus not guaranteed by our theory of Subsections 4.3.2 or 4.3.3. The convergence of the method with  $\omega = 0.2$  is additionally illustrated by Figs. 4.4–4.5, where the iteration up to 4th are plotted and we see clearly that the iterative process has stabilized.

As a conclusion of these first numerical experiments, we can say that additional Assumptions 4.4 or 4.5 are not really necessary for Algorithm 4.1 to converge (contrary to the relaxation, which can be indeed necessary). One needs a subtler theory to investigate Algorithm 4.1 without Assumptions 4.4 or 4.5.



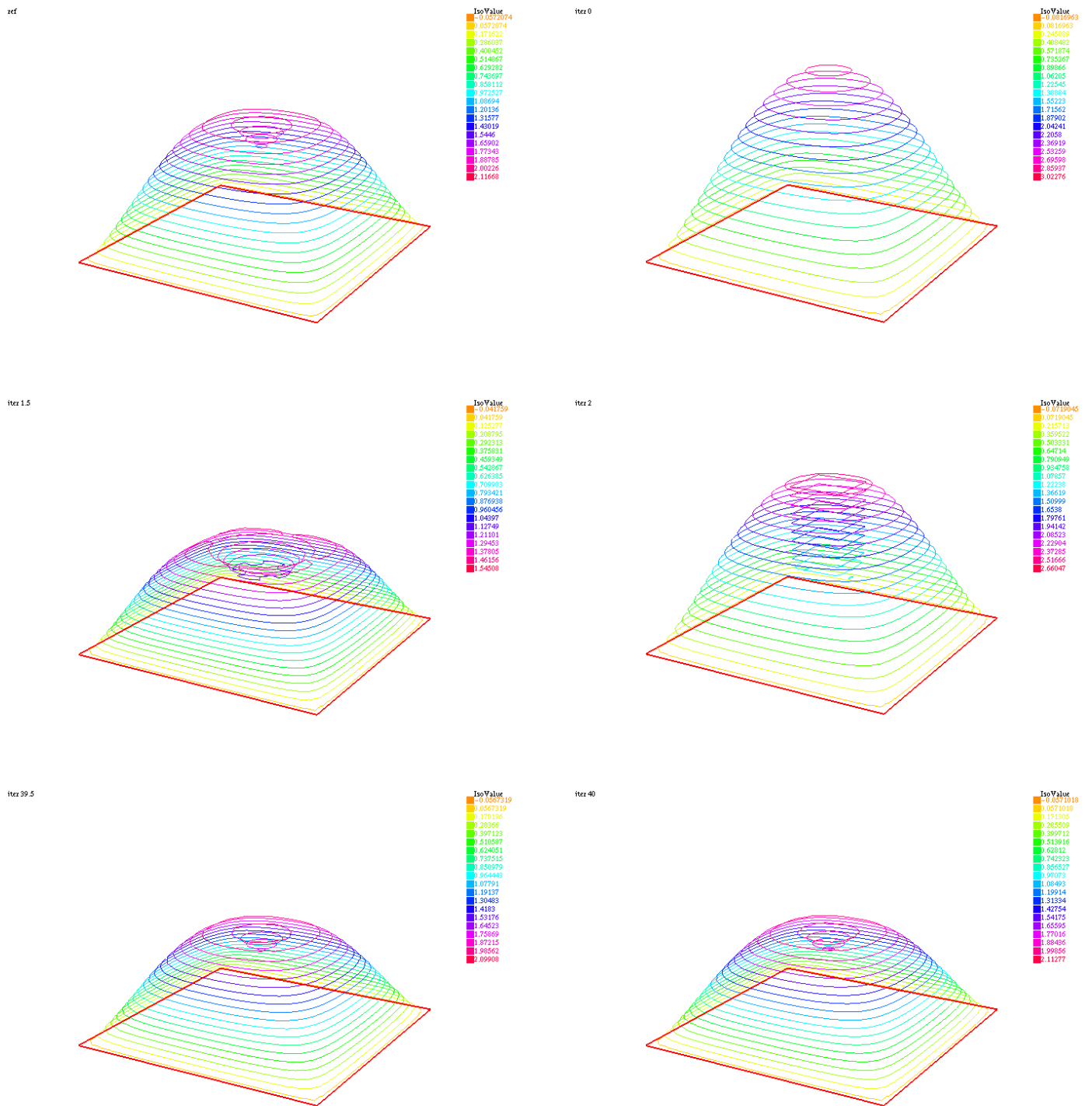


FIGURE 4.1: Evolution on iterations of Algorithm 4.1. The test case (4.11)–(4.35) with  $r = \sqrt{0.02}$ ,  $\eta = f = 10$ , the mesh sizes  $H = 0.1$ ,  $h = 0.01$  on the patch  $\Lambda = (-0.2, 0.2)^2$ . The reference solution, the initial coarse approximation (Iter 0,  $u_H^0$ ) and several subsequent iterations ( $u_{Hh}^{1.5}$ ,  $u_{Hh}^2$ ,  $u_{Hh}^{39.5}$ ,  $u_{Hh}^{40}$ ) of Algorithm 4.1 are presented from top to bottom, left to right.

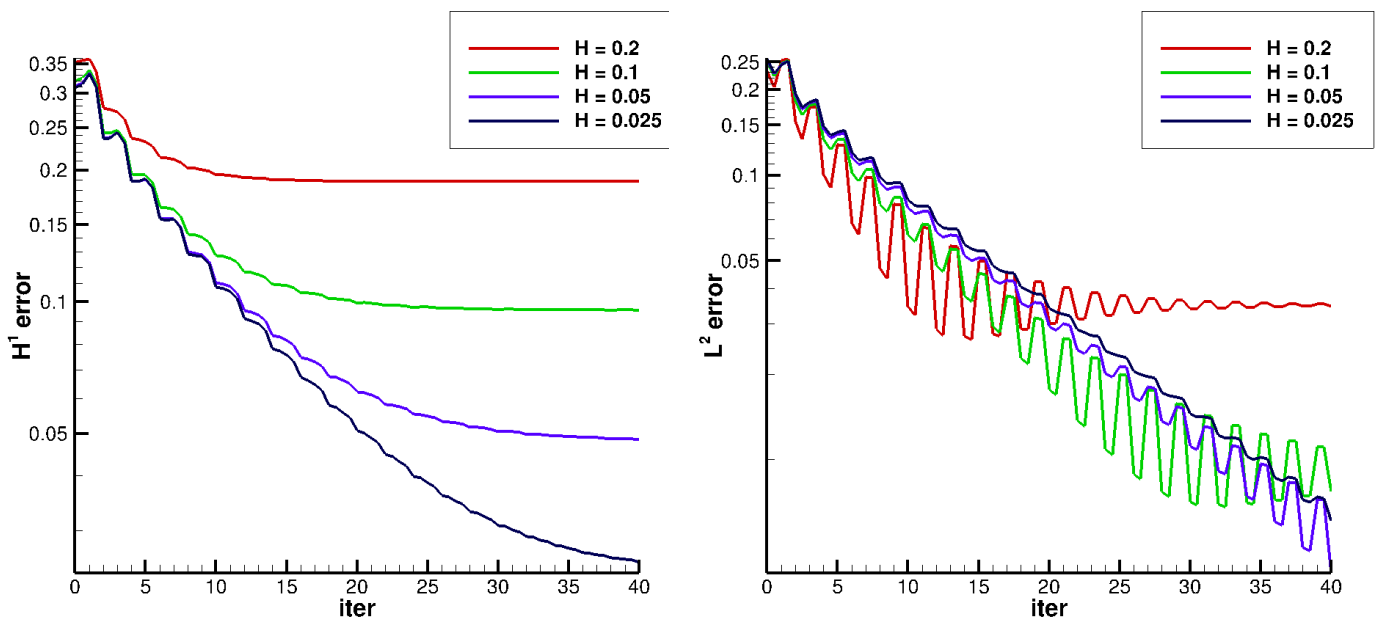


FIGURE 4.2: Convergence of Algorithm 4.1 under the mesh refinement for the same test case as in Fig. 4.1, the varying mesh size  $H$ , and the fine mesh size  $h = H/20$  on the patch  $\Lambda = (-0.2, 0.2)^2$ .

Left: the relative  $H^1$ -error on iterations; Right: the relative  $L^2$ -error on iterations.

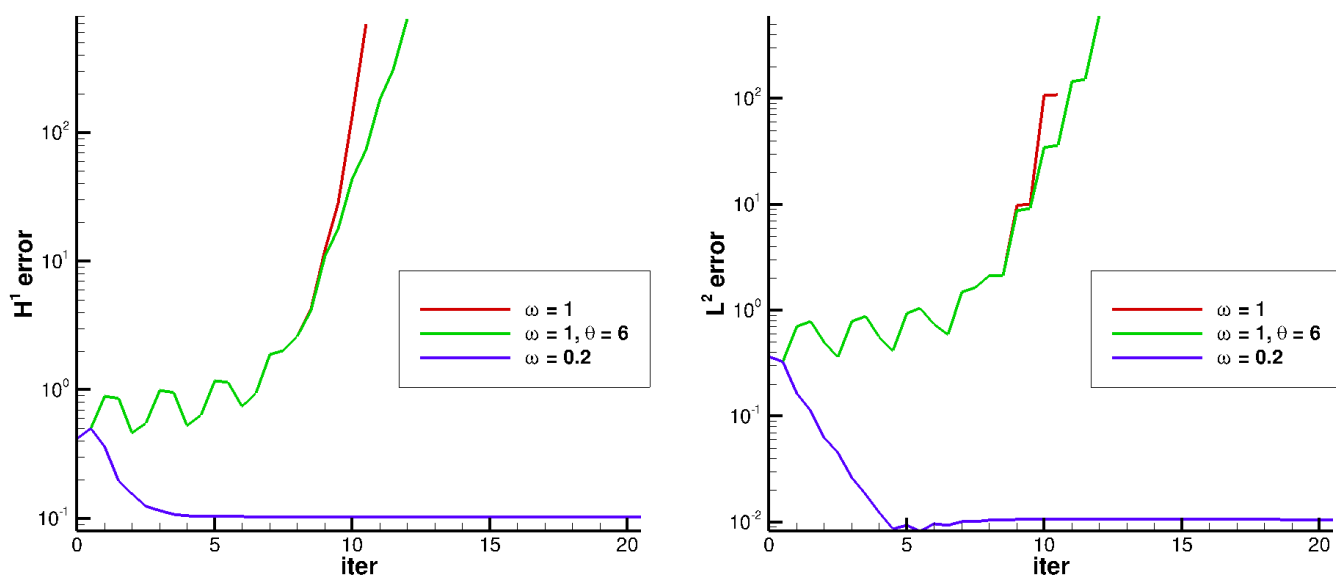


FIGURE 4.3: Convergence of Algorithm 4.1 . The test case (4.11)–(4.35) with  $r = 0.02$ ,  $\eta = f = 10$ , the mesh sizes  $H = 0.1$ ,  $h = 0.01$  on the patch  $\Lambda = (-0.2, 0.2)^2$ . We present 3 variants: i) no relaxation ( $\omega = 1$ ); ii) no relaxation ( $\omega = 1$ ) but a cut-off on the non-linearity ( $\theta = 6$ ); iii) relaxation ( $\omega = 0.2$ ), no cut-off. Left: the relative  $H^1$ -error on iterations; Right: the relative  $L^2$ -error on iterations.

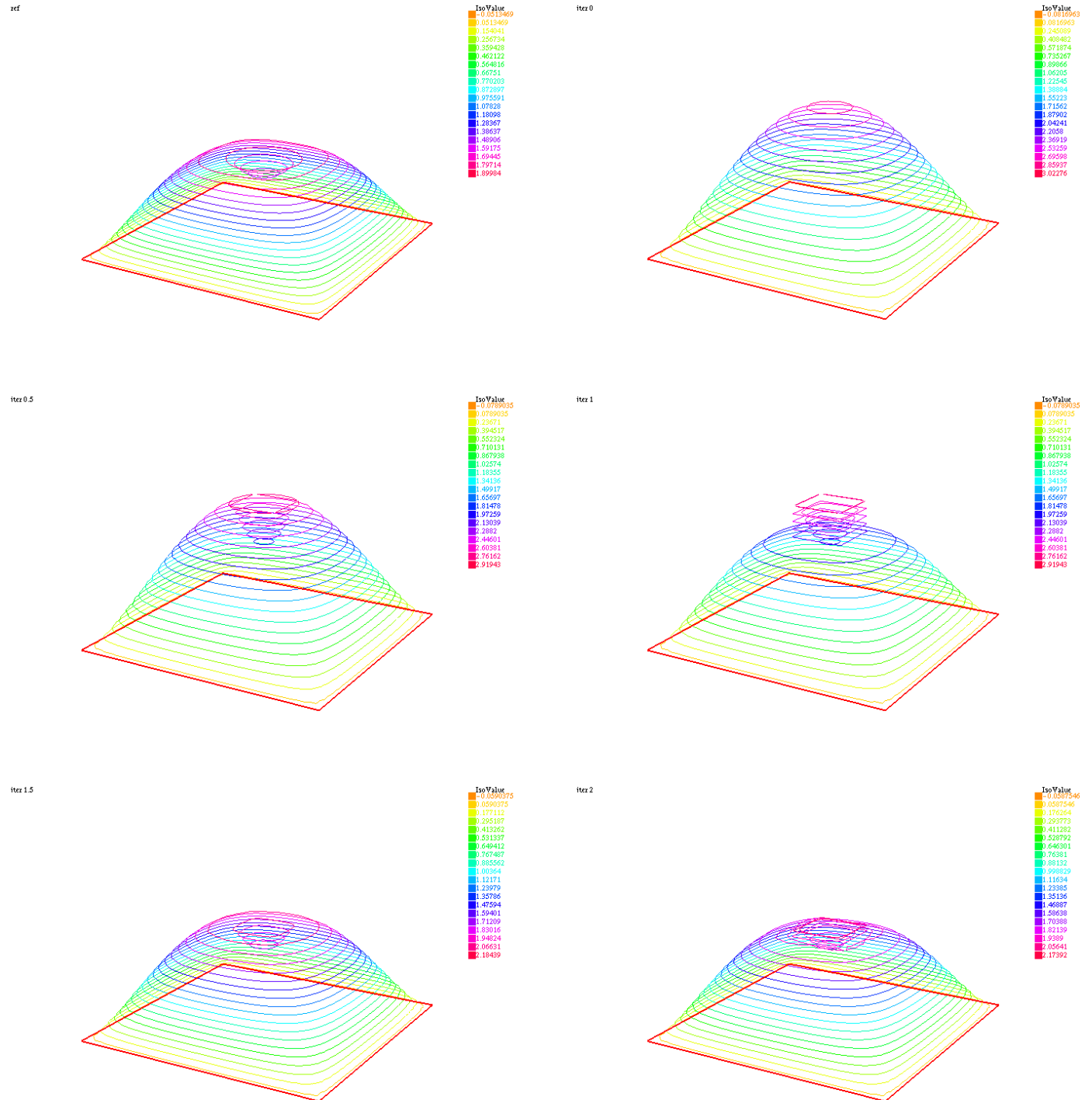


FIGURE 4.4: Evolution on iterations of Algorithm 4.1 on the same test case and the meshes as in Fig. 4.3. The reference solution, the initial coarse approximation (Iter 0,  $u_H^0$ ) and several first iterations ( $u_{Hh}^{0.5}$ ,  $u_{Hh}^1$ ,  $u_{Hh}^{1.5}$ ,  $u_{Hh}^2$ ) of Algorithm 4.1 are presented from top to bottom, left to right.

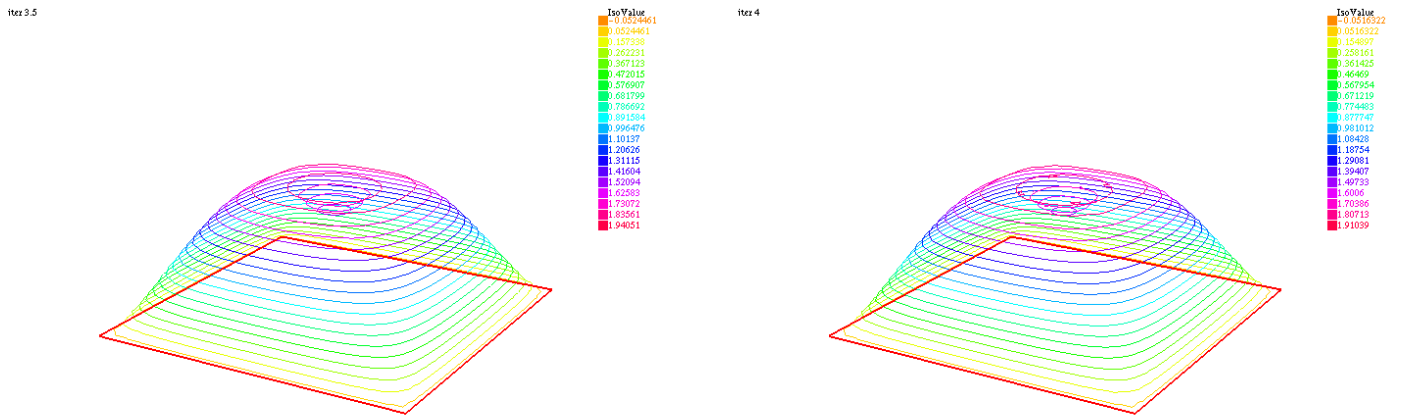


FIGURE 4.5: Continued from Fig. 4.4. iterations  $u_{Hh}^{3.5}$  and  $u_{Hh}^4$ .

# Bibliography

- [1] R. Adams and J. Fournier. *Sobolev Spaces*, volume 140 of *Pure and Applied Mathematics*. Elsevier Science, Oxford, 2nd edition, 2003.
- [2] H. W. Alt and S. Luckhaus. Quasilinear elliptic-parabolic differential equations. *Mathematische Zeitschrift*, 183(3):311–341, 1983.
- [3] C. Amrouche, V. Girault, and J. Giroire. Dirichlet and neumann exterior problems for the n-dimensional laplace operator an approach in weighted sobolev spaces. *Journal de mathématiques pures et appliquées*, 76(1):55–81, 1997.
- [4] J.-B. Apoung Kamga and O. Pironneau. Numerical zoom for multiscale problems with an application to nuclear waste disposal. *J. Comput. Phys.*, 224(1):403–413, 2007.
- [5] H. J. C. Barbosa and T. J. R. Hughes. The finite element method with Lagrange multipliers on the boundary: circumventing the Babuška-Brezzi condition. *Comput. Methods Appl. Mech. Engrg.*, 85(1):109–128, 1991.
- [6] F. Ben Belgacem and Y. Renard. Hybrid finite element methods for the Signorini problem. *Math. Comp.*, 72(243):1117–1145 (electronic), 2003.
- [7] C. Bernardi and V. Girault. A local regularization operator for triangular and quadrilateral finite elements. *SIAM journal on numerical analysis*, 35(5):1893–1916, 1998.
- [8] H. Berninger, R. Kornhuber, and O. Sander. Fast and robust numerical solution of the richards equation in homogeneous soil. *SIAM Journal on Numerical Analysis*, 49(6):2576–2597, 2011.
- [9] V. Bonnaillie-Noël. *Analyse asymptotique, spectrale et numérique pour quelques problèmes elliptiques issus de la physique ou de la mécanique*. Habilitation à diriger les recherches, 2011.
- [10] V. Bonnaillie-Noël, D. Brancherie, M. Dambrine, F. Héreau, S. Tordeux, and G. Vial. Multiscale expansion and numerical approximation for surface defects. In *ESAIM: Proceedings*, volume 33, pages 22–35. EDP Sciences, 2011.
- [11] V. Bonnaillie-Noël, D. Brancherie, M. Dambrine, S. Tordeux, and G. Vial. Effect of micro-defects on structure failure coupling asymptotic analysis and strong discontinuity. *European Journal of Computational Mechanics/Revue Européenne de Mécanique Numérique*, 19(1-3):165–175, 2010.

- [12] F. Brezzi and M. Fortin. *Mixed and hybrid finite element methods*, volume 15 of *Springer Series in Computational Mathematics*. Springer-Verlag, New York, 1991.
- [13] E. Chahine, P. Laborde, and Y. Renard. A non-conformal eXtended finite element approach: integral matching Xfem. *Appl. Numer. Math.*, 61(3):322–343, 2011.
- [14] M. Chevreuril, A. Nouy, and E. Safatly. A multiscale method with patch for the solution of stochastic partial differential equations with localized uncertainties. *Computer Methods in Applied Mechanics and Engineering*, 255:255–274, 2013.
- [15] P. G. Ciarlet. *The finite element method for elliptic problems*. North-Holland Publishing Co., Amsterdam-New York-Oxford, 1978. Studies in Mathematics and its Applications, Vol. 4.
- [16] M. Duval, A. Lozinski, J.-C. Passieux, and M. Salaün. Residual error based adaptive mesh refinement with the non-intrusive patch algorithm. *Computer Methods in Applied Mechanics and Engineering*, 329:118–143, 2018.
- [17] M. Duval, J.-C. Passieux, M. Salaün, and S. Guinard. Non-intrusive coupling: recent advances and scalable nonlinear domain decomposition. *Archives of Computational Methods in Engineering*, pages 1–22, 2014.
- [18] L. Gendre, O. Allix, and P. Gosselet. A two-scale approximation of the schur complement and its use for non-intrusive coupling. *International Journal for Numerical Methods in Engineering*, 87(9):889–905, 2011.
- [19] L. Gendre, O. Allix, P. Gosselet, and F. Comte. Non-intrusive and exact global/local techniques for structural problems with local plasticity. *Computational Mechanics*, 44(2):233–245, 2009.
- [20] R. Glowinski, J. He, A. Lozinski, J. Rappaz, and J. Wagner. Finite element approximation of multi-scale elliptic problems using patches of elements. *Numer. Math.*, 101(4):663–687, 2005.
- [21] R. Glowinski, J. He, A. Lozinski, J. Rappaz, and J. Wagner. Finite element approximation of multi-scale elliptic problems using patches of elements. *Numer. Math.*, 101(4):663–687, 2005.
- [22] R. Glowinski, J. He, J. Rappaz, and J. Wagner. Approximation of multi-scale elliptic problems using patches of finite elements. *C. R. Acad. Sci. Paris, Ser. I*, 337:679–684, 2003.
- [23] C. Hager, P. Hauret, P. Le Tallec, and B. I. Wohlmuth. Solving dynamic contact problems with local refinement in space and time. *Computer Methods in Applied Mechanics and Engineering*, 201:25–41, 2012.

- 
- [24] J. Haslinger and Y. Renard. A new fictitious domain approach inspired by the extended finite element method. *SIAM Journal on Numerical Analysis*, 47(2):1474–1499, 2009.
- [25] J. He, A. Lozinski, and J. Rappaz. Accelerating the method of finite element patches using approximately harmonic functions. *Comptes Rendus Mathématique*, 345(2):107–112, 2007.
- [26] F. Hecht. New development in freefem++. *J. Numer. Math.*, 20(3-4):251–265, 2012.
- [27] F. Hecht, A. Lozinski, and O. Pironneau. Numerical zoom and the schwarz algorithm. In *Domain decomposition methods in science and engineering XVIII*, pages 63–73. Springer, 2009.
- [28] A. Il'in. *Matching of asymptotic expansions of solutions of boundary value problems*. 1992.
- [29] F. D. J.L. Steger and J. Benek. A chimera grid scheme. In *Advances in Grid Generation*. K. N. Chis and U. Ghia ed., ASME FED-Vol. 5. June 1983.
- [30] A. Lozinski. *Méthodes numériques et modélisation pour certains problèmes multi-échelles*. Habilitation à diriger les recherches. Université Paul Sabatier, Toulouse 3, 2010.
- [31] A. Lozinski and P. Laborde. Numerical zoom for multi-scale and multi-model problems. *in preparation*, 2018.
- [32] A. Lozinski and O. Pironneau. Numerical zoom for advection diffusion problems with localized multiscales. *Numerical Methods for Partial Differential Equations*, 27(1):197–207, 2011.
- [33] V. Maz'ya, S. Nazarov, and B. Plamenevskij. *Asymptotic theory of elliptic boundary value problems in singularly perturbed domains*, volume 1. Birkhäuser, 2012.
- [34] A. Nouy and F. Pled. A multiscale method for semi-linear elliptic equations with localized uncertainties and non-linearities. *ESAIM: Mathematical Modelling and Numerical Analysis*, 52(5):1763–1802, 2018.
- [35] M. Renardy and R. C. Rogers. *An introduction to partial differential equations*, volume 13. Springer Science & Business Media, 2006.
- [36] E. Safatly. *Méthode multiéchelle et réduction de modèle pour la propagation d'incertitudes localisées dans les modèles stochastiques*. Thèse de doctorat, Université de Nantes, 2012.
- [37] L. R. Scott and S. Zhang. Finite element interpolation of nonsmooth functions satisfying boundary conditions. *Math. Comp.*, 54(190):483–493, 1990.



- [38] E. Stein. *Singular integrals and differentiability properties of functions (PMS-30)*, volume 30. Princeton university press, 1971.
- [39] L. Tartar. Sur un lemme d'équivalence utilisé en analyse numérique. *Calcolo*, 24(2):129–140 (1988), 1987.
- [40] M. Tirvaudey, L. Chamoin, R. Bouclier, and J.-C. Passieux. A posteriori error estimation and adaptivity in non-intrusive couplings between concurrent models. *Computer Methods in Applied Mechanics and Engineering*, 367:113104, 2020.
- [41] R. Verfürth. *A review of a posteriori estimation and adaptive mesh-refinement techniques*. Wiley-Teubner, Stuttgart, 1996.
- [42] G. Vial. *Perturbations singulières de problèmes elliptiques, analyse asymptotique et calcul scientifique*. Habilitation à diriger les recherches. Université Paul Sabatier, Toulouse 3, 2011.



**titre** La méthode de Zoom Numérique pour des problèmes elliptiques perturbés et des problèmes non linéaires

**Mots clés** elements finis, zoom numérique, problèmes non linéaires

**Résumé** Nous proposons plusieurs nouvelles variantes de la méthode du Zoom Numérique et les étudions mathématiquement. Nous considérons principalement la situation suivante simple, mais pertinente aux applications pratiques : l'équation de Poisson dans un domaine contenant un petit trou. Nous utilisons un maillage global grossier qui ne voit pas le trou et corrigeons ce défaut grâce à un maillage fin placé autour du trou et conforme à celui-ci. Un algorithme itératif (zoom numérique multi-modèles ou couplage des modèles non intrusif) est alors proposé, résolvant alternativement les problèmes sur les maillages global et local. Nous introduisons un cadre mathématique pour ces méthodes sous des hypothèses très générales sur les maillages : le maillage fin peut être placé sur le maillage grossier de manière arbitraire. Nous analysons ensuite théoriquement à la fois la précision de la méthode par rapport aux raffinements du maillage et le taux de convergence des itérations. Nous comparons également cette approche avec la méthode des développements asymptotiques. Enfin, nous adaptons notre méthode aux problèmes monotones avec des non-linéarités localisées, en modifiant la preuve de convergence et en donnant une estimation d'erreur a priori.

**Title :** The Numerical Zoom method for the elliptic perturbed problems and non-linear problems

Keywords :] finite elements, numerical zoom, nonlinear problems

**Abstract :** We propose several new variants of the method of Numerical Zoom and study them mathematically on several model problems. We consider mostly the following simple situation, yet pertinent to some practical application: Poisson equation in a domain containing a small hole. We employ a coarse global mesh that does not see the hole and correct this defect using an additional fine mesh placed around the hole and conforming with it. An iterative algorithm (multi-model numerical zoom or non intrusive model coupling) is then proposed, solving alternatively the problems on global and local meshes. We introduce a mathematical framework for these methods under very general assumptions on the meshes: the fine mesh may be placed over the coarse one in an arbitrary manner. We perform then a complete theoretical analysis both of the accuracy with respect to a mesh refinement and of the convergence rate of iterations. We also compare this approach with the method of matched asymptotic expansions. Finally, we adapt our method to monotone problems with localized non-linearities, adapting the convergence proof and giving an a priori error estimate.